
***FLUXES OF ENERGY AND WATER VAPOUR FROM
GRAZED PASTURE ON A MINERAL SOIL IN THE
WAIKATO***

A thesis
submitted in part fulfilment
of the requirements for the Degree
of
Master of Science in Earth Science
at
The University of Waikato
by

TEHANI JANELLE KUSKE



The University of Waikato

2009

Abstract

The eddy covariance (EC) technique was used to measure half hourly fluxes of energy and evaporation from 15 December 2007 to 30 November 2008 at the Scott Research Farm, located 7 km east of Hamilton. Many other supporting measurements of climate and soil variables were also made.

The research addressed three objectives:

1. To examine the accuracy of the eddy covariance measurement technique.
2. Understand the surface partitioning of energy and water vapour on a diurnal to annual timescale.
3. Compare measurements of evaporation to methods of estimation.

Average energy balance closure at Scott Farm was deficient by 24%, comparable to published studies of up to 30%. Three lysimeter studies were carried out to help verify eddy covariance data. These resulted in the conclusions that; 1) lysimeter pots needed to be deeper to allow for vegetation rooting depths to be encompassed adequately; 2) forcing energy balance closure was not supported by two of the studies (summer and winter); 3) latent heat flux (λE) gap filling of night time EC data during winter over estimated values by about 10 W m^{-2} ; and 4) the spring lysimeter study verified eddy covariance measurements including the closure forcing method. Some uncertainty still exists as to the accuracy of both lysimeter and EC methods of evaporation measurement because both methods still have potential biases, however for the purpose of this study, it would appear data are sufficiently accurate to have confidence in results.

Energy and water vapour fluxes varied on both a diurnal and seasonal timescale. Diurnally, fluxes were small or negative at night and were highest during the day, usually at solar noon. Seasonally, spring and summer had the highest energy and evaporation fluxes and winter rates were small but tended to exceed available energy supply. Evaporation was constrained by soil moisture availability during summer and by energy availability during winter. Estimated annual evaporation at Scott Farm was 755 mm, 72% of precipitation.

Two evaporation models were compared to eddy covariance evaporation (E_{EC}) measurements; the FAO₅₆ Penman-Monteith model (E_o) and the Priestley-Taylor model (E_{PT}). Both models over estimated evaporation during dry conditions and slightly under estimated during winter. The α coefficient that is applied to E_{PT} was not constant and a seasonally adjusted value would be most appropriate. A crop coefficient of 1.13 is needed for E_o measurements during moist conditions. E_o began over estimating evaporation when soil moisture contents dropped below ~44%. A water stress adjustment was applied to both models which improved evaporation estimates, however early onset of drying was not able to be adjusted for. The adjusted E_o model is the most accurate overall, when compared to E_{EC} .

Acknowledgements

I have many people to thank for providing help and positive support throughout the course of this thesis. I would therefore like to acknowledge the following people:

My first thanks go to Dave Campbell, my primary supervisor who always made time for me, showed enthusiasm, and who showed a lot of patience during every part of my graduate experience.

To Louis Schipper, my secondary supervisor, who was always positive and supportive and a great person for discussions.

A big thank you to Susanna Rutledge for her support and consistent help using MatLab and analysing data.

Craig Hosking, for his technical support and eagerness whether in the field or in the lab, who always provided a good laugh and home baking on field trips, and to the Annette Rodgers and Chris McKinnon for their technical support.

Paul Mudge for his support in our joint field areas.

Thanks to Willem de Lange for his assistance for gaining SST data.

Thank you to Leah Adlam, Sarah Ewen and Justin Wyatt for their fabulous proof reading work.

To Renee Schicker for her help using GIS.

Thank you to my field assistants; James Cooper, Fiona Sanders and Leah Adlam who either braved the early, icy morning frosts or the soggy, muddy fields to help me with my data collection.

Thank you to Dairy NZ and Scott Farm management and staff for providing such a great field site and allowing access to the farm for this study.

The New Zealand Hydrological Society for their aid with travel and conference costs to help me present my research at their annual joint conference in Greymouth.

To all the funding providers who made it possible for this research to go ahead – Environment Waikato, Landcare Research, Earth and Ocean Sciences, The University of Waikato and the C. Alma Baker Trust.

Thank you to all my fellow students who were always there to support each other and help each other through the tough times of Masters.

And finally, but certainly not least, to Sydney Wright, for all her help throughout my time at The University of Waikato. What would we do without you?

Table of Contents

ABSTRACT	III
ACKNOWLEDGEMENTS.....	V
TABLE OF CONTENTS.....	VII
LIST OF FIGURES	XI
LIST OF TABLES	XVII
LIST OF SYMBOLS AND ABBREVIATIONS	XIX
1 INTRODUCTION	1
1.1 THE EVAPORATION PROCESS	1
1.2 WHY GRAZED PASTURE?.....	2
1.3 AIMS AND OBJECTIVES.....	3
1.4 RELATED STUDIES	3
1.5 OUTLINE OF THESIS STRUCTURE	4
2 BACKGROUND AND LITERATURE REVIEW	5
2.1 INTRODUCTION	5
2.2 SURFACE ENERGY BALANCE	5
2.2.1 <i>The diurnal energy balance</i>	7
2.3 EVAPORATION	9
2.3.1 <i>Factors affecting evaporation</i>	9
2.3.2 <i>Evaporation measurement</i>	11
2.3.3 <i>Estimating evaporation</i>	19
2.3.4 <i>Correcting for soil water stress conditions</i>	22
2.4 PASTURE – THE ENERGY BALANCE AND EVAPORATION.....	24
2.4.1 <i>New Zealand’s maritime environment</i>	25
3 METHODS AND SITE DESCRIPTION	27
3.1 INTRODUCTION	27
3.2 SITE DESCRIPTION.....	27
3.2.1 <i>Scott Farm</i>	27
3.2.2 <i>Climate</i>	29
3.2.3 <i>Soil properties</i>	32
3.2.4 <i>Local hydrology</i>	32

3.3 INSTRUMENTATION	33
3.3.1 Eddy covariance measurements	36
3.3.2 Lysimeters.....	38
3.3.3 Data loggers.....	40
3.4 PROCESSING DATA	41
3.4.1 WPL corrections.....	42
3.4.2 Other calculations and corrections.....	43
3.4.3 Data quality, filtering, missing data and gap-filling.....	45
3.5 EVAPORATION ESTIMATION.....	52
3.5.1 Calculating E_{PT} and E_o	52
3.5.2 Water stress adjustment and crop coefficient	52
3.6 FOOTPRINT ANALYSIS AND AIR DISTURBANCES	53
4 ACCURACY OF THE EDDY COVARIANCE TECHNIQUE	59
4.1 INTRODUCTION	59
4.2 ENERGY BALANCE CLOSURE	59
4.2.1 Energy balance closure and wind direction.....	63
4.2.2 Seasonal closure.....	64
4.3 EFFECTS OF GAP-FILLING	67
4.4 LYSIMETERS AS AN INDEPENDENT MEASUREMENT OF E	68
4.4.1 Autumn lysimeter study	69
4.4.2 Winter lysimeter study.....	70
4.4.3 Spring lysimeter study.....	72
4.4.4 Overall lysimeter/EC accuracy	74
4.5 DISCUSSION	75
5 SURFACE ENERGY BALANCE AND EVAPORATION.....	79
5.1 INTRODUCTION	79
5.2 SURFACE RADIATION BALANCES	79
5.2.1 Longwave and shortwave radiation	79
5.2.2 Albedo.....	81
5.3 SURFACE ENERGY BALANCE.....	82
5.3.1 Diurnal energy balances	82
5.3.2 Seasonal energy balances	85
5.3.3 Advection.....	88

5.4 EVAPORATION	90
5.5 DISCUSSION	92
6 EVAPORATION ESTIMATION	95
6.1 INTRODUCTION	95
6.2 PRIESTLEY-TAYLOR AND FAO ₅₆ MODELS	95
6.2.1 <i>The Priestley-Taylor alpha (α)</i>	98
6.2.2 <i>Critical soil moisture values during drought</i>	101
6.2.3 <i>Model corrections</i>	105
6.2.4 <i>Sensitivity analysis</i>	110
6.3 DISCUSSION	114
7 CONCLUSIONS	119
7.1 ACCURACY OF EDDY COVARIANCE MEASUREMENTS OF EVAPORATION	119
7.3 RADIATION AND ENERGY BALANCES, AND EVAPORATION	120
7.4 ESTIMATING EVAPORATION	121
7.5 FURTHER RESEARCH RECOMMENDATIONS	122
REFERENCES	125
APPENDICES	137
A APPENDIX A	139
B APPENDIX B	141
C APPENDIX C	145
D APPENDIX D	149
E APPENDIX E	151

List of figures

<i>Figure 2.1 Typical proportions of energy transfers during daytime and night time (adapted from Oke, 1987).....</i>	<i>8</i>
<i>Figure 2.2 Soil moisture balance using a lysimeter.....</i>	<i>15</i>
<i>Figure 2.3 Determination of evaporative and vegetative area (adapted from Allen et al. 1991).....</i>	<i>17</i>
<i>Figure 3.1 Map of East/South Hamilton and location of Scott Farm.....</i>	<i>28</i>
<i>Figure 3.2 Scott Farm EC site and layout of surrounding paddocks.</i>	<i>28</i>
<i>Figure 3.3 40 year (1947 - 2007) average monthly rainfall at Ruakura with maximum and minimum values shown as bounding shaded area and total rainfall at Ruakura for 2008 (data from NIWA climate database, accessed 29 September 2008) and 2008 Scott Farm rainfall.</i>	<i>30</i>
<i>Figure 3.4 15-day running means of a) R_n, b) air temperature, and daily c) rainfall and d) volumetric moisture content.</i>	<i>31</i>
<i>Figure 3.5 Installation of eddy covariance instrumentation.....</i>	<i>34</i>
<i>Figure 3.6 The eddy covariance instruments. CSAT3 sonic anemometer and LI-7500 gas analyser (vertical cable ties are used to deter birds).</i>	<i>37</i>
<i>Figure 3.7 The progression of data processing.</i>	<i>42</i>
<i>Figure 3.8 Timeseries for 1 – 3 January 2008 showing 30-minute raw soil heat flux (G_z) and the temperature, moisture, and depth corrected G using Equation 3.4.</i>	<i>45</i>
<i>Figure 3.9 Regression of LI-7500 and HMP45A vapour pressure, where black data points are accepted and grey points are rejected for the period 15 December 2007 to 30 November 2008.</i>	<i>46</i>
<i>Figure 3.10 Scatter plot of λE against R_n to determine the gap-filling model required for each moisture content range for January 2008.</i>	<i>48</i>
<i>Figure 3.11 Scatter plot of H against R_n to determine the gap-filling model required for each moisture content range for January 2008.</i>	<i>48</i>
<i>Figure 3.12 Volumetric moisture content changes and thresholds for January 2008.</i>	<i>49</i>

<i>Figure 3.13 Time series of latent heat flux for 2–5 January 2008 showing example of measured and gap-filled data.</i>	<i>50</i>
<i>Figure 3.14 Comparison of net radiation data measured by REBS and NR01 instruments for the period 19 January 2008 to 20 June 2008. Diagonal line is 1:1.</i>	<i>51</i>
<i>Figure 3.15 Image of (a) REBS net radiometer and (b) NR01 four component net radiometer at Scott Farm.</i>	<i>51</i>
<i>Figure 3.16 Footprint analysis for 1 February 2008 12:00 NZST under unstable conditions.</i>	<i>54</i>
<i>Figure 3.17 Footprint analysis for 10 March 2008 02:00 NZST under stable conditions.</i>	<i>54</i>
<i>Figure 3.18 Spatial distribution of half hourly daytime (unstable) x_{MAX} values surrounding the EC tower site (central location) for the period 15 December 2007 to 30 November 2008.</i>	<i>55</i>
<i>Figure 3.19 Spatial distribution of half hourly night time (stable) x_{MAX} values surrounding the EC tower site (central location) for the period 15 December 2007 to 30 November 2008.</i>	<i>56</i>
<i>Figure 3.20 Spatial distribution of half hourly daytime (unstable) CNF_{80} values surrounding the EC tower site (central location) for the period 15 December 2007 to 30 November 2008.</i>	<i>56</i>
<i>Figure 3.21 Spatial distribution of half hourly night time (stable) CNF_{80} values surrounding the EC tower site (central location) for the period 15 December 2007 to 30 November 2008 (NOTE: axis scale different to Figure 3.20).</i>	<i>57</i>
<i>Figure 4.1 Half hourly energy balance ratio ($\lambda E + H$ against $R_n - G$) to show average lack of closure for 15 December 2007 to 30 November 2008. Dashed line shows regression.</i>	<i>60</i>
<i>Figure 4.2 Energy balance for 1 January 2008 showing lack of closure due to probable underestimation of λE and H.</i>	<i>61</i>
<i>Figure 4.3 Energy balance for 25 July 2008 showing lack of closure due to probable underestimation of λE and H.</i>	<i>61</i>
<i>Figure 4.4 Diurnal time series of the two net radiometer instruments (REBS and NR01) for the four day period 7–10 February 2008.</i>	<i>63</i>

<i>Figure 4.5 30-minute energy balance ratio (day time values only $R_n > 100 \text{ W m}^{-2}$) compared to wind direction for 15 December 2007 to 30 November 2008. Vertical dashed line shows orientation of tower.</i>	<i>64</i>
<i>Figure 4.6 Daily energy balance ratio for the period 15 December 2007 to 30 November 2008 to show lack of closure.</i>	<i>65</i>
<i>Figure 4.7 Daily energy balance closure for the period 15th December 2007 to 30 November 2008.</i>	<i>66</i>
<i>Figure 4.8 Cumulative evaporation for the period 15 December 2007 to 30 November 2008 showing forced data and un-forced data.</i>	<i>66</i>
<i>Figure 4.9 Time series for 1 July 2008 showing data that required gap-filling where the grey shaded area shows how λE is over calculated at night by the gap-filling model when it should be closer to zero. Note: scale small to show small night time fluxes where day time fluxes are much higher.</i>	<i>68</i>
<i>Figure 4.10 a) Comparison between eddy covariance (E_{EC}) and lysimeter (E_{lys}) measurements of daily evaporation for 6–15 March 2008. E_{lys} is the mean measurement from all 10 lysimeters, bars indicate 95% confidence limits around the mean. $E_{EC}(*)$ are EC measurements where night-time gaps in λE data were set to zero and $E_{EC(closure)}$ is EC closure forced evaporation. b) is volumetric moisture content for the same period.</i>	<i>69</i>
<i>Figure 4.11 a) Comparison between eddy covariance (E_{EC}) and lysimeter (E_{lys}) measurements of daily evaporation for 8–10 July 2008. E_{lys} is the mean measurement from all 10 lysimeters, bars indicate 95% confidence limits around the mean. $E_{EC}(*)$ are EC measurements where night-time gaps in λE data were set to zero and $E_{EC(closure)}$ is EC closure forced evaporation. b) is volumetric moisture content for the same period.</i>	<i>71</i>
<i>Figure 4.12 a) Comparison between eddy covariance (E_{EC}) and lysimeter (E_{lys}) measurements of daily evaporation for 8–14 November 2008. E_{lys} is the mean measurement from all 10 lysimeters, bars indicate 95% confidence limits around the mean. $E_{EC}(*)$ are EC measurements where night-time gaps in λE data were set to zero and $E_{EC(closure)}$ is EC closure forced evaporation. b) is volumetric moisture content for the same period.</i>	<i>73</i>
<i>Figure 4.13 Scatter plot of measured eddy covariance and measured lysimeter evaporation for all lysimeter studies.</i>	<i>74</i>

Figure 5.1 a) Radiation balance. R_n , $K\uparrow$, $K\downarrow$, $L\uparrow$ and $L\downarrow$ for 26-28 January 2008 and b) the albedo for the same period. For convenience, $K\uparrow$ and $L\uparrow$ are shown as positive values.	80
Figure 5.2 a) Daily albedo, b) rain and c) θ_v from 19 Jan to 29 Jun 2008.....	82
Figure 5.3 a) Diurnal energy balance components and Bowen ratio for the three days 31 December 2007 to 2 January 2008 and b) Bowen ratio for the same period.	83
Figure 5.4 a) Diurnal energy components and b) Bowen ratio for the three days 4–6 February 2008.	85
Figure 5.5 Diurnal energy balance ensembles including Bowen ratios for a) January, b) April, c) July, and d) October 2008.....	86
Figure 5.6 a) Annual 15 day running mean energy balance for Scott Farm and b) the ratio $\lambda E/R_n$ for 15 December 2007 to 30 November 2008.	88
Figure 5.7 Mean monthly sea surface temperature (SST) from the Tasman sea and soil temperature (0.1 m) measured at Scott Farm for January 2008 to October 2008. Coordinates Lat 173.5°(E) Long 38' (S).	89
Figure 5.8 Mean, minimum and maximum daily evaporation for each month for Scott Farm from 15 December 2007 to 30 November 2008. Note: December is only a part month from 15 December 2007 to 31 December 2007 so some bias may exist for this month.	91
Figure 6.1 Cumulative evaporation for measured (E_{EC}), modelled FAO ₅₆ (E_o) and Priestley-Taylor (E_{PT}) for 15 December 2007 to 30 November 2008.	96
Figure 6.2 Scatter plot of estimated E_o evaporation versus measured E_{EC} . All values are 24 hour totals.	97
Figure 6.3 Scatter plot of estimated E_{PT} evaporation versus measured E_{EC} where α is set to the standard 1.26. All values are 24 hour totals.....	97
Figure 6.4 Time series of daily Priestley-Taylor alpha values calculated as $\alpha = E_{EC}/E_{EQ}$. Horizontal line is $\alpha = 1.26$	98
Figure 6.5 Regression of E_{EQ} to E_{EC} for data after 1 May 2008 (no drought effects) forced through the origin where the slope is equal to $1/\alpha$. The initial regression equation is also shown to display the magnitude of change when forced through zero.....	99

- Figure 6.6 Regression of E_{EQ} to E_{EC} for data from 15 December 2007 to 30 April 2008 (during drought conditions) forced through the origin where the slope is equal to $1/\alpha$ 100
- Figure 6.7 Regression of E_{EQ} to E_{EC} for data from 1 September 2008 to 30 November 2008 forced through the origin where the slope is equal to $1/\alpha$. . 100
- Figure 6.8 Ratio of E_o to E_{EC} evaporation against θ_v . Shaded area represents the estimated critical moisture content limit. θ_v probes are 5 and 10 cm deep.. 102
- Figure 6.9 a) Daily rainfall and b) θ_v for 15 December 07 to 30 June 08 with two drying events indicated during the 2008 summer drought. Shaded area is estimated critical moisture content. 103
- Figure 6.10 E_o/E_{EC} against θ_v for the two major drying events during the 2008 drought. Shaded area shows estimated critical moisture content. 104
- Figure 6.11 Regression of E_o to E_{EC} for data after 1 May 2008 (no drought effects) forced through the origin where the slope is equal to the inverse of the crop coefficient, K_c 104
- Figure 6.12 Effect the water stress adjustment model (using $K_c = 1.13$) has on estimated evaporation data by showing regression of E_o and E_{EC} 106
- Figure 6.13 Measured E_{EC} evaporation and estimated E_o (using $K_c = 1.13$) and E_{PT} ($\alpha = 1.26$) evaporation throughout the year (December 2007 only part month so adjusted to equivalent of a 31-day month). 107
- Figure 6.14 Measured E_{EC} evaporation and estimated E_o (using $K_c = 1.13$) and E_{PT} ($\alpha = 1.26$) evaporation adjusted for water stress conditions throughout the year (December 2007 only part month so adjusted to equivalent of a 31-day month). 107
- Figure 6.15 Cumulative evaporation for measured E_{EC} and estimated E_o , E_{PT} and $E_{o(adj)}$ and $E_{PT(adj)}$ for water stress conditions using $K_c = 1.13$ 108
- Figure 6.16 For the time period 1 January 2008 to 31 March 2008 a) change in water stress coefficient with different rooting depths, b) volumetric moisture content and c) cumulative E_o using different rooting depths and $K_c = 1.13$ and E_{EC} evaporation. 111
- Figure 6.17 Scatter plot with regression of $E_{o(adj)}$ with a rooting depth of 1.0 m against daily E_{EC} for data from 15 December 2007 to 30 November 2008. . 112
- Figure 6.18 For the time period 1 January 2008 to 31 March 2008 a) change in water stress coefficient with different field capacity (FC) values, and b)

*cumulative E_o using different field capacity values where $K_c = 1.13$ and
cumulative E_{EC} evaporation..... 113*

*Figure 6.19 For the time period 1 January 2008 to 31 March 2008 a) change in
water stress coefficient with different wilting point (WP) values, and b)
cumulative E_o using different wilting point values where $K_c = 1.13$ and
cumulative E_{EC} evaporation..... 114*

List of tables

<i>Table 3.1 Soil properties measured at Scott Farm for seven cores each 7.5 cm by 10 cm in size taken 1 September 2008. Organic matter fraction determined from a bulked subsample.</i>	<i>32</i>
<i>Table 3.2 Details of permanently deployed instruments at Scott Farm EC site. ...</i>	<i>35</i>
<i>Table 3.3 Details of temporary variables measured and instrumentation used at Scott Farm EC site.</i>	<i>36</i>
<i>Table 3.4 Company details of instruments listed in Table 3.2 and 3.3.</i>	<i>36</i>
<i>Table 5.1 Daily totals of energy fluxes, Bowen ratio, evaporative fraction and θ_v for 31 December 2007 - 2 January 2008 and 4 - 6 February 2008. Refer to Figure 5.3 and 5.4.</i>	<i>84</i>
<i>Table 5.2 Daily average total energy fluxes for the months representing each season (Figure 5.5a, b, c and d) including β, evaporative fraction and θ_v. ...</i>	<i>87</i>
<i>Table 5.3 Total monthly evaporation and rainfall (mm) and the evaporation percentage of rainfall showing the months of drying and wetting. Note that December 2007 is only a half month.</i>	<i>91</i>
<i>Table 6.1 Values used for the estimated evaporation adjustment after Allen et al. (1998).</i>	<i>105</i>

List of symbols and abbreviations

A	Area (m^2)
C_s	Volumetric soil heat capacity ($\text{J m}^{-3} \text{ }^\circ\text{C}^{-1}$)
D	Vapour pressure deficit (kPa)
D_r	Root zone depletion
E	Evaporation (mm)
E_{EC}	Eddy covariance evaporation (mm)
E_{EQ}	Equilibrium evaporation (mm)
E_{lys}	Evaporation from lysimeter (mm)
E_o	FAO ₅₆ evaporation (mm)
$E_{o(\text{adj})}$	FAO ₅₆ evaporation adjusted for moisture stress (mm)
E_{pen}	Penman evaporation (mm)
E_{PM}	Penman-Monteith evaporation (mm)
E_{PT}	Priestley-Taylor evaporation (mm)
$E_{\text{PT}(\text{adj})}$	Priestley-Taylor evaporation adjusted for moisture stress (mm)
G	Soil heat flux density (W m^{-2} or $\text{MJ m}^{-2} \text{ day}^{-1}$)
G_z	Measured soil heat flux at a given depth z (W m^{-2})
H	Sensible heat flux density (W m^{-2} or $\text{MJ m}^{-2} \text{ day}^{-1}$)
H_f	Sensible heat flux forced energy balance closure via Bowen ratio (W m^{-2} or $\text{MJ m}^{-2} \text{ day}^{-1}$)
K^*	Net shortwave radiation flux density (W m^{-2})
K_\uparrow	Outgoing shortwave radiation flux density (W m^{-2})
K_\downarrow	Incoming shortwave radiation flux density (W m^{-2})
K_c	Crop coefficient
K_s	Water stress coefficient
L^*	Net longwave radiation flux density (W m^{-2})
L_\uparrow	Outgoing longwave radiation flux density (W m^{-2})
L_\downarrow	Incoming longwave radiation flux density (W m^{-2})

P	Precipitation (mm)
P_s	Photosynthetic energy flux (W m^{-2} or $\text{MJ m}^{-2} \text{ day}^{-1}$)
Q	Discharge (mm)
R_n	Net radiation flux density (W m^{-2} or $\text{MJ m}^{-2} \text{ day}^{-1}$)
T	Temperature ($^{\circ}\text{C}$)
T_s	Mean soil temperature between the surface and the depth of measurement ($^{\circ}\text{C}$)
Z_r	Rooting depth (m)
c_p	Specific heat of air (J kg^{-1})
c_w	Specific heat of water ($\text{J kg}^{-1} \text{ }^{\circ}\text{C}^{-1}$)
e_s	Saturation vapour pressure (kg m^{-3})
p	depletion factor
r_a	Aerodynamic resistance (s m^{-1})
r_c	Canopy resistance (s m^{-1})
s	Slope of the saturation vapour pressure versus temperature curve ($\text{kPa }^{\circ}\text{C}^{-1}$)
t	Time interval (s)
u	Wind speed (m s^{-1})
u_2	Wind speed at 2 m height (m s^{-1})
w	Vertical wind velocity (m s^{-1})
z	Depth or height (m)
ΔS	Change in storage (mm)
ΔW	Change in weight (kg)
α	albedo or Priestley-Taylor coefficient
β	Bowen ratio
γ	Psychrometric constant ($\text{kPa }^{\circ}\text{C}^{-1}$)
θ_g	Gravimetric soil moisture content (kg kg^{-1})

θ_v	Volumetric soil moisture content ($\text{m}^3 \text{m}^{-3}$)
λ	latent heat of vaporisation of water (MJ kg^{-1})
λE	Latent heat flux (W m^{-2} or $\text{MJ m}^{-2} \text{day}^{-1}$)
λE_f	Latent heat flux forced energy balance closure via Bowen ratio (W m^{-2} or $\text{MJ m}^{-2} \text{day}^{-1}$)
μ	Ratio of molecular masses of dry air and water vapour
ρ	Density of air (kg m^{-3})
ρ_v	Density of water vapour in air
ρ_b	Bulk density (kg m^{-3})
σ	Ratio of the mean densities of water vapour and dry air
CNF ₈₀	Horizontal distance from measurement position to cumulative normalised flux at which 80% of the measured flux at a given height (m)
EBR	Energy balance ratio
FC	Field capacity ($\text{m}^3 \text{m}^{-3}$)
LAI	Leaf area index
RAW	Readily available water ($\text{m}^3 \text{m}^{-3}$)
TAW	Total available water ($\text{m}^3 \text{m}^{-3}$)
WP	Wilting point ($\text{m}^3 \text{m}^{-3}$)
x _{MAX}	Position of the peak of the flux footprint (m)

1 Introduction

1.1 The evaporation process

Evaporation is the process of vaporisation of liquid water and is the means by which water enters the atmosphere. Because evaporation is often a large component of the land-based hydrological cycle, it is important for hydrologists to understand and be able to determine its seasonal and annual magnitude. A thorough understanding will assist in water use efficiency models for water users including agricultural industries, energy users who depend on water, and for scientists who develop climate models on a local, regional or global scale.

The main driving force of evaporation is available energy, i.e. solar radiation or sensible heat from the environment, which are dependent on various factors such as solar angle (including latitude, season, time of day and slope or orientation of the surface), cloudiness, and altitude. However, rates of evaporation can also depend on the type of surface and the amount of water available at the site of interest (e.g. vegetation types can sometimes conserve water loss via transpiration rates).

Most early measurements of evaporation used various water balance methods such as the soil water budget method involving rainfall, and change in soil water content, but this was very time consuming and labour intensive (Burman and Pochop, 1994). The hydrological budget (or catchment water balance) is another well known method which is a mass balance equation used on larger areas and includes inflows and outflows from an area (Burman and Pochop, 1994). This method has many restrictions and only gives an average measure of evaporation, but is often still used.

There are several newer ways to attempt to measure evaporation such as the eddy covariance method, weighing lysimeters, or the Bowen ratio method. Each method has its pros and cons and some methods are more realistic than others.

Methods of estimation also exist which use locally collected meteorological data such as wind speed, temperature, and radiation measurements to estimate an average evaporation rate, with varying success (Shuttleworth, 2007). Another commonly used method of estimation is the open-pan evaporation method. This approach has many restrictions and assumptions and is therefore not always a practical approach, particularly when applying the technique to a vegetated area.

1.2 Why grazed pasture?

In the Waikato region of New Zealand, 58% of landuse is pastoral farming while on a whole, pastoral farming accounts for 39% of all landuses (Ministry for the Environment, 2001/2002). Since pastoral farming accounts for such large proportions, it is important to understand the major processes controlling these systems. A water and energy budget will assist in the management of irrigation schemes or annual optimum pasture growth. Land management users, particularly within the dairy industry, must maintain output production for export of products, while reducing costs of production. These users will benefit from a more comprehensive understanding of the water budget, particularly one that can ultimately be correlated to areas of analogous climates. As water resources come under more and more pressure, there is demand for users to pay for the water they use, making the efficient use of the resource under irrigation scenarios more important than ever, particularly for private users such as farmers.

There is a need for evaporation data in soil science, plant growth models and surface-atmosphere models. Plant and soil microbe function rely on the presence of water. For plants to grow and photosynthesise, water is needed, helping them gain mass which is a store of carbon (Baldocchi, 2008). Soil microbes require moisture to function, providing them with the means to respire and release carbon to the atmosphere (Baldocchi, 2008). To gain an in-depth understanding into any of these processes, moisture and evaporation data are required. This data is important when creating and producing models for the prediction of these processes and when developing water use efficiency models for pasture during drought conditions.

1.3 Aims and objectives

This research project sets out to determine fluxes of energy and water vapour from a typical grazed pasture on a mineral soil. Results obtained will be compared to estimation methods.

This will be achieved by the following objectives:

- Establish the accuracy of the eddy covariance method for measuring fluxes of energy and water vapour by making a comparison with weighing lysimeters.
- Comprehend the surface partitioning of energy and water vapour on a diurnal to annual timescale and determine the factors affecting these processes.
- Compare these measurement results to methods of estimation which use limited meteorological data.

1.4 Related studies

A vast number of studies have been done on evaporative processes, particularly on the effects of landuse change and the water balance. Fewer studies have been carried out that focus directly on one landuse (notably pasture) in which evaporation is the main focus.

In a New Zealand context, studies have been done to determine water and energy balances for several different land uses including tussock grasslands in Otago (Campbell, 1989; Campbell and Murray, 1990; Fahey and Watson, 1991), wetlands in the Waikato (Campbell and Williamson, 1997; and Thompson *et al.* 1999), forests in the Otago, Marlborough and Tasman areas (Fahey and Jackson, 1997), and some crops in Manawatu (Clothier *et al.* 1982). These studies all either measure or estimate evaporation rates over these landuses, however only few studies compare estimation techniques to measurement methods to find their capabilities or limitations in an environment such as New Zealand (Clothier *et al.* 1982; and McAneney and Judd, 1983).

Internationally, similar studies have been undertaken which use estimation methods to assess evaporation rates over various landuses (Sumner and Jacobs, 2005; Villa Nova *et al.* 2007; Marc and Robinson, 2007). More recently, reports have emerged such as those by Pauwels and Samson (2006) and Aires *et al.* (2008), who compared various methods of measuring evaporation to common estimation methods and models, with varying success. The most common methods of measuring evaporation in these studies involve the eddy covariance and/or Bowen ratio energy balance method. These are most commonly compared to estimation models such as the Priestley-Taylor, Penman-Monteith or FAO₅₆ Penman-Monteith equations (Pauwels and Samson, 2006; Aires *et al.* 2008). What becomes of even greater use is when these methods and models are tested under environmental stress conditions such as drought (Aires *et al.* 2008) so a better understanding can be gained as to how such factors affect water availability and energy partitioning.

1.5 Outline of thesis structure

First an explanation of the background to concepts and a review of existing literature are provided. This is followed by a site description for this study and a description of instruments and methods used for measurement, ground-truthing, and calculating variables. The methods used for correcting, processing, and gap-filling data, and the footprint analysis of the site is assessed. This is then followed by a discussion of results for; 1) the accuracy of eddy covariance, comparing measurements to lysimeter measurements, and the necessity of forcing energy balance closure; 2) an analysis of energy and water vapour partitioning at the Earth's surface, and; 3) an assessment of the accuracy of two estimation models used to estimate evaporation and how drought conditions may affect model outcomes. This is then followed up with a conclusion of the overall results and findings from this research and recommendations for future research.

2 Background and literature review

2.1 Introduction

Evaporation is defined as the combined processes of interception loss, transpiration and evaporation from bare soil surfaces, where interception loss is the evaporation of temporarily stored rain water from a plant canopy, and transpiration is the water transpired by plants (McNaughton and Jarvis, 1983; McConchie, 2001).

Evaporation is both an energy balance and a water balance term. Components of the energy balance include net radiation which is the dominant source of energy that drives ground (or soil) heat flux, sensible heat flux (energy used to heat the air), and latent heat flux (the energy used for evaporation) (McNaughton and Jarvis, 1983). In terms of the water balance of terrestrial surfaces, evaporation represents a loss from the system.

This chapter will begin by specifying evaporation in terms of the energy balance, followed by a section defining evaporation as a whole, the factors that affect it, ways of measuring and estimating it and ways of correcting estimates for soil water stress conditions. These concepts will then be discussed in a pastoral setting in New Zealand and globally, and compared to other landuses.

2.2 Surface energy balance

Fluxes of solar energy (or radiation) from the sun ultimately drive evaporation at the Earth's surface. Solar radiation is the factor which determines latent and sensible heat fluxes, wind strengths and directions (by causing thermal gradients in air masses).

Solar radiation enters the top of the Earth's atmosphere as the extraterrestrial shortwave radiation flux. Some of this radiation is returned to space by being

backscattered by air, reflected by clouds and the Earth's surface. The rest is absorbed by gases in the atmosphere, clouds and by the Earth's surface (Sturman and Tapper, 2006). The Earth's surface shortwave radiation balance is:

$$K^* = K \downarrow + K \uparrow \quad 2.1$$

where K^* is net shortwave radiation flux density, $K \downarrow$ is incoming shortwave radiation and $K \uparrow$ is outgoing shortwave radiation (which is defined as negative because it is a loss from the surface system). This term can only exist during daylight hours since the energy is derived from the sun. The absorption of shortwave radiation results in heating, where this energy is then emitted as terrestrial or longwave radiation (Sturman and Tapper, 2006). Longwave radiation is absorbed and emitted at the surface and in all layers of the atmosphere and is a very complicated process that occurs day and night. The surface longwave radiation balance is:

$$L^* = L \downarrow + L \uparrow \quad 2.2$$

where L^* is net longwave radiation flux density, $L \downarrow$ is incoming longwave radiation and $L \uparrow$ is outgoing longwave radiation (which is also defined as negative due to the loss from the system). The all-wave surface radiation balance is then:

$$R_n = K^* + L^* \quad 2.3$$

where R_n is the net all-wave radiation flux density. The Earth's surface is continuously losing energy by heating the air and by evaporating water which eventually releases its energy to the atmosphere when the water vapour condenses (Oke, 1987). At the scale of the Earth-Atmosphere system, all incoming radiation should equal outgoing radiation over long enough timescales. At short timescales the Earth's surface is usually either heating or cooling, depending on whether more or less radiation is leaving the surface in relation to that entering it (Oke, 1987).

The Earth's surface does not absorb all the energy arriving from the sun. Much is reflected back into the atmosphere and the rate at which the surface absorbs or reflects this energy is termed the surface albedo (α) (Sturman and Tapper, 2006). Albedo is calculated as:

$$\alpha = \frac{K \uparrow}{K \downarrow} \quad 2.4$$

Dark surfaces such as a wet organic soil have a small α (~0.05) (Sturman and Tapper, 2006 Table 2.2, pg 42) because most of the $K \downarrow$ is absorbed and heats the ground. Light-coloured surfaces such as snow have very large α (~0.40 – 0.95) so most of the energy is reflected away from the surface. Typical values of α for grass are often dependent on grass height but range between 0.16 – 0.26 (Sturman and Tapper, 2006 Table 2.2, pg 42).

2.2.1 The diurnal energy balance

A surface receives ($K \downarrow$ and $L \downarrow$) and reflects ($K \uparrow$) or emits ($L \uparrow$) radiation. The net radiation balance (Equation 2.3) results in a net surplus or deficit of energy at the surface. By day R_n is positive and is a surplus, while at night it is negative and is a loss from the surface. The daytime surplus radiation is converted to heat energy and is transported away from the surface as either the conductive soil heat flux (G), or as the convective fluxes sensible heat (H), or latent heat (λE) (Figure 2.1):

$$R_n = H + \lambda E + G + (P_s + \Delta S) \quad 2.5$$

When plants are growing a photosynthetic energy flux, P_s , is also present however it is usually very small (up to 5%) and usually prominent under a large amount of active vegetation with low-light conditions (Hillel, 2004). ΔS is a storage change component which should be equal to zero over a diurnal timescale or larger.

During the night time deficit when R_n is negative, the energy is made up by any or all of the flux components, providing heat at the surface which is then converted to longwave radiation and lost from the surface system as $L \uparrow$ (Figure 2.1).

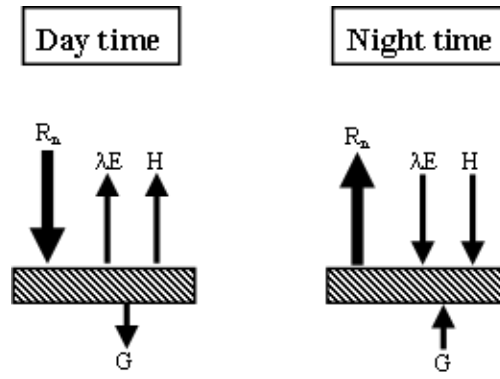


Figure 2.1 Typical proportions of energy transfers during daytime and night time (adapted from Oke, 1987).

The energy available for the division into H and λE at the lands' surface is given by $(R_n - G)$ so the fluxes are at their maximum when R_n is large and G is small (Sturman and Tapper, 2006; Gavilan and Berengena, 2007). The partitioning of available energy into H and λE is controlled mainly by the availability of water at the surface. If water is available, either for evaporation or transpiration, then more energy is likely to be partitioned as λE than H (Sturman and Tapper, 2006). The Bowen ratio, β , is the ratio of H to λE which is a useful diagnostic for identifying the partitioning of energy at the surface:

$$\beta = \frac{H}{\lambda E} \quad 2.6$$

Under abundant water conditions, β is low (usually $\beta < 1$), while during drier conditions, β is more likely to be higher ($\beta > 1$) due to more energy being partitioned into sensible heat, H , instead of latent heat, λE (Oke, 1987; Spronken-Smith, 2001; Sturman and Tapper, 2006). Energy partitioning is highly dependent on plant, as well as soil and climate factors. For instance, Campbell and Williamson (1997) found daytime $\beta > 3$ in a peat bog where soil moisture was not limiting, but plants had extremely constrained transpiration rates and a dense, largely dead, canopy acted as a mulch preventing evaporation from the moist peat.

2.3 Evaporation

Evaporation is the process by which energy is used for the vaporisation of water, changing the phase of water from a liquid to a gaseous state. For this reason we consider both interception loss, evaporation from bare soil and transpiration to be components of evaporation. Evaporation is the process by which water enters the atmosphere. When this water condenses, latent heat energy is released and precipitation is eventually formed. This section discusses the principle factors that affect the rate of evaporation, how it can be measured and estimated, and finally some correcting techniques needed when water stress conditions exist.

2.3.1 Factors affecting evaporation

Evaporation is a process essentially driven by energy from the sun, but this does not mean it is always the main driver affecting the rate of evaporation. There are several primary factors which influence evaporation foremost as well as secondary factors which could also influence the rate of evaporation at a finer scale (Kelliher and Jackson, 2001). Studies have been done to determine which factors are most influential (Law *et al.* 2002), however the degree to which a certain driver effects evaporation will also depend on the biome in which it is being measured (Zhang *et al.* 2007), making it difficult to develop a universal evaporation model.

Much literature discusses ‘potential’ and ‘actual’ evaporation, the former being the maximum evaporation which would occur if no factors other than energy supply were limiting the evaporation rate (Baumgartner & Reichel, 1975; Zhou *et al.* 2008), a function of solar radiation, vapour pressure deficit and wind speed (McConchie, 2001). Conversely, ‘actual’ evaporation is the amount of water evaporated with all other controls influencing it, a function of atmospheric demand (including those factors listed above) as well as water availability, and crop coefficients (McConchie, 2001). There has been some contest over the relevance of using potential evaporation in hydrological models (McNaughton, 1976; McNaughton *et al.* 1979), however it is often still used.

The two primary factors which dominate the rate of evaporation are the availability of energy from the sun or the environment (Zhang *et al.* 2007), and the availability of water, either at the surface or in the soil (Rodriguez-Iturbe, 2000). The amount of water available for evaporation will be dependent on the amount of rainfall that has previously occurred, the capacity for vegetation to intercept rainfall, and the amount of water in the soil layer that is accessible to plants. If no water is present at a surface, no interception evaporation can occur, however a plant will still lose water via transpiration, given sufficient access to soil water.

This is where the vegetation type becomes important. Plants have the ability to control the amount of water they transpire to the atmosphere via stomata. These are essentially pores in their leaves which can open or close to allow water to be released back into the atmosphere (Kelliher and Jackson, 2001). In hydrological terms, the rate at which plants control their water loss is determined by canopy (ecosystem scale) or stomatal (leaf scale) resistance, meaning that there is a resistance to water vapour flow out of the leaves (McNaughton and Jarvis, 1991; Daamen and McNaughton, 2000).

The structure of the vegetation also affects turbulence which can influence evaporation rates. There is a thin layer of static air just above any evaporating surface within which water vapour transfer is via molecular diffusion and is inefficient in comparison to the transport of water vapour in surrounding turbulent air (Kelliher and Jackson, 2001). This still air layer decreases in thickness with windier conditions and turbulence; hence the roughness and height of vegetation from a surface will cause turbulence and will have an impact on evaporation rates (Kelliher and Jackson, 2001). The aerodynamic resistance describes the efficiency of turbulent transport processes, and when coupled with canopy resistance provides a model for vapour transport from vegetated surfaces to the atmosphere (Monteith and Unsworth, 1990).

Because evaporation is the movement of water from a moist surface into the drier air above, the rate at which evaporation occurs is dependent on the vapour pressure of the air at the surface compared to that of the air above, and how easily the water vapour can be transported from one to the other (dependent on

turbulence) (Scotter and Kelliher, 2004). When the vapour pressure at the evaporating surface is larger than that of the overlying air, then evaporation can occur freely. But when vapour pressures between the surface and the overlying air become equal (i.e. the air becomes saturated), no gradient exists and evaporation ceases (Scotter and Kelliher, 2004).

2.3.2 Evaporation measurement

There is a difference between evaporation measurement and evaporation estimation but the distinction is sometimes unclear. Measurement uses sensors, instruments and gauges to quantify evaporation, or the rate of flow of water vapour or equivalent latent heat between the surface and the atmosphere. This is in contrast to estimation methods that rely on factors that are likely to be driving evaporation and are most often in the form of equations which use various climate variables to estimate the potential or actual evaporation, some of which can be fairly accurate but often have shortcomings (Allen *et al.* 2005), and in all cases should be validated against measurements of actual evaporation.

Shuttleworth (2007) describes how evaporation measurement techniques have progressed through the last 40 years, from using the ‘aerodynamic method’ and energy or water balance methods in the 1960’s and 70’s through to the eddy covariance (or eddy correlation) method. All these methods are still used but eddy covariance has been further developed to produce more accurate and instantaneous data with more durable sensors suitable for permanent installations (Baldocchi, 2008).

Today there are several measurement methods which are utilised, all of which require careful application in ‘real world’ situations to be able to minimise critical assumptions and error, and comparison with other methods to ensure accuracy may be required. These include lysimeters which measure changes in weight of a soil column due to evaporation (see Section 2.3.2.2), sap flow measurements (Wilson *et al.* 2001), catchment water balances, and micrometeorology, including Bowen ratio and energy balance (BREB) and eddy covariance. There are also biological methods available which measure transpiration rates of plants to

determine the various components of evaporation (Burman and Pochop, 1994) which can be helpful when determining effect of landuse changes on hydrological processes. The rest of this section describes the major measurement and estimation methods.

2.3.2.1 Eddy covariance and energy balance closure

The eddy covariance method measures fluxes of energy and mass (usually H₂O and CO₂) at the hectare or larger scale (ecosystem scale) by evaluating the characteristics of wind eddies as they pass through a set of sensors, in particular; air temperature, three dimensional wind speeds, vapour density and CO₂ density (Baldochhi, 2008). It seems the first ‘eddy covariance’ system was primarily based on an instrument developed by Swinbank (1951) and later described and tested by scientists such as Dyer and Maher (1965) called the ‘Evapotron.’ Its design involved sensors such as wet and dry bulb resistance thermometers and a heated wake anemometer along with a wind vane for wind direction measurements (Dyer and Maher, 1965). Technology has progressed these instruments into much more accurate and reliable flux measuring devices which can now be used in most weather conditions and for much longer time periods without constant supervision.

Wilson *et al.* (2001) compared the eddy covariance method for measuring evaporation to several other methods including sap-flow, soil water budget, and catchment water balance for a forest and found that the eddy covariance method had reasonably good agreement with all these other methods of measurement. The authors also pointed out several weaknesses of the eddy covariance system which included; not knowing the exact shape and extent of the region or area being measured by the system, having little confidence or having difficulty with data for low wind conditions, and not being able to directly account for advection in non-uniform landscapes which limits its use in many locations (Wilson *et al.* 2001).

Missing data is recognised as a universal issue with eddy covariance time series data (Falge *et al.* 2001) and gap-filling is required for many reasons including sensor spikes, deficiencies in frequency capture due to the inevitable spatial separation of instruments (Beyrich *et al.* 2006), and instrument malfunction due to poor weather or certain meteorological conditions, resulting in the need to reject some data (Falge *et al.* 2001). Weather conditions which can often result in invalid data include low wind speeds leading to insufficient mixing; rain impacting on sensors can cause λE to spike erratically; and water or dew on sensor windows can obstruct accurate measurements.

Because it has been found that eddy covariance will often underestimate energy fluxes (either sensible heat or latent heat or both) by 10–30% (Twine *et al.* 2000; Wilson *et al.* 2002), many correction techniques have been suggested. For example, Villalobos (1997) suggests using a second thermocouple (temperature sensor) with the standard sensors to calculate the underestimation of sensible heat which can then help account for the error of the latent heat flux.

It became evident that the eddy covariance technique may underestimate energy fluxes, leading to a lack of closure of the energy balance (Dugas *et al.* 1991). This means that the sum of sensible and latent heat fluxes (λE and H) is less than the available energy ($R_n - G$) if energy conservation was true (Twine *et al.* 2000).

$$R_n - G = H + \lambda E \quad 2.7$$

Energy balance closure is often lacking by up to 30% (Twine *et al.* 2000; Wilson *et al.* 2002; Aires *et al.* 2008) so by ‘forcing’ energy balance closure (adjusting the magnitude of λE and H), this underestimation can be crudely eliminated. Twine *et al.* (2000) first of all tested the accuracy of net radiation and soil heat flux measurements and concluded that their combined uncertainty was only about 10%. Therefore the sensible and latent heat fluxes are the two terms of significant error for energy balance closure. Twine *et al.* (2000) described two methods of energy balance closure: (1) *residual- λE closure* which assumes that the sensible heat flux is measured correctly so the latent heat flux is adjusted as the residual, or (2) *Bowen Ratio closure* which assumes that the ratio $\beta = H/\lambda E$ is measured correctly so H and λE are increased proportionately. Twine *et al.* (2000) suggested the use of the Bowen ratio closure method because they found no evidence to

suggest that one heat flux is underestimated more than the other. This assumption is re-enforced by Campbell and Nieveen (in prep), who found that the Bowen Ratio closure method best matched the estimated evaporation for pasture near Hamilton, New Zealand, when compared to the Penman-Monteith (FAO₅₆, Allen *et al.* 1998), while the residual- λE closure method resulted in a significant overestimation of evaporation. Oncley *et al.* (2007) proposed that a lack in energy balance closure is not due entirely to instrument error but that other energy terms are not taken properly into account. Horizontal and vertical advection may also play a critical role in providing energy for evaporation and Oncley *et al.* (2007) described how advection can be calculated. However they did suggest several improvements that could be made to their calculations and data to result in a more accurate data set such as more sensors to measure profiles, documenting the day time boundary layer, or 3-D mapping of wind, temperature and humidity. They also mentioned they had a lack of information of upwind fluxes from all wind directions. Foken (2008) suggested the lack of energy balance closure was due to a scale problem in which eddy covariance measures the energy components of small wind eddies, however larger eddies in the lower atmospheric boundary layer which do not make contact with the Earth's surface also make a contribution to the energy balance at the surface itself. These exchanges of larger eddies can currently only be measured at a large cost using such systems as scintillometers or airborne sensors, so Foken (2008) recommended the use of the Bowen ratio closure method described by Twine *et al.* (2000) as a temporary method of achieving closure.

2.3.2.2 Soil moisture balance via lysimeters

A lysimeter is a water balance measurement device which helps hydrologists gain an understanding of the various components that make up the water balance. A measure of evaporation can be calculated using a mass balance approach which has often been used as a way of ground-truthing other methods of evaporation measurement (Allen *et al.* 1991). A water balance can be formulated for a contained soil volume using the equation:

$$\Delta S = P + E + Q \quad 2.8a$$

Therefore:

$$E = \Delta S - P - Q \quad 2.8b$$

Where ΔS is net change in stored soil moisture, P is precipitation, E is evaporation, and Q is liquid water discharge (where E and Q are both defined as negative due to the loss of water from the lysimeter volume) (Figure 2.2).

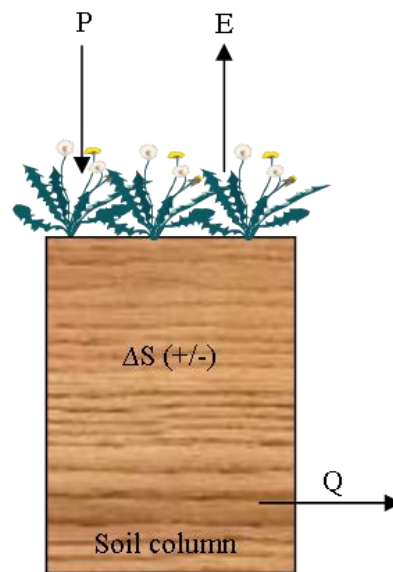


Figure 2.2 Soil moisture balance using a lysimeter.

This type of equation may incur some errors due to the assumption that significant vertical exchanges are absent, i.e. no infiltration or interaction with the water table (Oke, 1987).

Measuring the P component of the soil moisture balance is done using one or more rain gauges, which can often result in underestimations of rainfall due to wind turbulence around the gauge rim (Ward and Robinson, 1999), but is an error that cannot be reduced in many instances. Q is a measure of discharge of water that exits out of the base of the lysimeter (surface water discharges are assumed not to occur). ΔS is the more difficult measure, however this is where lysimeters become the most useful.

Many types of lysimeters exist. Essentially they are a tank in which a mass of soil contains growing plants and is isolated from the surrounding soil (Burman & Pochop, 1994). They can range in size from tens of centimetres in diameter up to several metres in diameter. The depth of lysimeters varies and usually depends on the rooting depth of the plants growing within them.

The types of lysimeters can be grouped into three classifications according to Burman and Pochop (1994);

- *Weighing* – directly measures a weight change which is converted to a change in stored water content. Many methods are available but the most commonly used ones have an automatic load cell connected to a data logger or a manually weighed soil core.
- *Non-weighing* – these rely on soil water budgets compiled from measurements of changes in soil moisture content.
- *Drainage* – measures outflows from a lysimeter to calculate evaporation via a water balance equation over periods of time that are long enough to assume ΔS is zero.

To get the most precise measure of evaporation, the soil structure inside the lysimeter should closely resemble that of the area being studied and should therefore consist of intact cores (Grimmond *et al.* 1992).

Campbell and Murray (1990) used a large weighing lysimeter to measure evaporation for tussock grassland in Otago, New Zealand. Evaporation was partitioned into interception loss and transpiration and hourly data were summed to give daily and monthly totals. Similarly, Klocke *et al.* (1990) conducted a study in which lysimeters were used to measure evaporation in conjunction with the catchment water balance method in which they found that the lysimeter method for measuring evaporation measured significantly higher values than the catchment water balance method. It was also discovered that mini-lysimeters, weighed daily, measured evaporation more accurately than the automatic weighing lysimeters (Klocke *et al.* 1990). In the study by Grimmond *et al.* (1992), miniature weighing lysimeters were used and the study concluded that, on a short-

term basis, these lysimeters resulted in fairly accurate and reliable evaporation measurements when compared to eddy covariance measurements.

After reporting several success stories of using lysimeters, we must remember that science is not so simple and there are many factors which need consideration when conducting an experiment such as using lysimeters and the water balance. Allen *et al.* (1991) report on many of the environmental requirements when using lysimeters and these will be briefly summarised now:

- The soil and vegetation of the lysimeter should closely imitate that of the surrounding environment since they are being used to characterise evaporation for large areas.
- The most common mistake when using lysimeters is miscalculating the correct evaporating area of the lysimeter when computing evaporation. The area should be calculated using the area including the lysimeter rim, but not including the area from the outside of the lysimeter to the surrounding ground, see Figure 2.3.

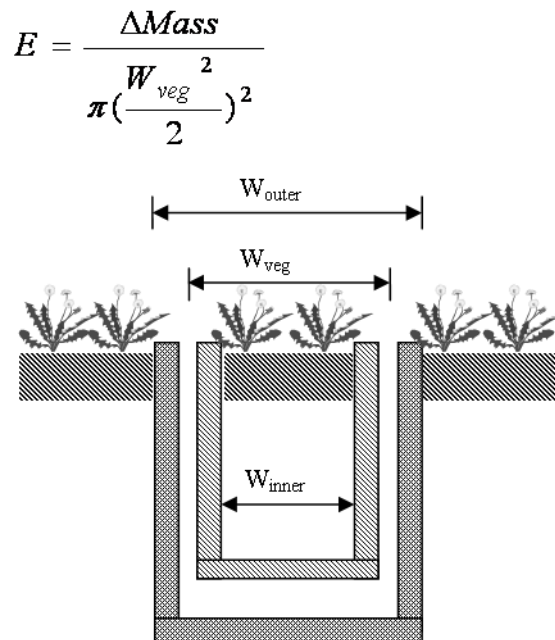


Figure 2.3 Determination of evaporative and vegetative area (adapted from Allen et al. 1991).

- There is a possibility that the lysimeter rim could reflect radiation to the vegetation which could result in micro-advection, causing a less accurate measure of evaporation.
- If the rim is too tall relative to the vegetation height, air mixing could be affected or the radiation balance may also be disturbed.
- The effect of plants leaning into or out of the lysimeter could result in a miscalculation of evaporation.
- A clothesline effect¹ could be created if plants growing in a lysimeter grow at a different rate to the vegetation surrounding the lysimeter.

These are all possible sources of error and should be minimised as best as possible when using lysimeters to measure evaporation in the field.

Dugas and Bland (1989) conducted a study to determine if lysimeter size affected the accuracy of evaporation measurements using small, medium and large lysimeters. They concluded that evaporation totals were often significantly different when leaf area index (LAI) was not accounted for due to increased variability in LAI with a reduction in lysimeter size, however as long as an adjustment was made for this variable, total rates were not significantly different (Dugas and Bland, 1989). Grimmond *et al.* (1992) also found that mini-lysimeters were fairly accurate, however only on a short-term basis since the study did not operate longer, and suggestions were also made that it is important to ensure the depth of lysimeters is sufficient to encompass the rooting depth for the crop being studied. A useful experiment was carried out by Daamen *et al.* (1993), who set out to find errors that may be associated with lysimeter size (both diameter and depth) and age. They found that the diameter of a lysimeter was not a significant source of error, however the depth of a lysimeter could cause error after an extended time period of several days. The time soil cores are collected may influence evaporation rates directly after a rain event, but after 2 or more days this no longer has an effect (Daamen *et al.* 1993).

¹ A clothesline effect is created when a crop or forest is bordered with a different landuse type which may have warmer and drier ground. The air entering the crop from that edge is warm and dry and will therefore increase heat supply and change the vapour pressure gradient, enhancing evaporation rates and depleting soil moisture at the crop stand border. This results in conditions being different to those further inside the crop (Oke, 1987).

2.3.3 Estimating evaporation

Over the past 50 years models have been developed which have led us to fairly accurate methods of estimation, such as the FAO₅₆ Penman-Monteith or the Priestley-Taylor equations. One of the first physically-based equations developed was the Penman equation which amalgamated the energy balance and Dalton equations to determine an evaporation rate using limited amounts of climatic data (Kelliher and Jackson, 2001), which was eventually developed into the Penman-Monteith equation. Before this however a model produced by Priestley and Taylor (1972) simplified the Penman equation to include only energy and temperature factors and an empirical adjustment (Shuttleworth, 2007):

$$E_{PT} = \alpha \frac{s(R_n - G)}{\lambda(s + \gamma)} \quad 2.9$$

Where α is a dimensionless constant often set to 1.26 (Priestley and Taylor, 1972; McNaughton, 1976; Kelliher and Jackson, 2001; and Shuttleworth, 2007), which allows for advection to be accounted for (McNaughton and Jarvis, 1983). s is the slope of the saturation vapour pressure versus temperature curve ($\text{kPa } ^\circ\text{C}^{-1}$) and γ is the psychrometric constant. When $\alpha = 1$, E_{PT} is equivalent to the so-called equilibrium equation:

$$E_{Eq} = \frac{s(R_n - G)}{\lambda(s + \gamma)} \quad 2.10$$

The Priestley-Taylor equation is therefore simply:

$$E_{PT} = \alpha E_{Eq} \quad 2.11$$

The addition of the dimensionless α value in Equation 2.9 and 2.11 attempts to account for other sources of energy which may affect the evaporation rate at the given location. Because E_{Eq} is temperature dependent (via s), Kelliher *et al.* (2001) explain that with a global average temperature of 15°C E_{Eq} will be within 10% of actual evaporation (E), however when temperature, R_n and λ are measured, a more accurate evaporation rate can be estimated.

The Penman-Monteith equation is a further development of the Penman equation which uses resistances to describe surface controls on vapour and heat transfers, providing a physically realistic model of evaporation, defined as (McNaughton and Jarvis, 1983):

$$E_{PM} = \frac{s(R_n - G) + \rho c_p D / r_a}{s + \gamma(1 + r_c / r_a)} \quad 2.12$$

Where ρ is density of air (kg m^{-3}), c_p is specific heat of air ($\text{J kg}^{-1} \text{ } ^\circ\text{C}^{-1}$), r_a is aerodynamic resistance and r_c is canopy resistance (both s m^{-1}). Equation 2.12 requires many data inputs and these are not often measured at all sites, which highlights the need to develop a more simplistic version, while still maintaining the accuracy of the model. Models have been developed based on these earlier equations, such as the FAO₅₆ Penman-Monteith equation, which are often used in global climate models to find rates of evaporation when climate data are available.

Many studies have been done using lysimeter or eddy covariance data to compare these and various other evaporation models both around the world (Sumner and Jacobs, 2005; Lopez-Urrea *et al.* 2006a and 2006b; and Paco *et al.* 2006) and in New Zealand (Clothier *et al.* 1982; McAneney and Judd, 1983).

2.3.3.1 FAO₅₆ Penman-Monteith method

The FAO₅₆ Penman-Monteith method is a further development of the original Penman-Monteith equation. Because evaporation data are often required for project planning or irrigation scheduling in agriculture, guidelines were developed and published in an earlier FAO publication which have now been developed further to allow the spatial and temporal comparison of evaporation for crops to be compared and related (Allen *et al.* 1998). The model was developed by a number of scientists and organisations and is now recommended as the standardised method for calculating reference crop evaporation by the Food and Agriculture Organisation of the United Nations. The FAO₅₆ Penman-Monteith reference crop evaporation is calculated as:

$$E_o = \frac{0.408s(R_n - G) + \gamma \frac{900}{(T + 273)} u_2 D}{s + \gamma(1 + 0.34u_2)} \quad 2.13$$

Where E_o is reference crop evaporation (mm day^{-1}), T is mean daily air temperature at 2 m height ($^{\circ}\text{C}$) and u_2 is wind speed at 2 m height (m s^{-1}). ‘Reference crop’ is defined by Allen *et al.* (1998) as a grass crop with an assumed height of 0.12 m, a fixed surface resistance of 70 s m^{-1} and an albedo of 0.23 where the surface is well-watered, actively growing and completely shading the ground.

This equation has been tested on several different agricultural land uses such as a peach orchard in Portugal by Paco *et al.* (2006), who compared the FAO₅₆ model results to lysimeter and eddy covariance measurements and found that when crop coefficients were used as an additional adjustment the equation made adequate estimations of evaporation. A crop coefficient will adjust the evaporation estimate according to the crop being measured when the crop characteristics do not match those of the reference crop.

A study conducted by Ventura *et al.* (1999), in which various Penman-Monteith equations were compared to lysimeter measurements and other estimation equations, on an irrigated pasture, found that all Penman-Monteith equations (including FAO₅₆) were most accurate. DehghaniSanij *et al.* (2004) also found that the Penman-Monteith model produced the most accurate estimates in a semiarid environment over irrigated alfalfa crops, while the Penman model was best for evaporation estimates in a humid temperate environment when compared to lysimeter measurements.

Lopez-Urrea *et al.* (2006a, 2006b) tested five different evaporation equations against lysimeter measurements in a semiarid climate in Spain, and found that in both high and low evaporative demand conditions, the FAO₅₆ Penman-Monteith equation was the most accurate, while in another paper they reported that FAO₅₆ Penman-Monteith performed very accurately when compared to lysimeter measurements in a semiarid environment in Spain.

Berengena and Gavilan (2005) evaluated the use of estimation methods in advective and semiarid environments. They discovered that many of the earlier FAO recommended equations often overestimated evaporation by 19% on average and when a correction factor was applied to several of the models, the values were even worse, being corrected in the wrong direction. They found that the Priestley-Taylor model tended to underestimate evaporation by an average of 23% however when a locally adjusted α value was calculated, results improved considerably (Berengena and Gavilan, 2005). When Berengena and Gavilan (2005) tested the FAO₅₆ Penman-Monteith equation, using carefully measured variables, the accuracy of the model was good with a slight underestimation of only 7% on average, and only a 2.9% underestimation on average when hourly data were used.

This equation has also been tested in New Zealand via comparisons to other estimation methods in which Scotter and Heng (2003) found that the FAO₅₆ calculation would give the most realistic estimates of evaporation when compared to evaporation values calculated using the Penman equation using values from around New Zealand. It is rare to find New Zealand studies in which measured evaporation is compared to estimation methods. Campbell and Nieveen (2005) undertook a study to compare eddy covariance measurements with the Priestley-Taylor and Penman-Monteith models and found that the Priestley-Taylor method underestimated evaporation in winter and overestimated evaporation in summer, even when no soil moisture deficit was present. They found that the α term varied between 1.0 and 2.0 on a seasonal basis. The FAO₅₆ model was found to perform well during all seasons due to its inclusion of all relevant controls on evaporation (Campbell and Nieveen, 2005).

2.3.4 Correcting for soil water stress conditions

The availability of soil moisture plays a key role in determining evaporation rates. Soil moisture can be available for evaporation in two ways, either via evaporation from the soil surface, or via transpiration through the stomata of plants. The

importance of understanding how drought (or soil moisture stress) conditions are affecting evaporation rates is becoming more recognised in the scientific community and several recent papers have reported on studies undertaken over different types of landuses (Hunt *et al.* 2002; Teuling *et al.* 2006; Alfieri *et al.* 2007; Aires *et al.* 2008; and Ryu *et al.* 2008). Alfieri *et al.* (2007) determined that water availability was the most dominant control on λE when soil conditions were dry. Below a threshold soil moisture value, plants and crops become water stressed (Allen *et al.* 1998) and growth rates decrease or cease completely. When this occurs, net radiation is no longer the sole driving force of evaporation so evaporation estimation methods and equations need adjusting to avoid over-estimation of evaporation rates in such conditions. The study done by Aires *et al.* (2008) describes how soil water deficits, in combination with a lower than usual leaf area index resulted in lower net radiation values during dry periods, due to a lower albedo which may also play a small role when estimating evaporation rates using climatic variables and equations. To determine the threshold below which evaporation is affected by soil moisture content, Aires *et al.* (2008), following the method of Baldocchi *et al.* (2004), found that when volumetric soil moisture content was below 13 – 14% evaporation rates dropped substantially, similar to the levels found by Baldocchi *et al.* (2004).

It is evident that soil moisture does control evaporation rates during drought conditions so how can this be accounted for using methods of estimation that do not have a soil moisture variable incorporated? The FAO₅₆ evaporation equation (Allen *et al.* 1998) has an adjustment factor for water limiting conditions:

$$E_{o(\text{adj})} = K_s K_c E_o \quad 2.14$$

Where K_s and K_c are the water stress and crop coefficients respectively. The methods used to measure or calculate these components can be found in Allen *et al.* (1998) and in Appendix A. K_c can vary depending on the type of crop but for a rotationally grazed pasture it varies between 0.40 and 1.05 (Allen *et al.* 1998, Table 12) which differs due to wind speeds, relative humidity and plant height. Little information and data exist on how well this correction formula by Allen *et al.* (1998) works for water stressed crops. Most studies that are conducted in arid climates are irrigated crops or orchards (Paco *et al.* 2006, Lopez-Urrea *et al.*

2006a, 2006b) so soil water stress is usually never an issue and estimation methods such as this have not been compared with measurements for drought conditions. Because grazed pasture is a significant landuse type in New Zealand, particularly non-irrigated, which is often subject to seasonal drought, it is important to be able to model evaporation accurately if measurements cannot be made directly.

2.4 Pasture – the energy balance and evaporation

In the context of comparing water use by pasture with various other landuses (and possibly the changing of a landuse) the primary factors to note are the differences between the vegetation types. Pasture has much lower interception abilities than a forest due to obvious canopy structural differences as well as surface roughness affecting wind velocities and turbulence. The colour of pasture is much lighter than forest, resulting in a higher albedo (more radiation reflected) and hence a lower net radiation value (Oke, 1987), and rooting depth differences mean that forests can source water from much deeper in the soil profile than pasture, which results in forests being less affected by drought.

The relative amounts of water evaporated via either transpiration or interception depends on the time the canopy is wetted by rain. Transpiration is usually higher for pasture than forests however forests have the ability to intercept much more rain which can therefore become a much larger evaporative component than that for transpiration (McNaughton and Jarvis, 1983). If the canopy is kept wet by regular small storm events, much more interception evaporation occurs than transpiration. However McNaughton and Jarvis (1983) illustrate that net radiation alone cannot explain rates of transpiration and interception evaporation but that advection of energy may supply large amounts of energy, especially for forests in steep or mountainous terrain.

Rosset *et al.* (1997) studied changes in radiation and energy balances with changes in altitude for pasture sites, but found that, on average, these changes

were very small. Fong (2001) conducted a study to see if slope or aspect had an effect on energy availability and evaporation for pasture. The study found that although radiation receipt varied with different slopes and aspects (north and south), evaporation rates did not show the same trend. This is thought to be due to local advection which acted to neutralise the differences in energy availability (Fong, 2001).

Some studies have been done in New Zealand to find the water regimes of tussock grasslands (Campbell, 1989; Campbell and Murray, 1990), various types of forest (Stewart, 1977; Pearce and Rowe, 1979; Pearce *et al.* 1980), and how a change in vegetation type from grassland to forest or vice versa can affect the hydrology and evaporation rates of a catchment (Fahey and Watson, 1991; Fahey and Jackson, 1997) which have all helped to develop a good understanding of evaporation rates and hydrological processes for different landuse types in New Zealand.

Not many studies have been carried out in New Zealand comparing methods of estimation to measured evaporation, and those that have been done have been short-term studies. Clothier *et al.* (1982) compared the Penman equation and the Priestley-Taylor equation with BREB evaporation measurements, and found that both equations were accurate. Clothier *et al.* (1982) recommended the use of the Priestley-Taylor model because it is simpler and requires less data inputs with an adequate evaporation result. A more recent study by Scotter and Heng (2003) simply assessed the accuracy of the FAO₅₆ Penman-Monteith method and suggested that it will give the most accurate estimates of evaporation for the time period they reviewed although they didn't have measured evaporation rates against which to compare their data.

2.4.1 New Zealand's maritime environment

In some situations, evaporation may exceed the net radiation available for evaporation. In these situations advection is most likely playing a role in providing extra energy for evaporation (Calder, 1990), either on a local or a larger

scale. Because New Zealand is surrounded by a fairly warm sea, sensible heat energy can be carried inland by winds (Kelliher and Jackson, 2001) which can provide energy for evaporation when net radiation is low (i.e. during rainfall events or night time), however during summer these temperature differences usually disappear or reverse so advection is not much of a contributor to evaporation (Scotter and Kelliher, 2004). Oncley *et al.* (2007) have attempted to calculate the energy made available via horizontal advection with some success but suggest more measures can be taken to develop a more accurate and reliable method, while Figuerola and Berliner (2005) also concluded that the lack of energy balance closure is due primarily to advection effects. No studies have been done in New Zealand to find how significant advection may be, however it is becoming clear that it is an important concept to consider when studying evaporation for a specific landuse.

3 Methods and site description

3.1 Introduction

First a site description will be provided, describing the location of the study, as well as climate, soil properties and hydrology of the area. This is followed by a description of the instrumentation used during the study and any associated errors that may have occurred. A detailed description of the data handling and processing techniques is provided, including corrections that were applied to raw measurements and the procedures used when data were error-prone or missing altogether. The data used for estimation models is briefly outlined and the soil moisture adjustment method is discussed. Finally, the method used to define the spatial area associated with flux measurements is described.

3.2 Site description

3.2.1 Scott Farm

Scott Farm is a dairy farm owned and run by DairyNZ. It is run as a research farm for large scale farm systems trials. The farm is located approximately 7 km east of Hamilton (Figure 3.1) and has an area of 120 ha on which 340 cows are grazed, however this number varies depending on trials being undertaken (~3 cows/ha in the vicinity of the tower). The location of the instrument tower within the farm is shown in Figure 3.2.

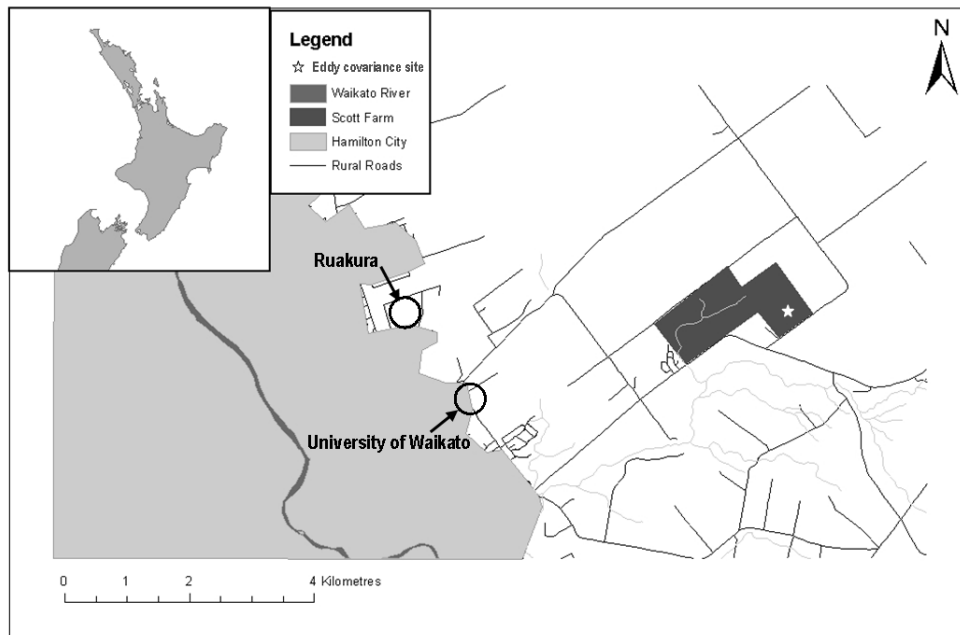


Figure 3.1 Map of East/South Hamilton and location of Scott Farm.

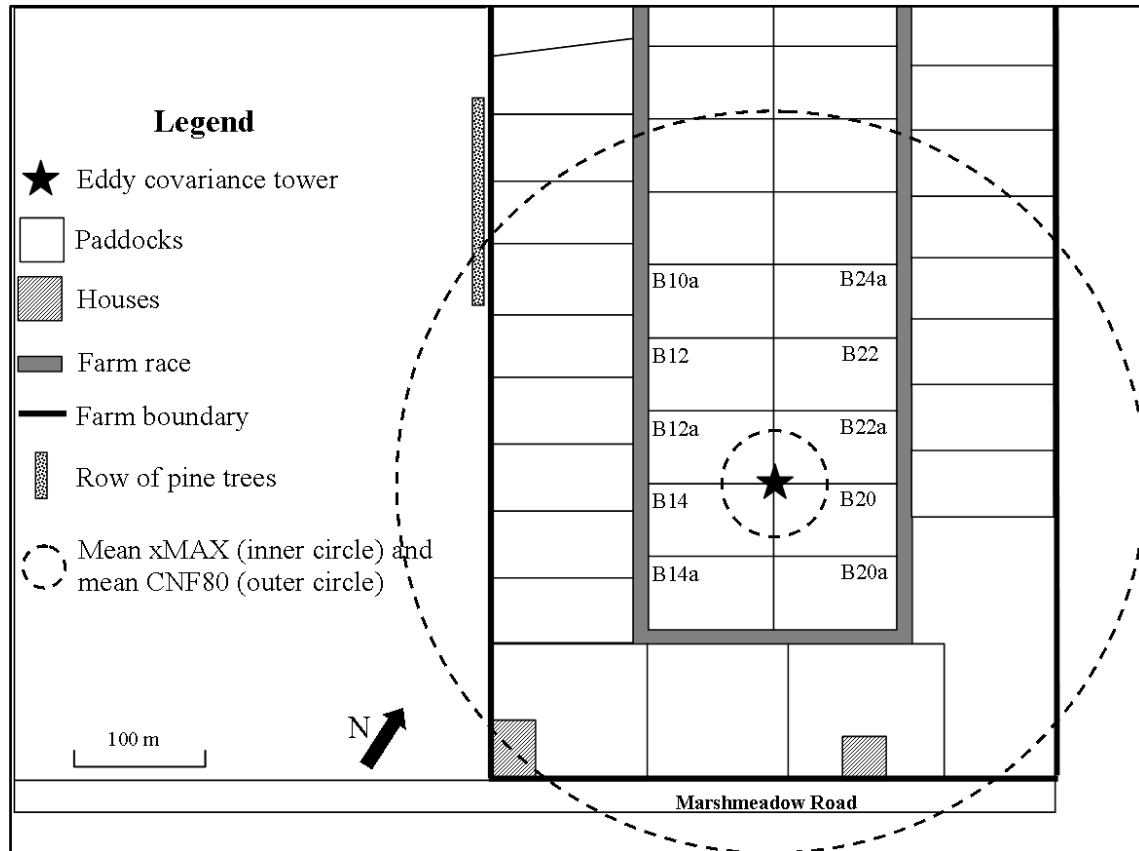


Figure 3.2 Scott Farm EC site and layout of surrounding paddocks.

3.2.2 Climate

The nearest climate station is at Ruakura which was relocated in 2005 but has rainfall records dating to 1906 and is situated 6 km northwest of Scott Farm. Annual mean rainfall for Ruakura is 1166 mm and mean annual temperature is 13.7°C with average wind speeds for the last 13 years measured at 2.9 m s⁻¹ (NIWA climate database, accessed 4 September 2008). Figure 3.3 shows mean monthly rainfall for the last 40 years measured at the Ruakura climate station, with maximum and minimum monthly rainfall values indicated via the shaded area, and rainfall measured at Scott Farm and Ruakura during 2008 are also plotted. The first 3 months of 2008 had significantly lower rainfall than the 40 year rainfall averages. The driest recorded monthly rainfall for January over the last 40 years was recorded as 10 mm in 1970 while that measured at Scott Farm and Ruakura in 2008 for January was 4.8 mm and 4.2 mm respectively. The rainfall measured at Ruakura for January 2008 was also the least amount of rainfall recorded in the past 100 years, however when combining the measures for the period January, February and March, the year 1911 was the driest period on record for the area with a total rainfall of only 62.3 mm, while at Ruakura in 2008 rainfall was measured at 66 mm and at Scott Farm 91.4 mm for the same period. The discrepancy is caused by localised rainfall differences in the area such as the one that occurred on 14 April 2008 where 27.4 mm of rain fell at Scott Farm but only 7.8 mm fell at Ruakura. Two days later, on 16 April 2008, only 3 mm of rainfall fell at Scott Farm while 37 mm fell at Ruakura. Therefore most discrepancies are a result of single rainfall events that have a higher intensity at one site compared to the other. The winter months (Figure 3.3) have recorded higher than the 40 year average rainfall (at Ruakura) but do not reach close to the maximum extremes.

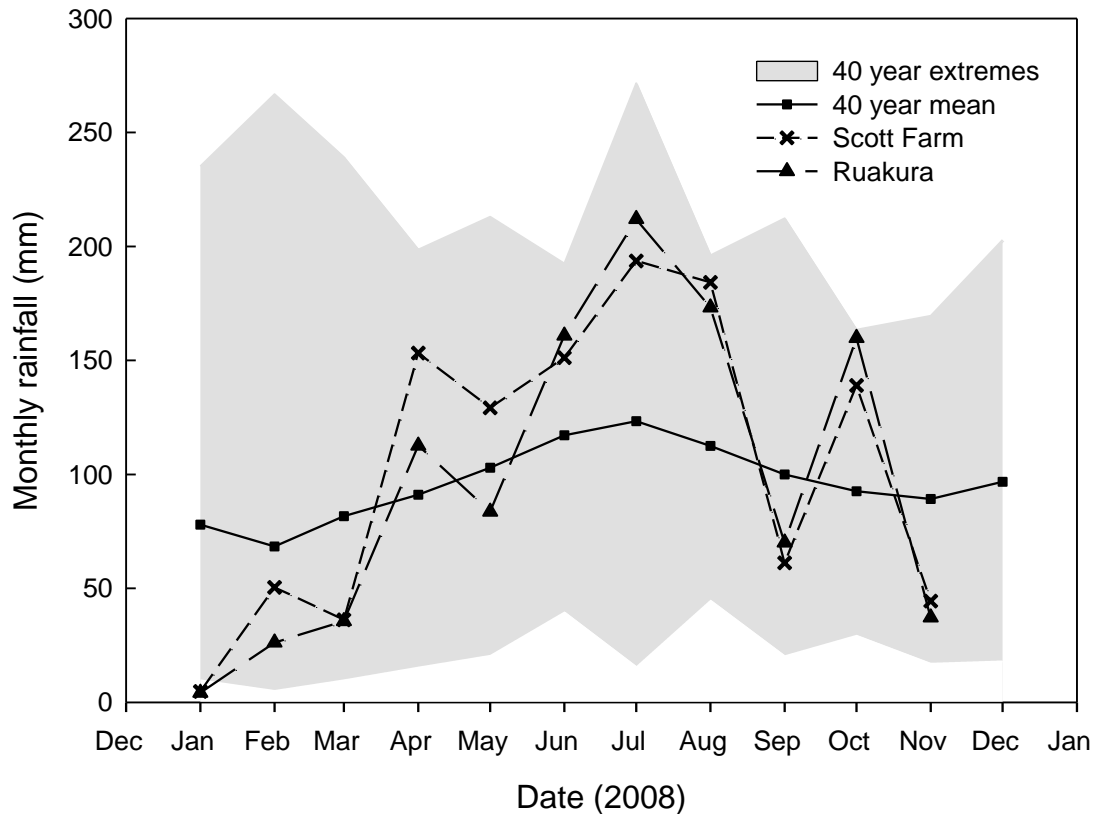


Figure 3.3 40 year (1947 - 2007) average monthly rainfall at Ruakura with maximum and minimum values shown as bounding shaded area and total rainfall at Ruakura for 2008 (data from NIWA climate database, accessed 29 September 2008) and 2008 Scott Farm rainfall.

Figure 3.4 shows daily rainfall and volumetric soil moisture content, and 15-day running means for net radiation (R_n) and air temperature for the year of measurements from 15 December 2007 to 30 November 2008 for Scott Farm. Seasonal patterns can be seen in which R_n is very high during summer reaching an average of approximately $17 \text{ MJ m}^{-2} \text{ day}^{-1}$ during January and February, then declining to a minimum of about $2 \text{ MJ m}^{-2} \text{ day}^{-1}$ during June and July, after which it began to increase again. Average daily air temperature ranged from about 20°C during summer to about 6°C in winter, after which it began increasing again with the onset of spring. Daily rainfall was sparse from the beginning of the measurement period until the beginning of April, with short and low intensity rainfall events occurring occasionally. From mid April, rainfall event frequency and magnitude increased. This can also be seen in the volumetric moisture content

data, where during the summer period values almost reached as low as 20%, with small increases with every rainfall event. Drying events are evident, the two major events occurring 22 December 2007 to 10 February 2008 and 5 March 2008 to 31 March 2008. After this time, rainfall frequency increased, providing the soil with sufficient water for θ_v values to reach an average of about 55% (Figure 3.4d).

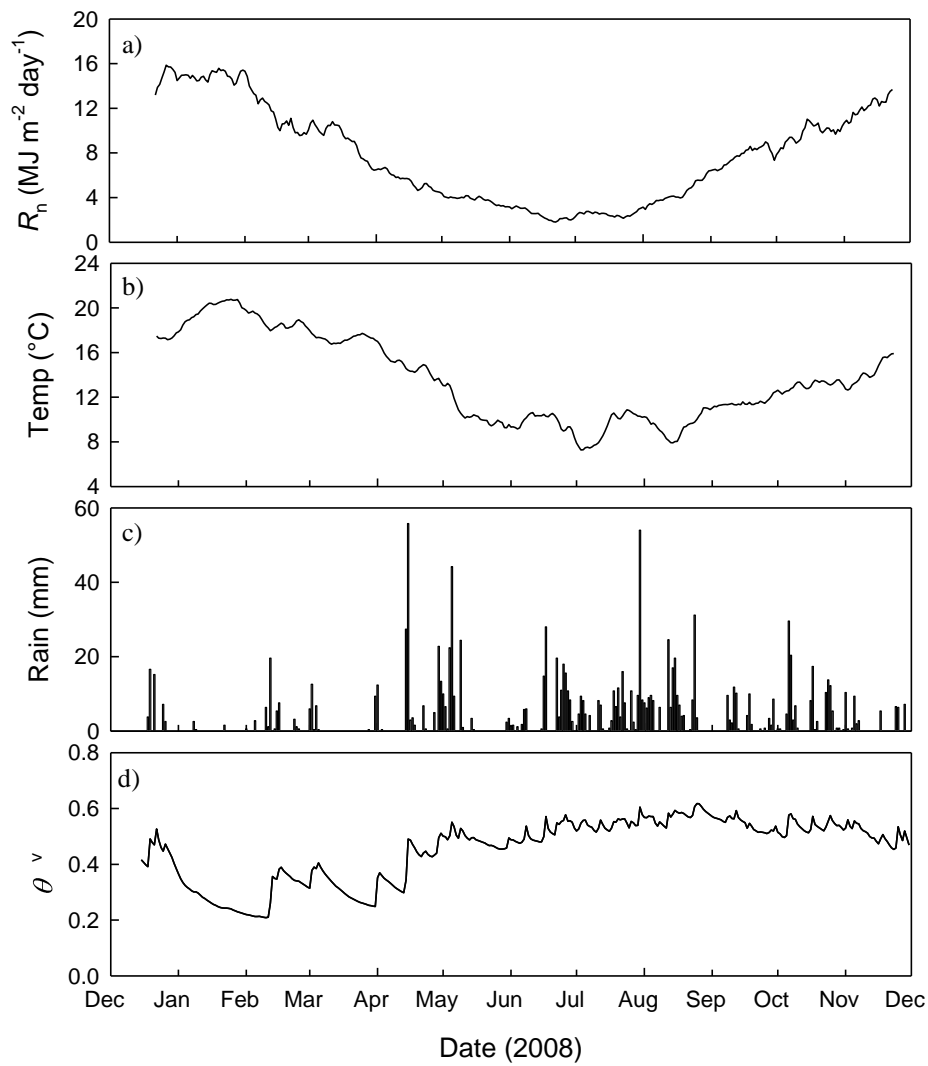


Figure 3.4 15-day running means of a) R_n , b) air temperature, and daily c) rainfall and d) volumetric moisture content.

3.2.3 Soil properties

Stiles (1998) undertook a study to develop a soil map for Scott Farm from which some generalisations can be made. The soil adjacent to the site of the present study is a Matangi silt loam which is classified as a typic orthic gley soil in the New Zealand soil classification (Hewitt, 1993). This type of soil is formed on layers of alluvium deposited by the ancestral Waikato River and may have both a humic and peaty topsoil while drainage is usually poor. Because drainage does not appear to be very restricted in the area of measurements, there is a possibility that soil types may cross into types such as the Bruntwood silt loam (typic impeded allophanic soil; Hewitt, 1993), which has also formed on layers of alluvium but is moderately well drained with a moderate permeability. Both types occur on flat to undulating land of the Hamilton plains (Singleton, 1991) and both have mottles present in deeper horizons indicating possible restrictions on drainage at some stage (Stiles, 1998). Due to scale and spatial restrictions, it can be difficult to determine which soil type is present at any given location. Table 3.1 gives the soil bulk density (calculated from seven core samples 7.5 cm * 10 cm in size) and the organic fraction at the field site, which are later used in the correction of the soil heat flux (G). The soil organic fraction was measured for the top 10 cm, using a bulked sample which was analysed using a LECO furnace (TruSpec, St Joseph, Mississippi) and corrected for moisture content.

Table 3.1 Soil properties measured at Scott Farm for seven cores each 7.5 cm by 10 cm in size taken 1 September 2008. Organic matter fraction determined from a bulked subsample.

	Mean	Std dev.
Dry bulk density	770 kg m ⁻³	17 kg m ⁻³
Organic fraction	0.14 kg kg ⁻¹	—

3.2.4 Local hydrology

Recharge of the groundwater in the area is primarily by infiltration of precipitation, and discharging via seepage into small streams which are dominated by the drainage pattern of the nearby Waikato River (Welten, 2005). The

groundwater flow in this region is in a westward direction and piezometric levels range from 35 – 45 m.a.s.l. \pm 1–2 m, so a similar direction and range is expected at Scott Farm (Welten, 2005). The Mangaonua Stream dissects Scott Farm and is the most dominant drainage destination of groundwater discharge for this study area.

3.3 Instrumentation

Most instrumentation was installed at Scott Farm on 15 December 2007. The site is powered by four 80-watt solar panels which charge a 440 A/hr 12 V battery bank connected to the data loggers. Most instruments are attached to a 3 m high, 40 cm triangular lattice tower, that is guyed and stable. A horizontal boom supporting eddy covariance instruments extends to the northwest. All other instruments are either attached to this tower at varying heights and orientations or are underground within a few metres of the tower. Figure 3.5 shows the installation of the field equipment while Table 3.2 includes a list of the instruments used, the model numbers and the height or depth at which they were deployed.



Figure 3.5 Installation of eddy covariance instrumentation.

Table 3.3 lists instruments that were deployed temporarily at Scott Farm and Table 3.4 gives a list of company details for the instruments used.

Table 3.2 Details of permanently deployed instruments at Scott Farm EC site.

Variable	Instrument/logger	Make & Model	Height/depth	Data logger connection
Data logger	CR3000	CSI	-	-
Data logger	CR10X(a)	CSI	-	-
3D wind velocity, sonic temperature *	3D sonic anemometer	CSI, CSAT3	2.84 m	CR3000
H ₂ O and CO ₂ concentration, density and atmospheric pressure *	Open path infrared CO ₂ /H ₂ O gas analyser, IRGA	LICOR, LI-7500	2.84 m	CR3000
Air temperature and vapour pressure	HMP 45A	Vaisala,	2.94 m	CR3000
Rainfall	Tipping bucket rain gauge	Hydrological Services TB5 0.2 mm/tip	0.4 m	CR3000 & CR10X(a)
Net radiation **	REBS	CSI Q 6.7.1	0.93 m	CR3000
Incoming solar radiation	Pyranometer	Kipp & Zonen SP Lite	3 m	CR3000
Quantum radiation		LI-COR, LI190SB	3 m	CR3000
Soil heat flux	REBS	CSI HF3	6 cm	CR3000
Soil temperature	Soil thermister	Local [†]	5 & 10 cm	CR10X(a)
Thermocouple reference temperature	Thermocouple reference thermister	Local [†]	0.6 m	CR3000
Soil heat storage	Spatially averaging thermocouple	CSI TCAV	2 cm & 4 cm	CR3000
Volumetric soil moisture content	Soil moisture reflectometer	CSI CS616 ^{††}	5 & 10 cm	CR10X(a)
Wind speed	Cup anemometer	Vector A101M	0.93 m	CR10X(a)
Wind direction	Wind vane	Vector W200P	3 m	CR10X(a)

* Instruments lowered to 1.5 m from 5 June 2008 to 27 June 2008 for data comparison with another site.

** Malfunction 18 February 2008 to 21 February 2008. [†] Equivalent to CSI 107B thermisters, individually calibrated. ^{††} Calibrated for soil type and conditions of Scott Farm.

Table 3.3 Details of temporary variables measured and instrumentation used at Scott Farm EC site.

Variable	Instrument	Make & Model	Height/ depth	Data logger connection	Date deployed
Data logger	CR10X(b)	CSI	-	-	19 Jan 2008 – 20 Jun 2008
Radiation fluxes ($K\downarrow$, $K\uparrow$, $L\downarrow$, $L\uparrow$, T_{surface})	4 component net radiometer	Hukseflux NR01	0.93 m	CR10X(b)	19 Jan 2008 – 20 Jun 2008
3D wind velocity, sonic temperature	3D sonic anemometer	RMY8100	0.93 m	CR3000	5 Mar 2008 – 27 Mar 2008
Rainfall	Storage rain gauge	Nylex RG1000	0.4 m	-	11 April 2008 – 30 Nov 2008

Table 3.4 Company details of instruments listed in Table 3.2 and 3.3.

Company	Details
CSI	Campbell Scientific Inc. Logan, UT, USA
LI-COR	Lincoln, NE, USA
Vaisala	Helsinki, Finland
Kipp and Zonen	Lincoln, UK
Vector	North Wales, UK
RM Young	R.M. Young Company, Michigan, USA
Hydrological Services	Liverpool, Sydney, Australia
Hukseflux	Delft, The Netherlands

3.3.1 Eddy covariance measurements

The 3D ultrasonic anemometer (CSAT3, Campbell Scientific Inc. (CSI), Logan UT) measured wind velocities relative to three axes (two horizontal and one vertical), and air temperature based on instantaneous speed of sound, all at a frequency of 20 Hz. By calculating the covariance between these variables, the sensible heat flux (H) was directly measured. Three dimensional wind velocities were determined by time-of-flight measurements of sound along the sonic axes

(non-orthogonal), which were then transformed into the orthogonal wind components u_x , u_y and u_z (Campbell Scientific, Inc. 2007).

The open path CO₂/H₂O gas analyser (LI-7500, LI-COR, Lincoln NE) measures densities of CO₂ and water vapour in air. These are measured by an infra red optical beam (1 cm diameter), which passes through windows 15 cm apart, determining the absorption of specific wavelengths to provide measures of CO₂ and H₂O gases (LI-COR, 2001). In this case, the LI-7500 sensor head was mounted horizontally (to allow water to run off sensor windows) and had a separation distance from the CSAT3 of 16 cm. It was calibrated according to the manufacturer's instructions several times throughout the study period. By using this instrument together with the CSAT3, fluxes of water vapour (and CO₂) can be measured from the Earth's surface, where the CSAT3 measures the vertical wind velocity and the LI-7500 measures the water vapour (and CO₂) concentration at a height of 2.84 cm. Figure 3.6 shows how these two instruments were deployed in the field.

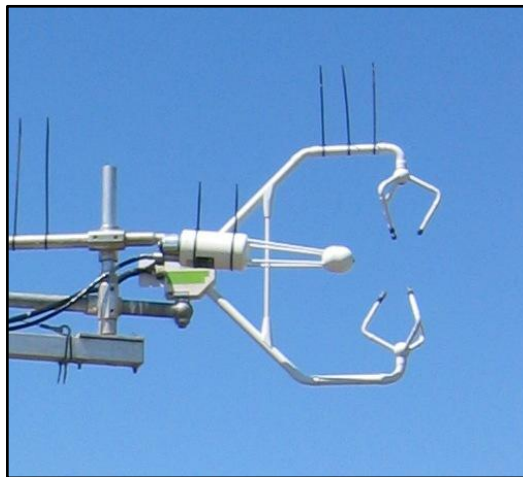


Figure 3.6 The eddy covariance instruments. CSAT3 sonic anemometer and LI-7500 gas analyser (vertical cable ties are used to deter birds).

3.3.1.1 Associated errors

The CSAT3 sonic transducers are well sealed and are not damaged when they become wet and wind measurements are still made during rainy conditions.

However if the transducers are obscured enough the CSAT3 cannot make valid readings. A diagnostic check variable allows online filtering of such corrupted data and they are excluded from flux calculations. Operating temperatures range between -30° to 50°C and wind speed accuracies are, for horizontal wind components (u_x and u_y) $\pm 4 \text{ cm s}^{-1}$ and $\pm 2 \text{ cm s}^{-1}$ for u_z . The CSAT3 faces into the prevailing wind direction to minimise any disturbance caused by the arms or other supporting structures of instruments, however when winds are coming from the direction in which disturbances are made, errors may exist.

The LI-7500 will have errors associated with measurements when water, dew or dust settles on the lenses through which the optical beam is transmitted. This is monitored using a diagnostic variable (AGC) which indicates if the beam's path is interfered with. This will also indicate if calibration is needed or when instrument chemicals may need replacing. Vapour density measurements are compared to those measured by the HMP instrument and data are discarded if there is a significant disagreement.

3.3.2 Lysimeters

Ten small pot lysimeters were used for a period of a few days during each season to calculate a soil moisture balance to determine daily evaporation totals. The pots were 0.152 m in diameter (outside diameter), 0.2 m deep and constructed of PVC pipe, with a wall thickness of 4 mm, formerly used by Fong (2001) for a MSc thesis. During operation, drainage holes in the base were sealed with tape to prevent drainage. Intact soil cores, including vegetation, were taken using a stainless steel corer with a diameter of 0.15 m. The corer had a sharpened edge to allow easy insertion into the ground and was removed by twisting using a steel handle. Cores were then carefully pushed out into the PVC lysimeter pots.

3.3.2.1 Deployment and operation

For every lysimeter trial, new cores were taken, and then discarded once the trial was complete. This ensured that soil conditions were kept as close as possible to

that of the natural field conditions and to ensure the vegetation growing in the pot would survive for the duration of the trial. Lysimeter locations were chosen along a transect for easy location for daily weighing within the two fields adjacent to the eddy covariance tower. Transect orientation varied for each season to try and maintain randomness.

During each lysimeter trial, the lysimeters were removed from the ground and weighed using electronic scales (Sartorius, MC1, 30 kg \pm 1 g) which were stored in a weather tight box at the eddy covariance climate station. The pots were then replaced immediately after weighing, the process only taking approximately 30 minutes to complete all 10 pots. This was done every morning at approximately 0730–0800 hours for 4–8 days in order to be able to calculate a daily evaporation total. All three trials were undertaken during rain-free periods so no additional calculations were required to account for any weight gain or drainage within the lysimeter pots.

3.3.2.2 Determining evaporation

Evaporation from a lysimeter was calculated as:

$$E_{\text{lys}} = \frac{\Delta W}{A} \quad 3.1$$

Where ΔW is the change in weight (kg) and A is the surface area of a lysimeter (0.0181 m²). The weighing resolution of \pm 0.05 g converts to an evaporation resolution of about \pm 0.03 mm. We assume that evaporation is the only cause of weight change (hence the reason for running the trials during rain-free conditions), while in reality rainfall, drainage, condensation or dew, and the growth or loss of plants can also contribute to changes in weight. Drainage was prevented by sealing holes at the base of pots and because of the short periods of deployment (no longer than 8 days), and avoiding periods of rainfall, all other factors were considered negligible and were therefore ignored for this study.

3.3.2.3 Lysimeter and weighing errors

Due to the short deployment periods of each lysimeter trial, many of the usual associated errors are not applicable. Some sources of error for lysimeters are still valid and need to be considered for this study:

- The effect of the grass leaning out of the lysimeter could result in a miscalculation of evaporation due to incorrect assumed surface area.
- The walls of the lysimeter could impact the thermal properties of the soil and alter the soil heat flux.
- Because the lysimeters are small, many replicates are required.
- The disturbance of the soil moisture distribution within the lysimeter, particularly after a rainfall event (dependent on the time when cores were taken and when the last rainfall event occurred previous to this).
- Restricted rooting depth can cause possible damage to plants and reduce soil water availability.
- Miscalculation of the lysimeter surface area.

3.3.3 Data loggers

Data loggers convert electrical signals from instruments into scientific units, perform calculations and store data outputs for later analysis. Electrical signals from instruments can be in several different forms such as voltage (e.g. solar radiation and relative humidity), voltage response to an excitation (e.g. wind vane), pulse (e.g. tipping bucket rain gauge and cup anemometer) and serial (CSAT3, LI7500).

Campbell Scientific data loggers were used, including one or more CR10X data loggers to measure supporting measurements such as soil moisture content, which required manual downloading of data via connection with a laptop. A CR3000 was used for all EC signal acquisition and on-line processing as well as some supporting measurements, from which data were downloaded via automated telemetry on a daily basis using a cell phone network (Wavecom WMOD2B GSM) as well as storing all high frequency data on a CF memory card. This

required replacing every 14–18 days. The CR10X collected mV signals from instruments and converted these into correct units to calculate half hourly averages or totals. The CR3000 recorded raw signals at 20 Hz and calculated covariances, averages or totals every half hour. The CR3000 logger allows the user to view output variables on a built-in screen on the data logger without the use of a laptop. See Table 3.2 and 3.3 for list of the instruments connected to the respective data loggers.

3.4 Processing data

Corrections applied to EC and other data were applied to the data using a custom software program running in the Matlab environment called Micrometlab (Nieveen *et al.* 2005). This software program automatically ran these corrections to produce a database containing all corrected data which were then used for analysis. Figure 3.7 shows the progression of data from instruments, to loggers, followed by the process of corrections and storage databases used.

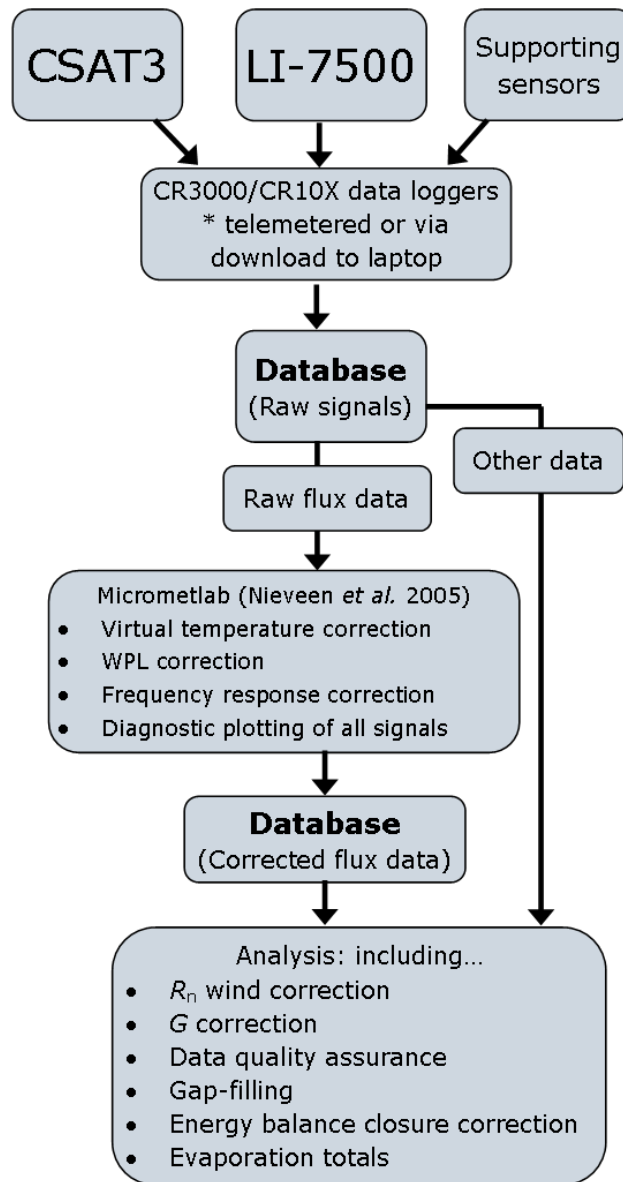


Figure 3.7 The progression of data processing.

3.4.1 WPL corrections

Corrections were applied to raw EC fluxes to account for the effects of air density on heat and water vapour measurements (Webb, Pearman and Leuning, 1980, henceforth abbreviated to WPL). The LI-7500 open path EC sensor measures water vapour and CO₂ densities on an air volumetric basis, so a correction is required to account for volume changes caused mainly by the transport of sensible heat. The corrected latent heat flux density is expressed as (WPL Equation 25):

$$\lambda E = \lambda(1 + \mu\sigma)[\overline{w'\rho'_v} + (\overline{\rho_v}/\overline{T})\overline{w'T'}] \quad 3.2$$

Where λ is the latent heat of vaporisation of water, $\mu = m_a/m_v$ is the ratio of molecular masses of dry air (a) and water vapour (v), $\sigma = \overline{\rho_v}/\overline{\rho_a}$ is the ratio of the mean densities of water vapour and dry air, w is the vertical wind velocity, $\overline{\rho_v}$ is the mean density of water vapour, \overline{T} is the mean absolute temperature at the measurement height, $\overline{w'\rho'_v}$ is the covariance between vertical wind speed and vapour density and $\overline{w'T'}$ is the covariance between vertical wind speed and air temperature fluctuations. The sensible heat flux density is expressed as (WPL Equation 40):

$$H = c_p \overline{\rho w'T'} \quad 3.3$$

Where c_p is the specific heat of moist air, and $\overline{\rho}$ is mean density of moist air.

3.4.2 Other calculations and corrections

“Virtual temperature corrections” were made following Schotanus *et al.* (1983), for the effect of humidity on sonic temperature. Co-ordinate rotation (McMillen, 1988) corrections were applied to the convective flux densities to account for instrument misalignment with the mean wind streamline. For frequency response and sensor separation, corrections following Moore (1986) were used (Nieveen *et al.* 2005).

For net radiation (R_n) a wind speed dependent correction (REBS, 1995) typically increased R_n (~5%) during the day, with little effect during night time (REBS, 1995). The REBS data were then compared to the data collected by the NR01 for quality control, discussed further in Section 3.4.3.1.

The surface soil heat flux (G) was calculated as the average of soil heat flux plate measurements inserted in the soil at a depth of 0.06 m and corrected for the storage of heat in the soil layer between the plate and soil surface.

$$G = \overline{G_z} + z \frac{\Delta T_s}{\Delta t} C_s \quad 3.4$$

Where

$$C_s = \rho_b (c_s + \theta_g c_w) \quad 3.5$$

Where $\overline{G_z}$ is the mean of measured soil heat flux at $z = 0.06$ m depth by the two soil heat flux plates, ΔT_s is the change in mean soil temperature between the surface and depth z over the time interval Δt (1800 s) and C_s is volumetric soil heat capacity in which ρ_b is soil dry bulk density, c_s is specific heat of soil, θ_g is gravimetric soil moisture content and c_w is specific heat of water (Thompson *et al.* 1999). Because ΔT_s was measured using a 4-junction averaging thermocouple (TCAV, CSI) inserted at 2 cm and 4 cm below the soil surface, a reference temperature was required. This was measured by a thermocouple reference junction which was located in a sealed PVC pipe at 0.6 m depth in the soil to provide a stable temperature environment, in order to minimise errors due to temperature gradients.

Figure 3.8 shows G corrected for heat storage and soil moisture for 1 January 2008 to 3 January 2008 together with the uncorrected G_z . By applying the correction (Equation 3.4) a more ‘spiky’ G is produced due to the effects of cloud cover and diurnal temperature variations on half hourly timescales. This means that G , once corrected, will show a larger diurnal energy range (more negative at night and more positive during the day) and weather conditions (presence of clouds) will also become evident. Figure 3.8 shows one cloudless day (1 January 2008) and two cloudy days (2–3 January 2008) where G is a smooth curve during the clear day and spiky during the two cloudy days.

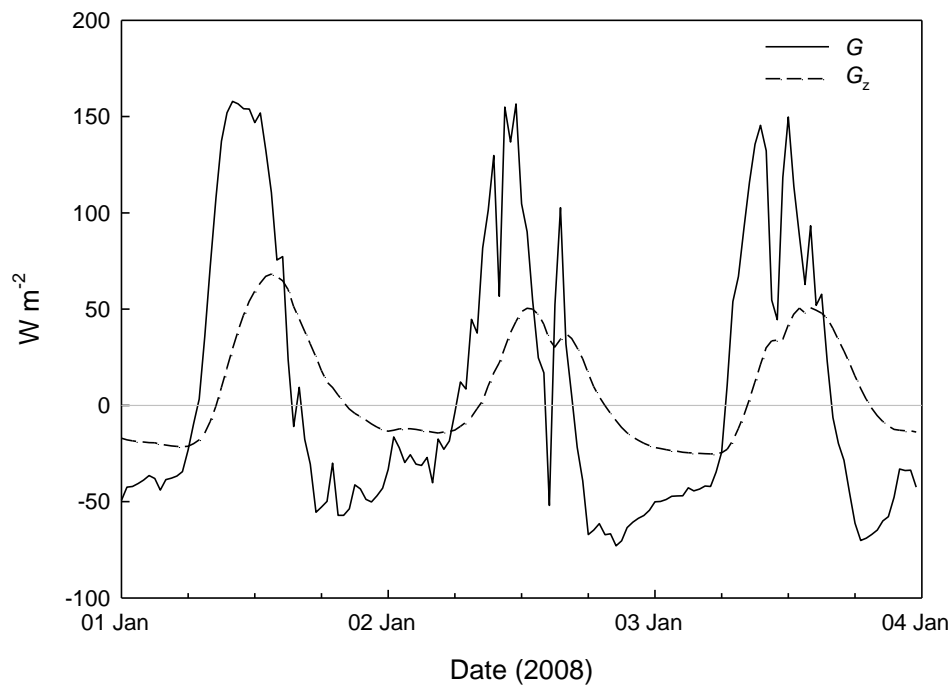


Figure 3.8 Timeseries for 1 – 3 January 2008 showing 30-minute raw soil heat flux (G) and the temperature, moisture, and depth corrected G using Equation 3.4.

3.4.3 Data quality, filtering, missing data and gap-filling

Once all corrections were made to the raw data and they were stored in a binary form for further processing and analysis, they were checked for quality, and filtered if required. For some analyses, such as calculating daily total E , a flux gap-filling methodology was developed. The quality assurance of the data included filtering ‘hard’ and ‘soft’ spikes, forcing energy balance closure and filtering out data with air disturbances which may present false readings. The filtering process will be discussed and the energy balance closure, air disturbance filtering and gap-filling methods are discussed in the following three sections.

3.4.3.1 Data quality and filtering

Hard spikes are those that are far outside possible natural ranges and are eliminated by simple threshold conditions (Smith, 2003; Thornburrow, 2005). Soft spikes are more difficult to determine. For the LI-7500 the diagnostic technique was done by comparing vapour pressure measurements made by the LI-7500 and the HMP45A, and rejecting discrepancies (Figure 3.9). The LI-7500 will often miscalculate values due to water droplets resting on the sensor windows as a result of rain or dew (Thornburrow, 2005; Campbell and Nieveen, in prep), requiring the data to be filtered and gap-filled.

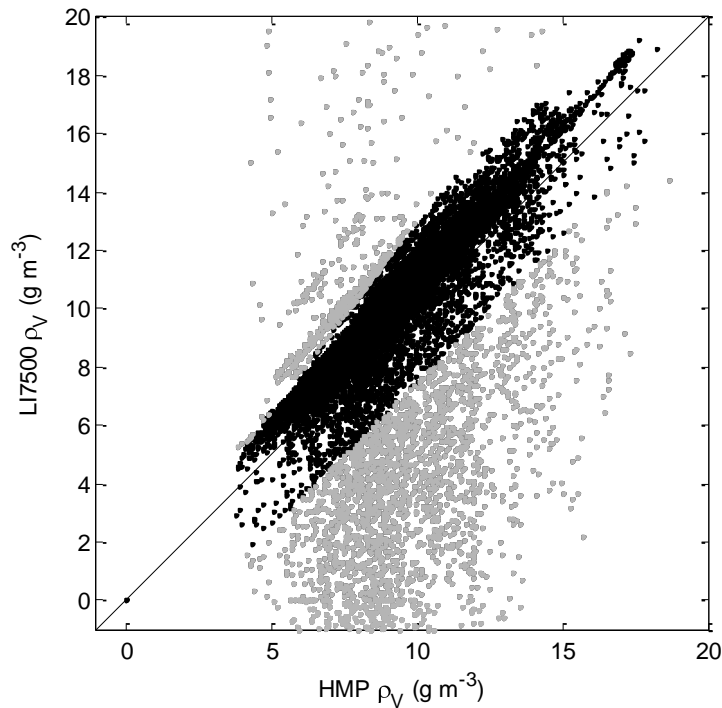


Figure 3.9 Regression of LI-7500 and HMP45A vapour pressure, where black data points are accepted and grey points are rejected for the period 15 December 2007 to 30 November 2008.

3.4.3.2 Missing data

For various sensors, occasional periods of missing data occurred, due either to instrument malfunction or when instruments required removal from the field for calibration. No more than five continuous days of missing data existed at any one time, and those sensors which did need filtering and gap-filling of missing data were easily accounted for using other sensor measurements and adjustments, i.e. HMP temperature required 5 days to be gap-filled using sonic temperature measurements and vapour pressure was gap-filled using data from another site 50 km away (Torehape), once an appropriate correlation relationship had been established on valid data.

3.4.3.3 Gap-filling

The two variables that required gap-filling models to be applied every month were H and λE due to water droplets forming on sensor windows (during rain events or when dew settled during early morning fog events). Overall, 25% of λE data required gap-filling and only 3% of H , in order to be able to make long term estimates. The gap-filling model was a simple empirical type which created synthetic flux data using inputs of net radiation and soil moisture, determined uniquely for each month.

Volumetric soil moisture content appeared to impose the greatest restriction on evaporation rates, particularly during the summer dry period. For this reason, during dry periods, separate models were used to adjust for the moisture conditions which restrict λE and therefore enhance H . Figure 3.10 shows how the relationship between λE and R_n varied with differing volumetric moisture contents during the month of January 2008 when drought conditions were present. H produced very similar results and the same concept was used to adjust values with moisture conditions (Figure 3.11). See Appendix B for all months.

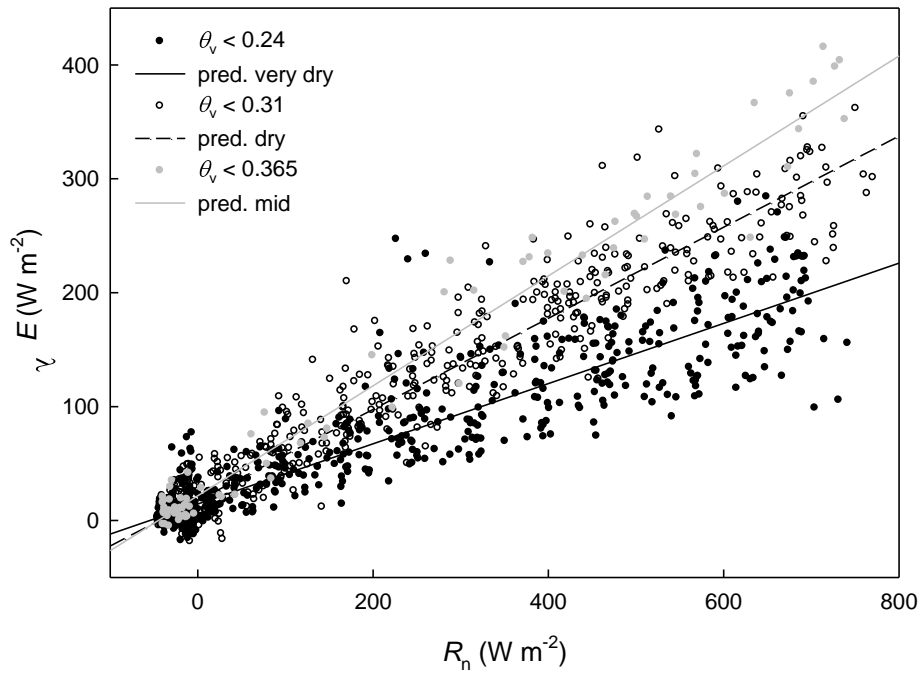


Figure 3.10 Scatter plot of λE against R_n to determine the gap-filling model required for each moisture content range for January 2008.

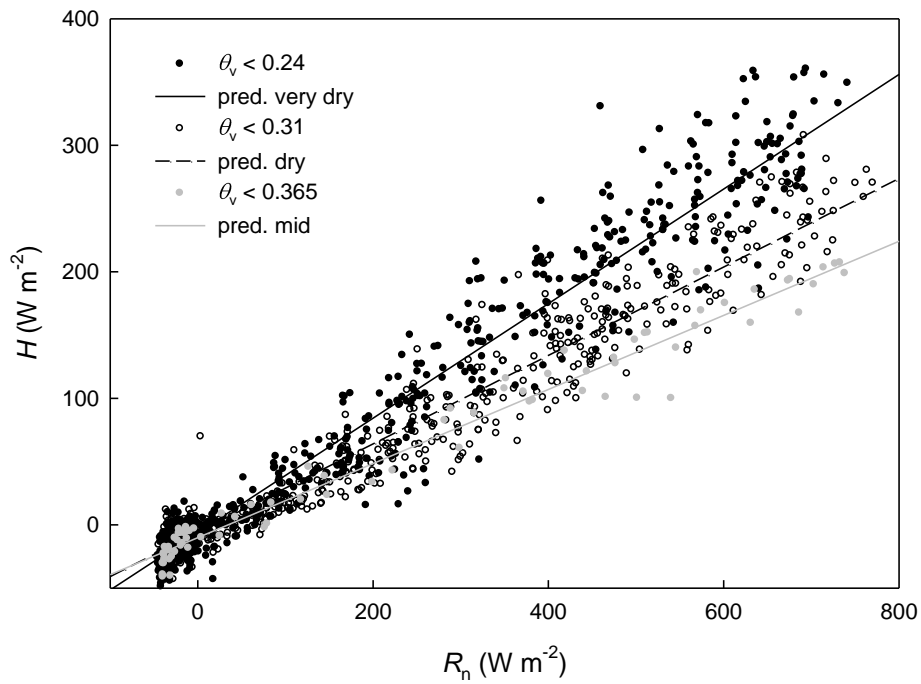


Figure 3.11 Scatter plot of H against R_n to determine the gap-filling model required for each moisture content range for January 2008.

Thresholds for volumetric moisture (θ_v) contents were chosen to determine separate models so the most accurate estimates could be made for gap-filling. Moisture contents below 0.24 were considered ‘very dry’, moisture contents between 0.24 – 0.31 were ‘dry’, moisture contents 0.31 – 0.365 were considered to be ‘mid’ (Figure 3.12) and any moisture content above 0.365 was considered as ‘wet’. Second order polynomial regression models were derived using these moisture thresholds and data were then gap-filled to result in datasets such as that in Figure 3.13, and regression coefficients were stored for use in on-line gap-filling during analysis.

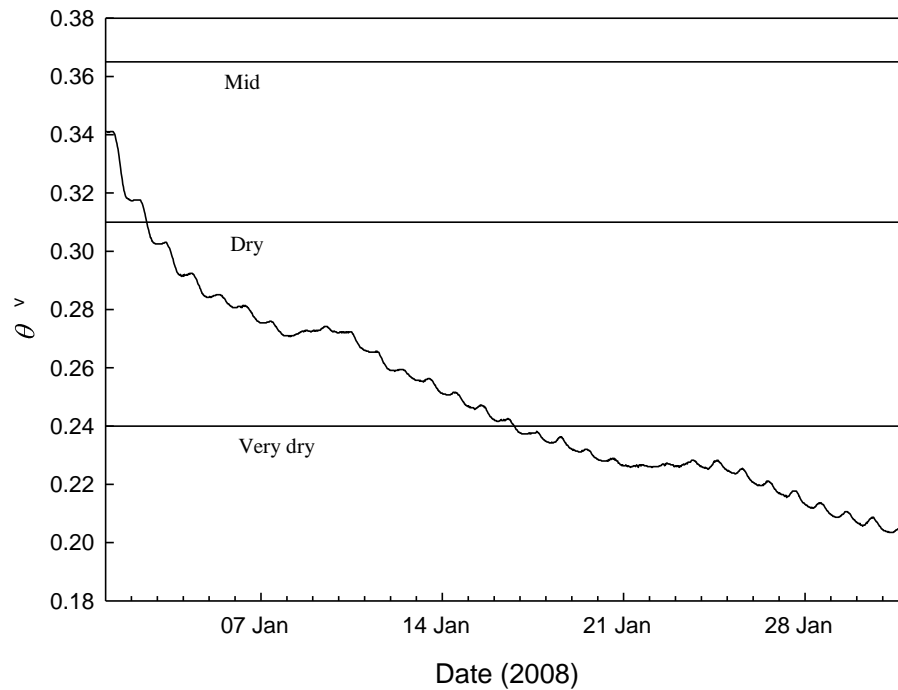


Figure 3.12 Volumetric moisture content changes and thresholds for January 2008.

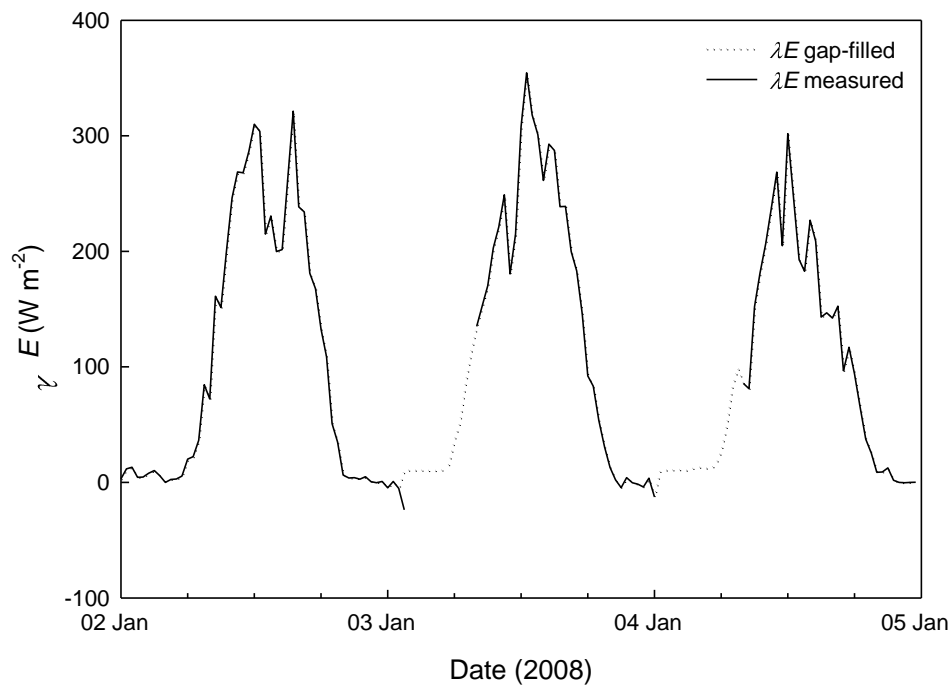


Figure 3.13 Time series of latent heat flux for 2–5 January 2008 showing example of measured and gap-filled data.

Net radiation required filtering and filling for short periods a few times throughout the year due to the REBS instrument malfunctioning, in one instance due to splits in hemispheres allowing water to enter. Net radiation was measured by both the REBS and NR01 instruments (Table 3.2 and 3.3) for approximately five and a half months to ensure measurements were accurate and to build confidence in measurements (thereafter all measurements were done only using the REBS instrument). Figure 3.14 shows a comparison of R_n measured by the two instruments and Figure 3.15 shows their deployment in the field.

All other variables measured occasionally had some missing data which usually only accounted for a half hour period every so often. These gaps were filled using a Matlab function which linearly interpolated between two valid data points. This method is only acceptable when very short periods of data are missing and should not be used for longer periods of time.

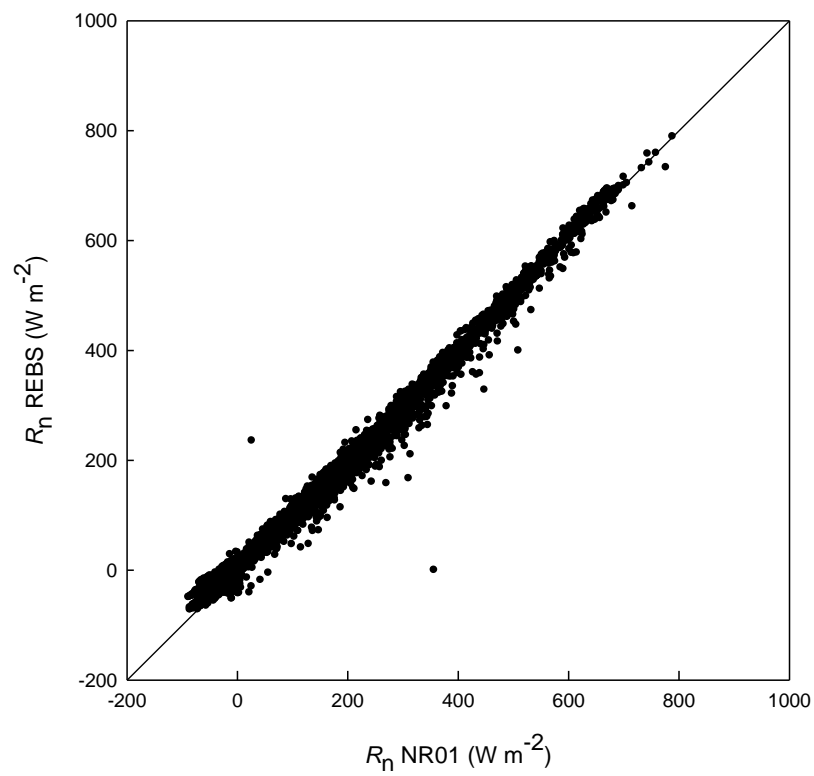


Figure 3.14 Comparison of net radiation data measured by REBS and NR01 instruments for the period 19 January 2008 to 20 June 2008. Diagonal line is 1:1.



Figure 3.15 Image of (a) REBS net radiometer and (b) NR01 four component net radiometer at Scott Farm.

3.5 Evaporation estimation

3.5.1 Calculating E_{PT} and E_o

Two evaporation estimation equations were used for comparison to measured evaporation; the first was the Priestley-Taylor (Equation 2.9) and the second was the FAO₅₆ (Equation 2.13). These models require daily input variables so daily averages were calculated and energy components converted to MJ m⁻² day⁻¹. For this reason, all evaporation results that compare estimated evaporation with measured evaporation are either daily averages or monthly totals. A soil moisture adjustment is occasionally required to adjust estimated evaporation during dry conditions and is outlined in the next section.

3.5.2 Water stress adjustment and crop coefficient

Section 2.3.4 outlines the need for an adjustment to evaporation models when soil moisture conditions become dry. As described in Section 2.3.4, Allen *et al.* (1998) give a correction method where the original estimated evaporation is multiplied by a water stress coefficient (K_s) and a crop coefficient (K_c), Equation 2.14. These water stress corrections can be applied to any methods of evaporation estimation to help account for the constraints that limiting moisture conditions have on evaporation models and have been applied to both models for this study. Crop coefficients can vary through seasons which can often affect results so a representative value needs to be decided on which will best describe the crop type for a site. Rooting depth of plants is very sensitive to the adjustment model. Plants are able to extract sufficient moisture from the upper soil layer. During summer, and particularly during a drought when water becomes very limited, plants no longer have access to enough moisture and may therefore be able to send their roots much deeper into the soil in order to find water to survive. The rooting depth value that is used for the model can affect results dramatically so an adequate rooting depth value is important for the K_s adjustment.

3.6 Footprint analysis and air disturbances

To minimise air disturbances from either the EC tower or surrounding trees, the EC tower was positioned at such a distance and orientation to allow adequate fetch (Figure 3.2) and positioned facing the direction of the most dominant wind directions.

The dominant wind directions vary through the year but are either north-westerly or easterly. The minimum fetch is limited to the west of the site with a distance of approximately 280 m where a line of tall pine trees may cause some disturbance (Figure 3.2). Diagnostic methods, following Schuepp *et al.* (1990), are commonly used (Thompson *et al.* 1999; Smith, 2003; and Thornburrow, 2005) to estimate the area contributing to flux measurements. Two parameters are used as diagnostic tools. The first is x_{MAX} which gives the upwind distance of the peak of the footprint. The second parameter is CNF_{80} or the upwind distance within which 80% of the cumulative normalised flux can be expected to come from (Schuepp *et al.* 1990). Figures 3.16 and 3.17 show x_{MAX} and CNF_{80} calculated for a.) predominantly unstable (day) and b.) predominantly stable (night) conditions for a single half hourly period for 1 February 2008 at 12:00 NZST and 10 March 2008 at 02:00 NZST respectively. During unstable conditions as in Figure 3.16, x_{MAX} is 15.2 m from the EC tower while during stable conditions (Figure 3.17) x_{MAX} is a lot larger at 54.8 m from the tower. CNF_{80} is 137 m during unstable conditions in Figure 3.16, allowing for sufficient fetch in all directions from the EC tower. During stable conditions however, CNF_{80} can become large (Figure 3.17 shows a distance of 492 m) and therefore occasionally exceeds the 280 m minimum fetch of the western boundary. This may explain discrepancies in data during night time conditions, however λE is commonly close to zero at night. For this reason, fetch is considered adequate for this study.

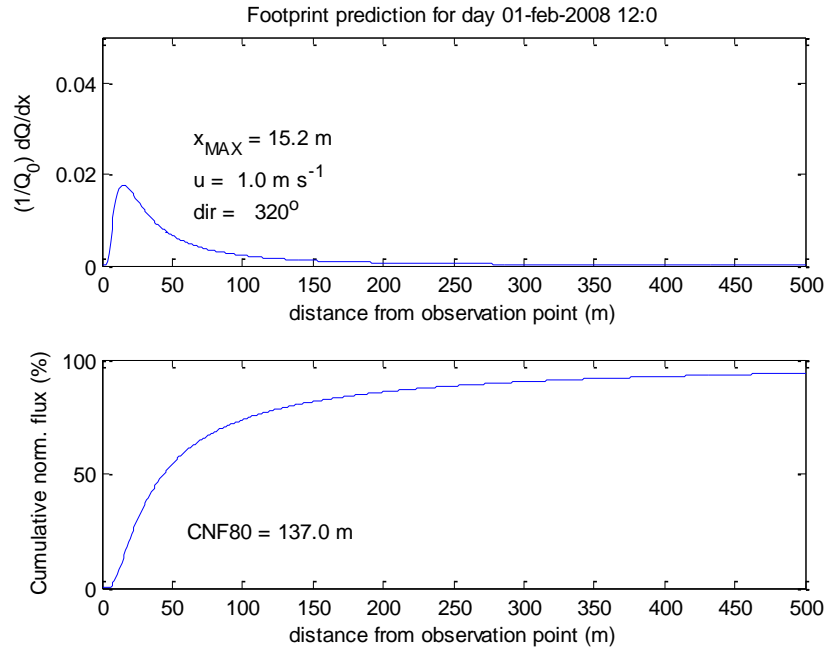


Figure 3.16 Footprint analysis for 1 February 2008 12:00 NZST under unstable conditions.

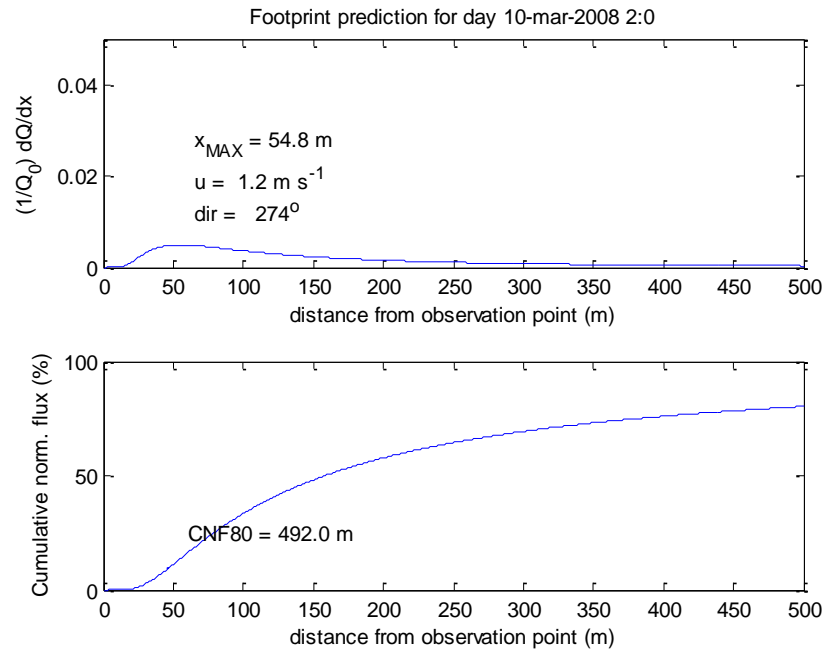


Figure 3.17 Footprint analysis for 10 March 2008 02:00 NZST under stable conditions.

The spatial representation of half hourly x_{MAX} and CNF_{80} parameters are displayed in Figure 3.18, 3.19, 3.20 and 3.21 for daytime (predominantly

unstable) and night time (predominantly stable) conditions. Values were plotted in conjunction with their corresponding wind directions (after Thornburrow, 2005). This results in a ‘map’ showing the position of calculated x_{MAX} and CNF_{80} for each half hourly measurement from the tower in metres. The influences of the dominant wind directions become apparent. During day time conditions, the surfaces of greatest influence on measured fluxes are on average about 20 m from the tower, while during night time conditions, fluxes are derived from much greater distances due to the lower wind conditions. CNF_{80} is proportional to x_{MAX} so therefore shows a similar distribution pattern around the EC site. Daytime values (Figure 3.20) seem well contained within about 250 m reinforcing the basis of adequate fetch.

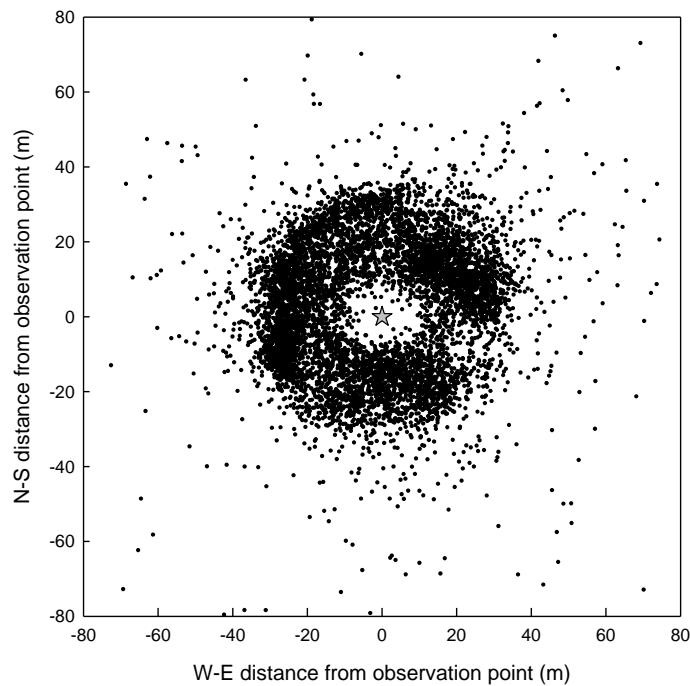


Figure 3.18 Spatial distribution of half hourly daytime (unstable) x_{MAX} values surrounding the EC tower site (central location) for the period 15 December 2007 to 30 November 2008.

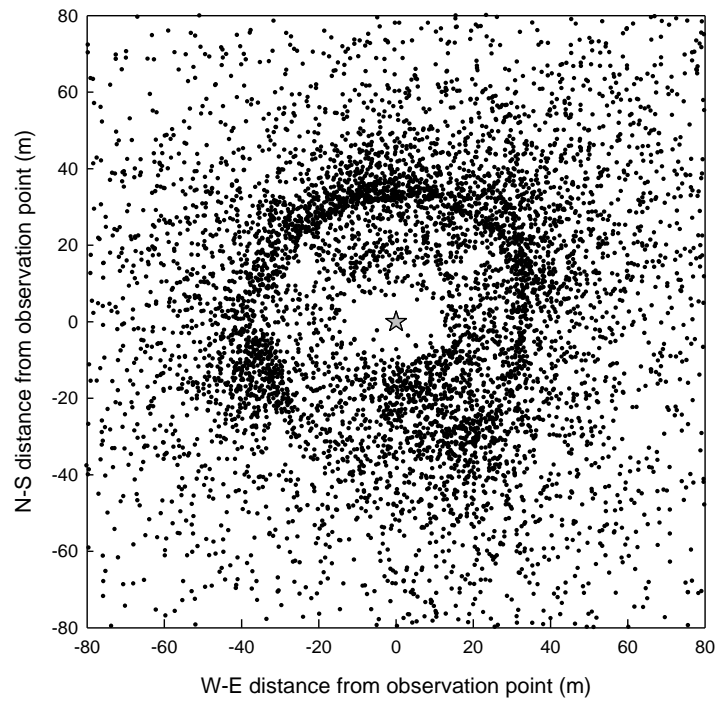


Figure 3.19 Spatial distribution of half hourly night time (stable) x_{MAX} values surrounding the EC tower site (central location) for the period 15 December 2007 to 30 November 2008.

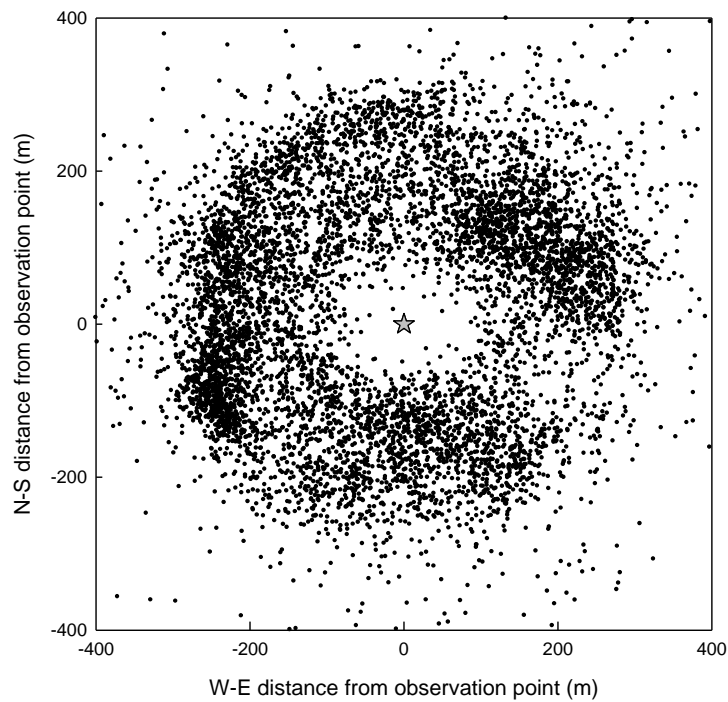


Figure 3.20 Spatial distribution of half hourly daytime (unstable) CNF_{80} values surrounding the EC tower site (central location) for the period 15 December 2007 to 30 November 2008.

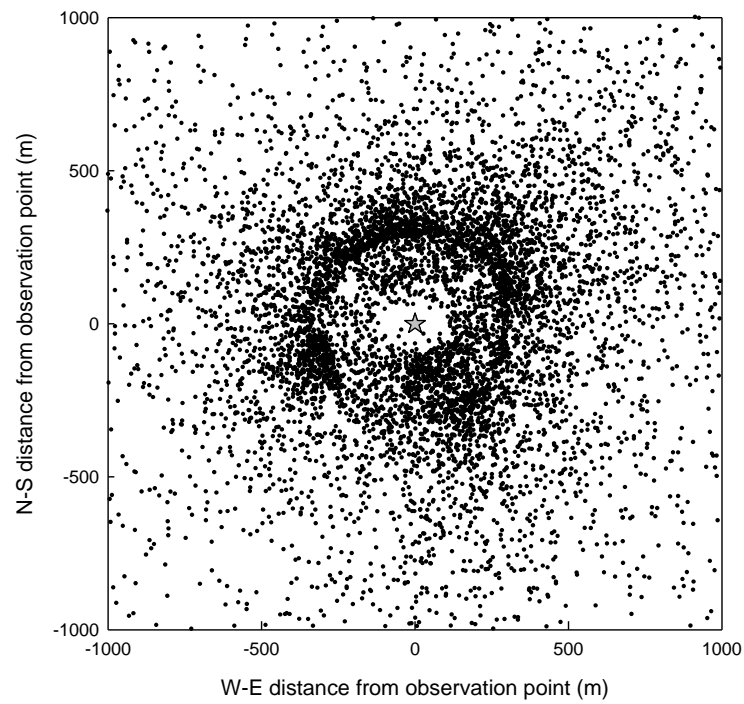


Figure 3.21 Spatial distribution of half hourly night time (stable) CNF_{80} values surrounding the EC tower site (central location) for the period 15 December 2007 to 30 November 2008 (NOTE: axis scale different to Figure 3.20).

4 Accuracy of the eddy covariance technique

4.1 Introduction

It is important to assess the accuracy of measurement methods to ensure results are as precise as possible and so confidence can be had in instruments and resulting data. In this chapter, an analysis of energy balance closure data for Scott Farm and the methods used to force closure for the site are discussed. This includes interpreting how energy balance closure varies throughout the year and what wind directions affect a lack of closure most significantly, related to available fetch and physical obstructions to wind by the tower. The results of a comparison between lysimeter and eddy covariance measurements of evaporation are then described. All results are then discussed in the context of other literature to gain a complete understanding of the outcomes.

4.2 Energy balance closure

Due to a lack of energy balance closure (Equation 2.7 in Section 2.3.2.1) when using eddy covariance instrumentation, corrections are required to force closure and account for the total available energy ($R_n - G$). Wilson *et al.* (2002) reported the average lack of closure to be about 20% for 22 eddy covariance sites and 50 site-years of data. For this study the Bowen ratio closure method is used, recommended by Twine *et al.* (2000) and Foken (2008), which assumes β is correctly measured so both λE and H are increased proportionately to close the energy balance while preserving measured β . Figure 4.1 shows the daily convective energy flux ($\lambda E + H$) plotted against available energy flux ($R_n - G$) for which a regression slope of 0.906 resulted, with a y-intercept of -9.92 W m^{-2} .

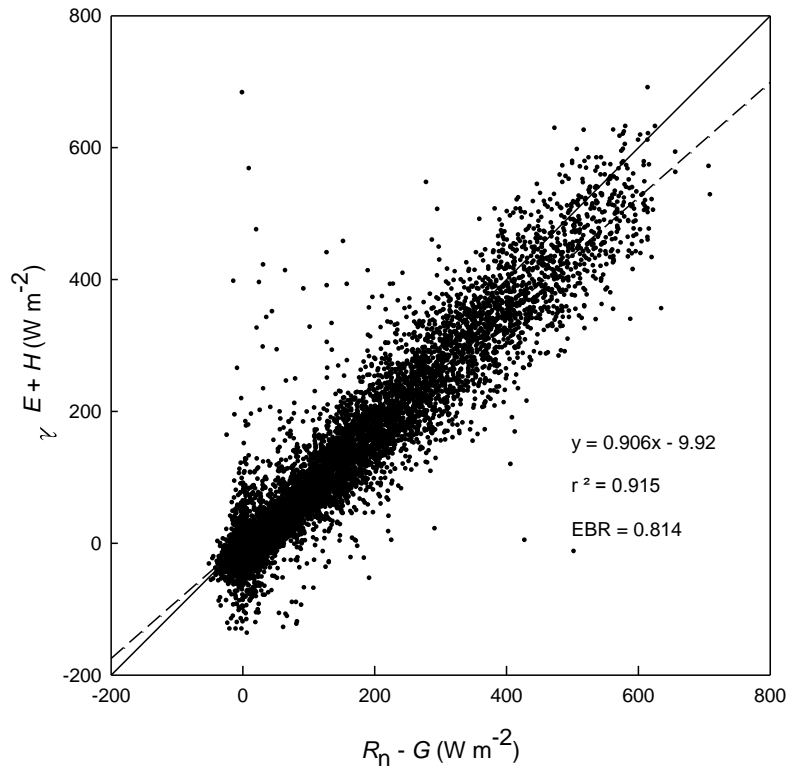


Figure 4.1 Half hourly energy balance ratio ($\lambda E+H$ against R_n-G) to show average lack of closure for 15 December 2007 to 30 November 2008. Dashed line shows regression

The energy balance ratio (EBR) is another way to assess energy balance closure:

$$\text{EBR} = \frac{\sum(\lambda E + H)}{\sum(R_n - G)} \quad 4.1$$

where summation of the fluxes is for the time period of interest (e.g. 30-minute, daily, annual). For the entire period of this study EBR was 0.814. This means that, on average, measured energy fluxes (λE and H) accounted for approximately 81% of available energy. Figure 4.2 shows a typical early summer day in which the energy balance was not closed due the under-measurement of the convective fluxes and Figure 4.3 shows a winter day (note scale differences of axes).

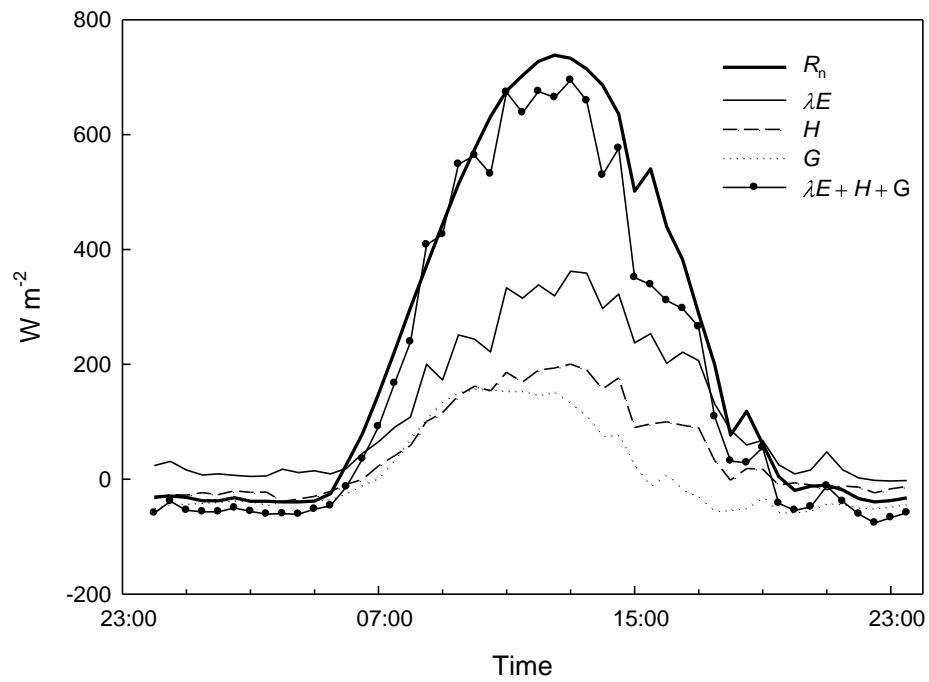


Figure 4.2 Energy balance for 1 January 2008 showing lack of closure due to probable underestimation of λE and H .

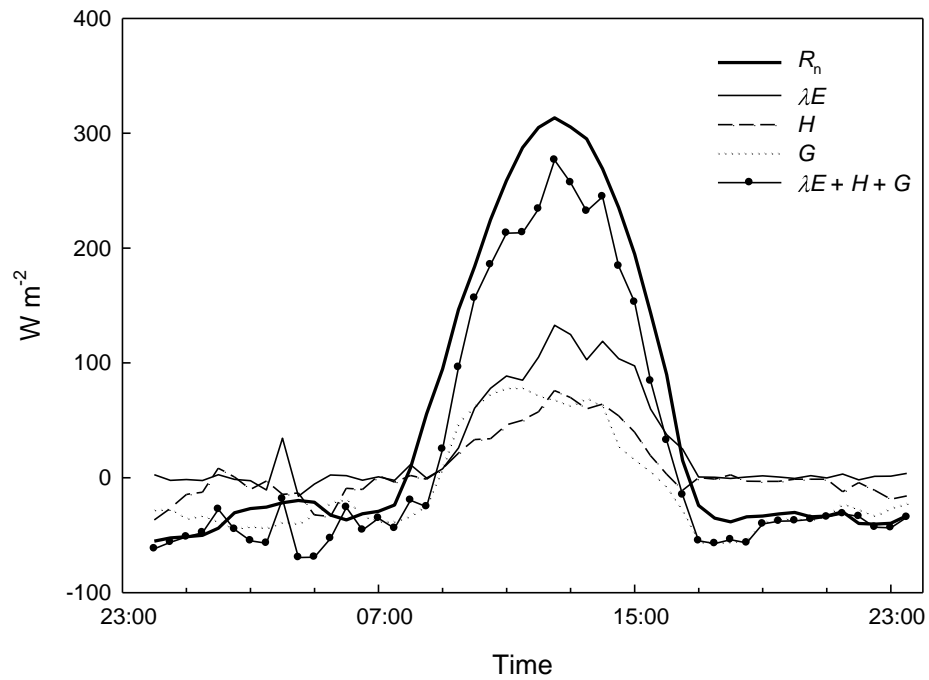


Figure 4.3 Energy balance for 25 July 2008 showing lack of closure due to probable underestimation of λE and H .

These need forcing in order to close the energy balance so that $LE+H+G$ are equal to R_n throughout the diurnal cycle. The equations to correct for turbulent fluxes and close the energy balance are:

$$\lambda E_f = \frac{R_n - G}{1 + \beta} \quad 4.2$$

$$H_f = \beta \lambda E_f \quad 4.3$$

Where the subscript f indicates fluxes forced to close the energy balance via the Bowen ratio. When fluxes are very small, usually during the early morning and evening, and when β approaches -1 , Equation 4.2 becomes undependable because the product approaches infinity. During such situations, the β method was not used and surplus available energy was evenly apportioned into H and λE (Thornburrow, 2005). Forcing closure using these methods does have serious problems however. A large amount of reliance is put on the accuracy of R_n-G measurements and it is assumed they are representative values within the measurement footprint. For this reason, R_n measurements from the permanent REBS instrument were compared with the NR01 instrument outlined in Section 3.4.3.3 to ensure data quality. In order to show diurnal differences between the two instruments, a time series (Figure 4.4) shows a combination of sunny and progressively cloudy days during February where the main discrepancy between the two measurements was during night time measurements where the REBS instrument measured a less negative flux than the NR01. Throughout the rest of a day, measurements were almost identical and matched together well.

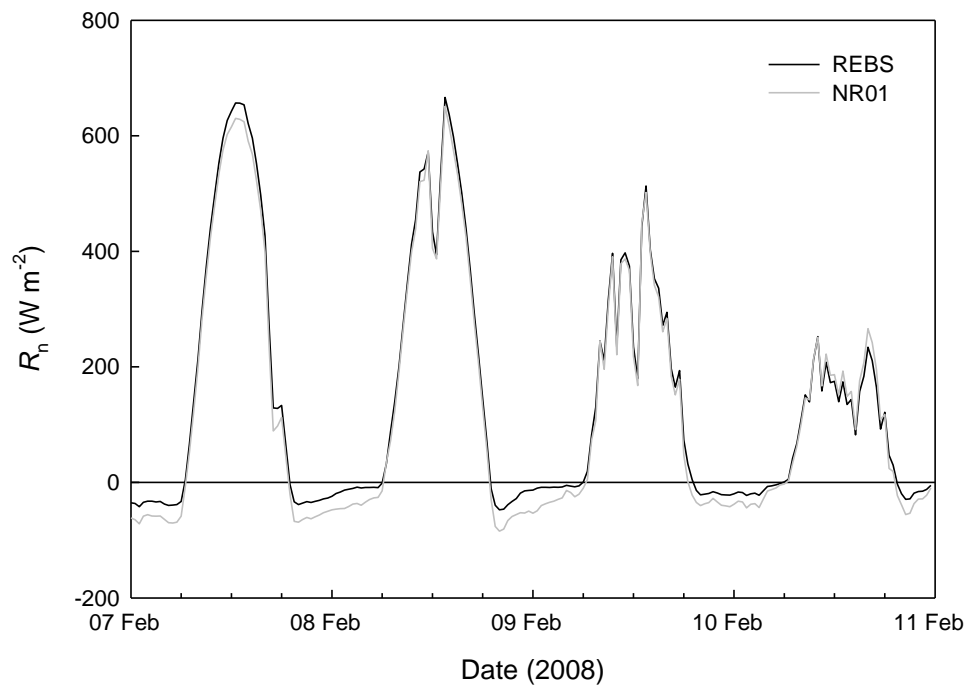


Figure 4.4 Diurnal time series of the two net radiometer instruments (REBS and NR01) for the four day period 7–10 February 2008.

4.2.1 Energy balance closure and wind direction

It was apparent that energy balance closure was worse during certain wind directions (Figure 4.5), in particular those winds coming from approximately 75–125°. This was the direction from which the least amount of winds came from during the year so only a small amount of data were affected and was most likely caused by the interference of the tower on which the instruments were mounted. Closure appeared to have scatter during all wind directions which was most likely caused by low wind speeds that occur from any wind direction.

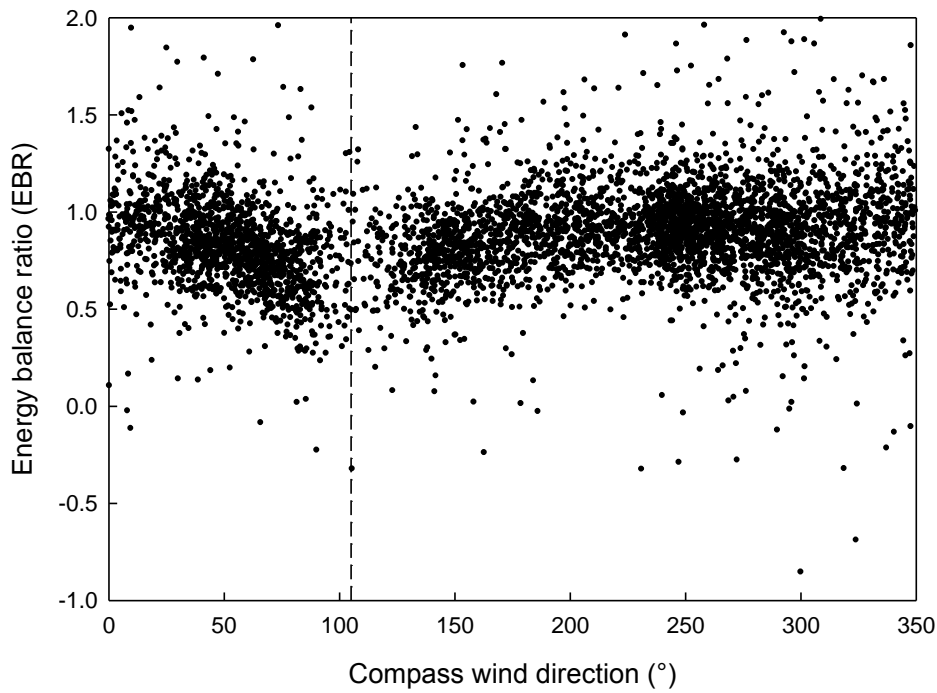


Figure 4.5 30-minute energy balance ratio (day time values only $R_n > 100 \text{ W m}^{-2}$) compared to wind direction for 15 December 2007 to 30 November 2008. Vertical dashed line shows orientation of tower.

4.2.2 Seasonal closure

To assess seasonal changes in energy balance closure, closure was calculated on a daily basis. Figure 4.6 shows the regression analysis of available energy ($R_n - G$) against convective energy ($\lambda E + H$) totals on a daily basis where the regression slope was 0.8699 and the y-intercept was $-0.207 \text{ MJ m}^{-2} \text{ day}^{-1}$. EBR on the daily scale was 0.8055 suggesting that on average, measured energy fluxes accounted for about 81% of available energy.

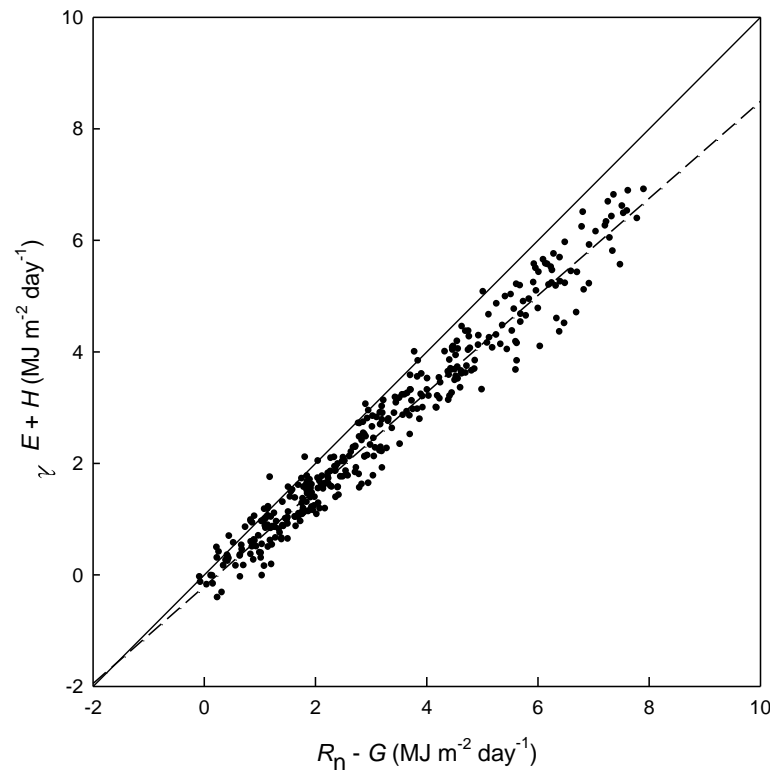


Figure 4.6 Daily energy balance ratio for the period 15 December 2007 to 30 November 2008 to show lack of closure.

Figure 4.7 shows the daily energy balance ratio through the year in order to see seasonal changes in closure. Energy balance ratios appeared to be about 0.8 during most of the year, with very little scatter for the months December 2007 to April 2008, however with a very slight downward trend. During April 2008, daily ratios were more scattered but remained around 0.75 until June, when ratio trends became highly variable and dropped suddenly to an average low of about 0.5. After September 2008, ratios became stable again at around 0.9 with some variability early October and November 2008. The reason for the sudden drop in closure was most likely due to lower energy inputs during this time of year.

Figure 4.8 shows the cumulative evaporation measured by eddy covariance comparing data that is not forced via energy balance closure and when it is forced using Equation 4.2. There was a very gradual separation between the two datasets as time progressed which shows the significant impact of forcing energy balance closure when using eddy covariance, particularly when analysing annual datasets

for comparison of long timescales. Unforced data resulted in a total evaporation of 655 mm of evaporation over the study period while when data was closure forced, evaporation totalled 752 mm, a difference of 97 mm.

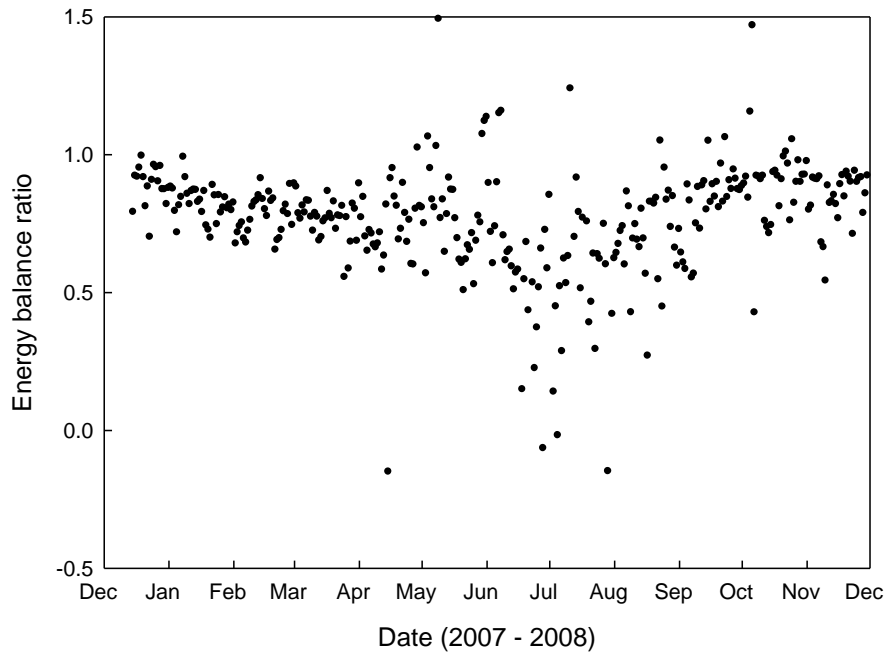


Figure 4.7 Daily energy balance closure for the period 15th December 2007 to 30 November 2008.

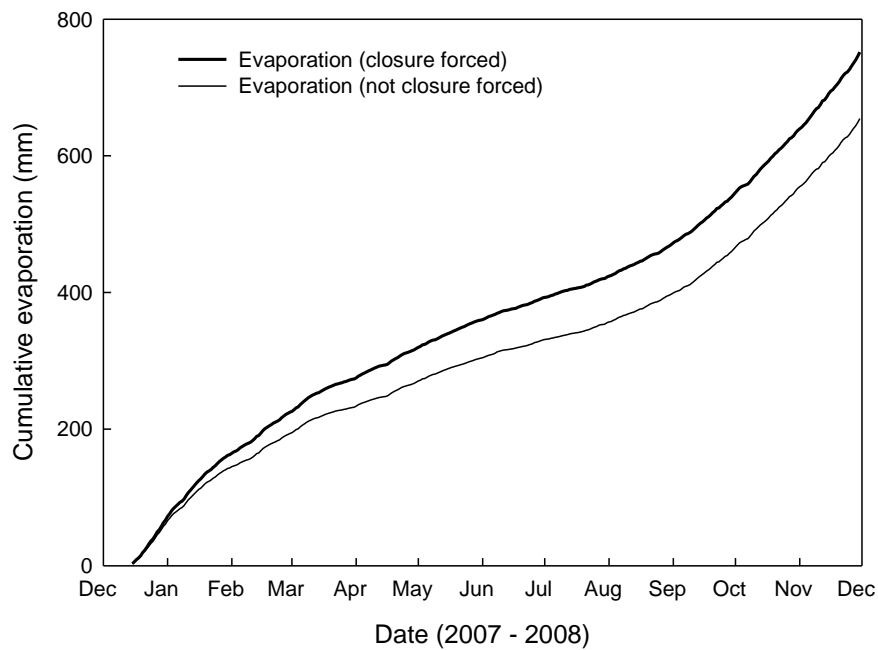


Figure 4.8 Cumulative evaporation for the period 15 December 2007 to 30 November 2008 showing forced data and un-forced data.

4.3 Effects of gap-filling

The gap-filling models that were used (described in Section 3.4.3.3) appeared to work well and filled missing data to an acceptable standard. However, what did appear to happen on a diurnal timescale was that when data required gap-filling at night, when R_n was negative, there was a tendency for the gap-filling model to over predict $\lambda E \sim 10 \text{ W m}^{-2}$ when it was expected to be about zero. Because this only occurred when gaps existed in the data, it was not always a problem, since gaps were not always present or were not continuous. Figure 4.9 shows the diurnal energy balance for 1 July 2008 where gaps have been filled using the gap-filling model. Filling was required for all of the early morning data but measurements were complete for the evening of that day. When actual measurements were present for night time, λE was zero (after 18:30 in Figure 4.9), however when λE required gap-filling, it was near 10 W m^{-2} (morning in Figure 4.9). The shaded area in Figure 4.9 indicates the area where λE was likely to be over adjusted by the gap-filling model. This over adjustment will mostly likely affect those seasons in which a large amount of gap-filling is required, such as winter when sensors are wet and when energy fluxes are low. About 10 W m^{-2} extra energy is not a large amount during summer when daily energy fluxes are very high, but in winter 10 W m^{-2} extra energy may make a large difference for the calculation of daily E due to the small daily flux. This could lead to a bias of increased evaporation calculated for days that require large amounts of gap-filling during night time hours.

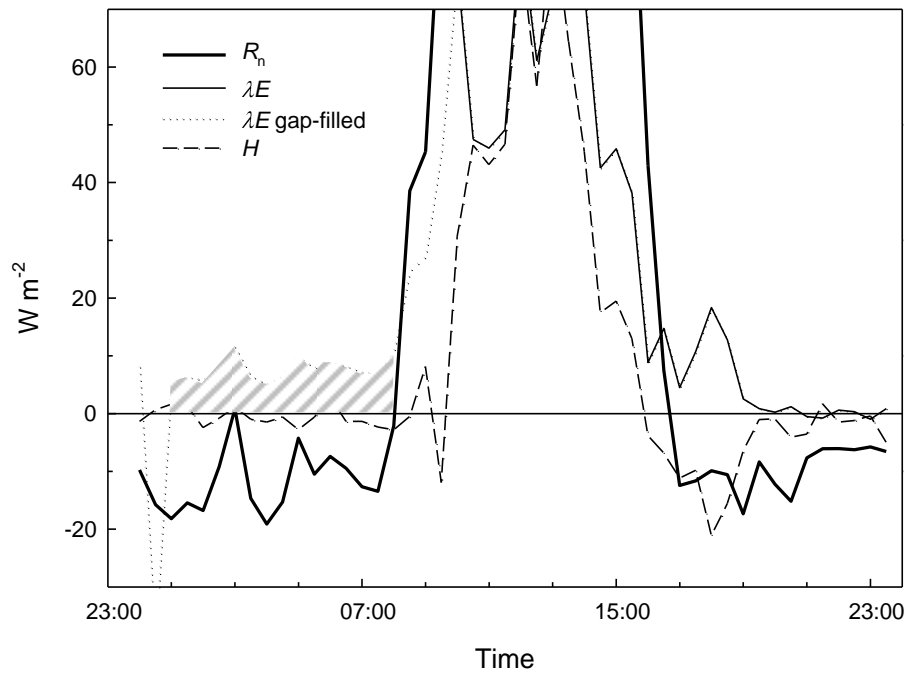


Figure 4.9 Time series for 1 July 2008 showing data that required gap-filling where the grey shaded area shows how λE is over calculated at night by the gap-filling model when it should be closer to zero.
 Note: scale small to show small night time fluxes where day time fluxes are much higher.

4.4 Lysimeters as an independent measurement of E

Small weighable lysimeters were used during three short campaigns to gain an independent measure of E for comparison with E_{EC} : autumn (6 – 15 March 2008), winter (8 – 10 July 2008), and spring (8 – 14 November) 2008. Methods of lysimeter deployment are described in Section 3.3.2. Daily E_{EC} was computed for each of these days by using 8.00 am to 8.00 am data to gain an exact measure of E to match the period of lysimeter measurement. Both closure forced and non-closure forced E were computed for comparison to evaporation from lysimeters (E_{lys}).

4.4.1 Autumn lysimeter study

Conditions for the period 6 March 2008 to 15 March 2008 were very dry. The last significant rainfall event that occurred before this study was on 4 March 2008 in which 6.8 mm fell in the 24 hour period followed by 0.4 mm the following day. No rainfall occurred during the study period and volumetric moisture contents dropped 9% from 39.5% to 30.5% during the 10-day lysimeter study (Figure 4.10b).

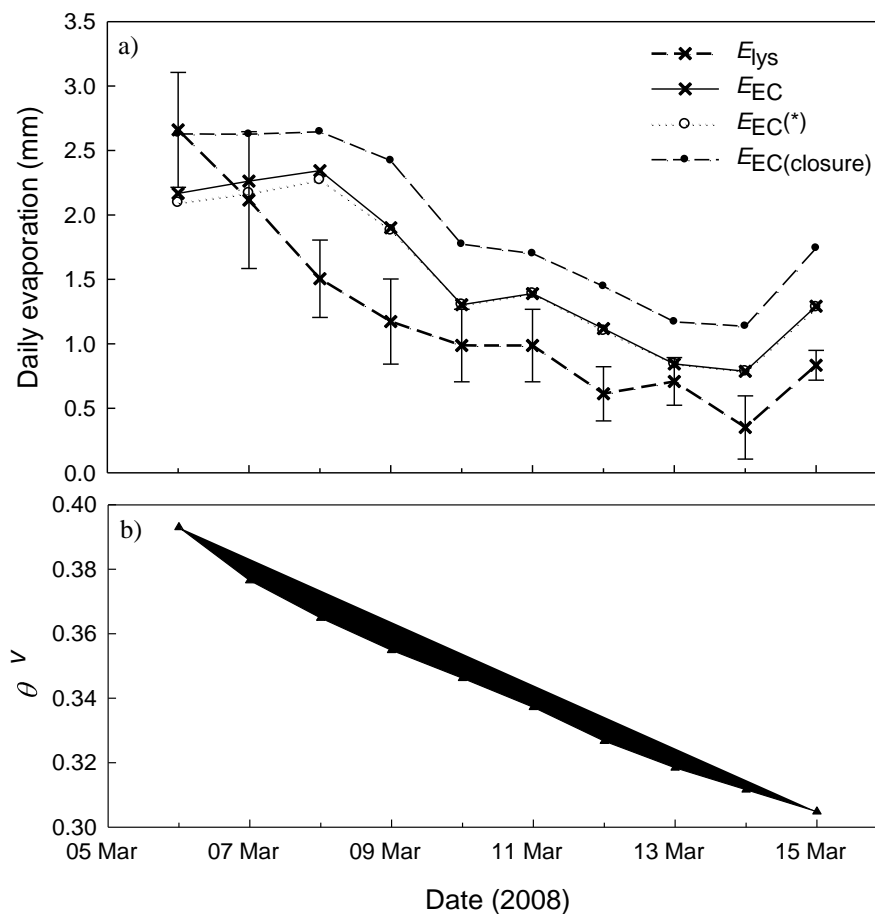


Figure 4.10 a) Comparison between eddy covariance (E_{EC}) and lysimeter (E_{lys}) measurements of daily evaporation for 6–15 March 2008. E_{lys} is the mean measurement from all 10 lysimeters, bars indicate 95% confidence limits around the mean. $E_{EC(*)}$ are EC measurements where night-time gaps in λE data were set to zero and $E_{EC(closure)}$ is EC closure forced evaporation. b) is volumetric moisture content for the same period.

Total evaporation measured by EC (E_{EC}) on 6 March 2008 (Figure 4.10a) was lower than that recorded by lysimeters. After this date however, mean lysimeter evaporation was lower than E_{EC} , but both followed the same trend of decreasing evaporation through the study period. On March 1, 10 and 13 E_{EC} measures were within 95% confidence bounds of lysimeter measurements. When E_{EC} was calculated by forcing energy balance closure ($E_{EC(closure)}$), evaporation measures resulted in an increase of 0.4 mm on average (or a 16% increase) in E from non-closure forced data (E_{EC}). This would suggest that the autumn lysimeter study did not support closure forcing, although faults with the lysimeter deployment may also have an effect on these results. Figure 4.10a also shows the measured E_{EC} when night time gap-filling was forced to zero due to the possible tendency for gap-filling models to over predict λE at night (see Section 4.3). During the autumn study this problem did not seem to affect results due to the high available energy during this season and very little missing data. Total evaporation measured by the lysimeters over this ten day period was 11.9 mm where evaporation measured by EC (not forced) totalled 15.4 mm. The lower evaporation rates measured by the lysimeters during this period were most likely a consequence of the shallow pots restricting plant rooting depth. During dry soil moisture conditions, when evaporative demand is high, plants struggle to find water for survival. This may allow some vegetation to extend their roots much deeper into the soil profile, resulting in higher rates of evaporation. Because the lysimeter pots were only 20 cm deep, plants growing inside them had limited access to soil water and could not access deeper soil moisture. This resulted in a lower evaporation rate from the lysimeters, in which most grass was dead by the end of the study period, than those evaporation rates measured by the eddy covariance technique, which was for the pasture as a whole.

4.4.2 Winter lysimeter study

During the winter study, conditions were cold with very frosty nights and mornings. Conditions were moist with a soil moisture content of about 54% on 8 July 2008 which dropped by almost 2% over the following two days (Figure 4.11b).

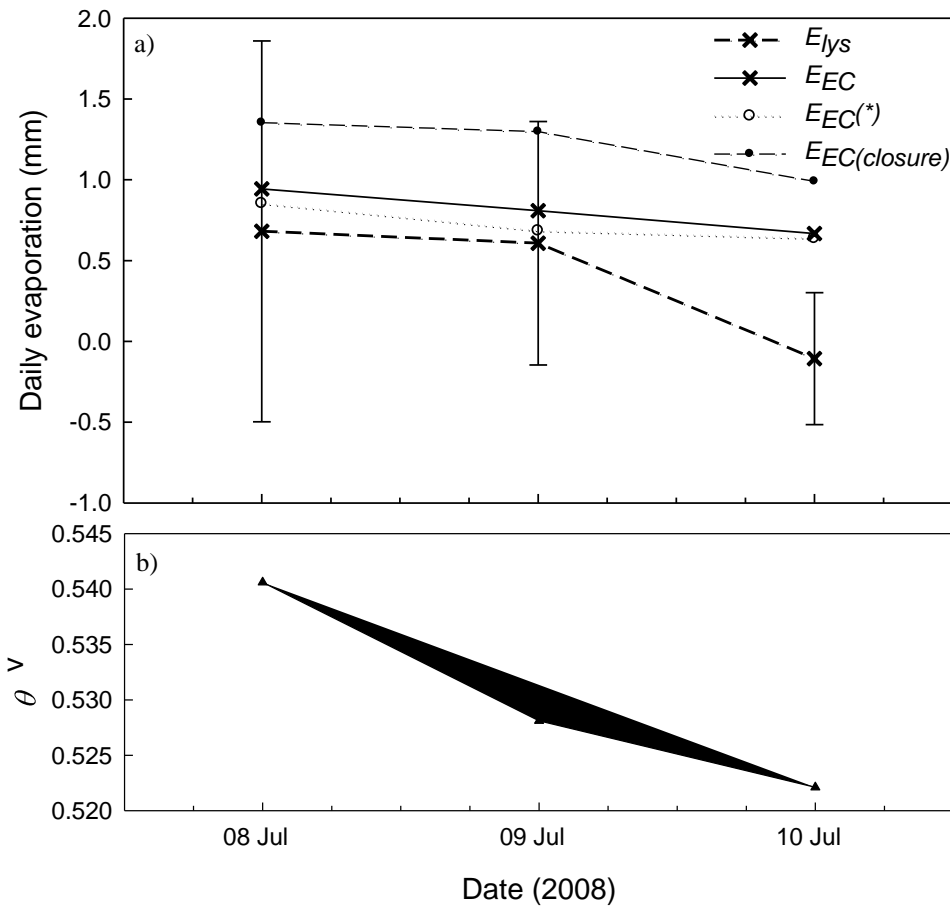


Figure 4.11 a) Comparison between eddy covariance (E_{EC}) and lysimeter (E_{lys}) measurements of daily evaporation for 8–10 July 2008. E_{lys} is the mean measurement from all 10 lysimeters, bars indicate 95% confidence limits around the mean. $E_{EC(*)}$ are EC measurements where night-time gaps in λE data were set to zero and $E_{EC(closure)}$ is EC closure forced evaporation. b) is volumetric moisture content for the same period.

Evaporation rates were fairly low due to lower available energy during winter. Some lysimeters recorded weight gains in a 24 hour period, resulting in negative evaporation. This is possible when net condensation is greater than net evaporation over the daily period but may also indicate other errors. Lysimeter measurements averaged lower than EC measurements (Figure 4.11a) however on the first two days (8 – 9 July 2008) evaporation differences were small (0.3 mm and 0.2 mm respectively) and EC measurements fell well within the 95% confidence bounds of the measured lysimeter rates. The measurement on 10 July 2008 was 0.8 mm lower than EC evaporation and could not be explained with certainty, but may have been caused by a number of lysimeters having negative evaporation (possible net condensation). Using closure-forced data to calculate E

resulted in a 0.4 mm average increase in E_{EC} which was an increase of 33.5% (due to the low rate of evaporation). Although this was a large difference, $E_{EC(closure)}$ still fell within the 95% confidence bounds of E_{lys} on the first two days of measurement. This result also suggests that this lysimeter study does not support closure forcing when using EC. Total E_{lys} for the period was 1.2 mm and E_{EC} totalled 2.2 mm. Although the rooting depth of the plants was likely to be deeper than the 20 cm depth of the pots, it is unlikely that this was restricting evaporation at this time of year because volumetric moisture contents were high (~53%, Figure 4.11b). The larger E_{EC} may be due to the night time gap-filling models that were applied. Gap-filling models appeared to over predict λE by about 10 W m^{-2} at night when rates should be about zero. This lead to an over measure of E when gaps existed in the data at night. Figure 4.11a also shows the E_{EC} when night time gap-filling models were set to zero which resulted in slightly lower E_{EC} by approximately 0.1 mm/day. This is a possible problem during winter conditions when energy rates are low, a small over estimation in the gap-filling models may have a large effect on E_{EC} rates when comparing to lysimeters.

4.4.3 Spring lysimeter study

Conditions during the spring study were moist with relatively high available energy, resulting in higher evaporation rates than the autumn and winter studies. Soil moisture content was 53% on 8 November 2008 (Figure 4.12b) and dropped by more than 4% over the 7 day period, to below 49%.

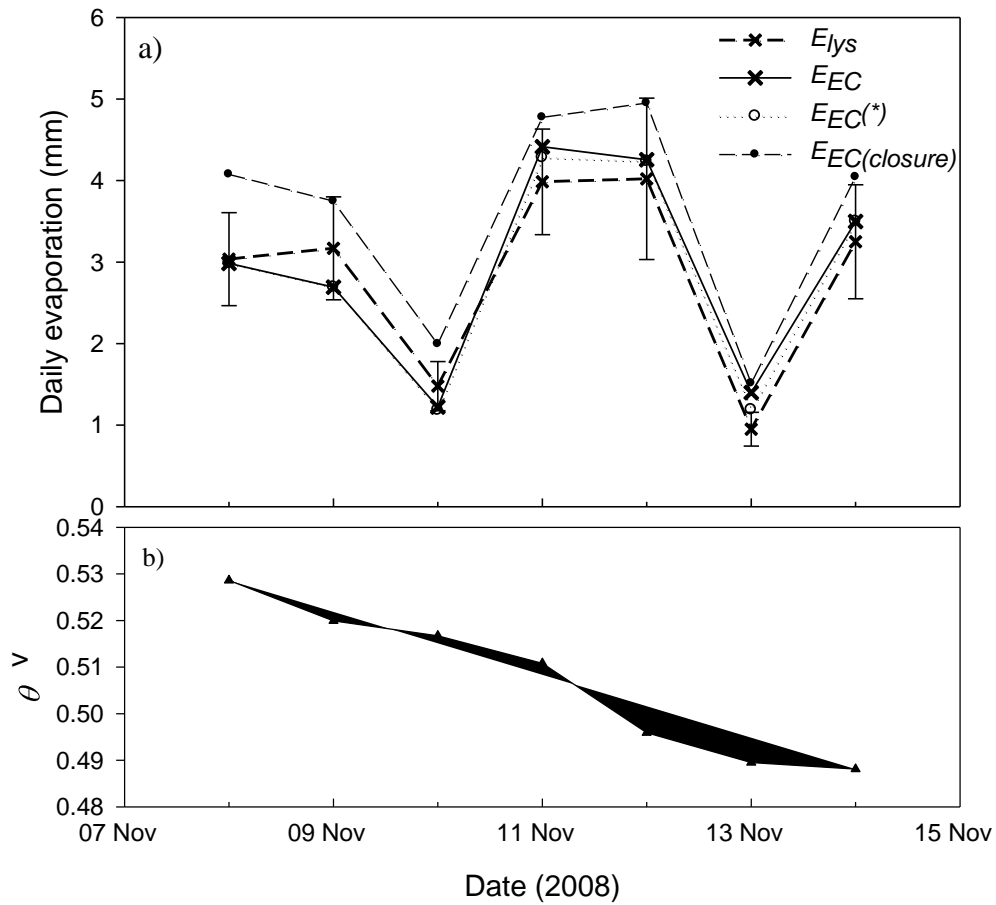


Figure 4.12 a) Comparison between eddy covariance (E_{EC}) and lysimeter (E_{lys}) measurements of daily evaporation for 8–14 November 2008. E_{lys} is the mean measurement from all 10 lysimeters, bars indicate 95% confidence limits around the mean. $E_{EC(*)}$ are EC measurements where night-time gaps in λE data were set to zero and $E_{EC(closure)}$ is EC closure forced evaporation. b) is volumetric moisture content for the same period.

Both E_{lys} and E_{EC} appeared to be highly dependent on available energy, hence the sudden drop on both 10 November 2008 and 13 November 2008 when cloud was present for most of the day. All other days were clear, sunny days with high rates of evaporation. Differences between E_{lys} and E_{EC} were very small and E_{EC} always fell within the 95% confidence bounds of E_{lys} except on 13 November. Once again, when closure was forced for the EC data, an increase of 0.66 mm on average resulted which was approximately 18% higher than non-forced E . Some $E_{EC(closure)}$ measurements still fell within the 95% confidence bounds but again, this result did not support forcing closure when using EC data. The limitation of lysimeter depth did not appear to be an issue during this study and biases due to night time gap-filling models did not appear to affect E_{EC} results during this

season. Totals for the period for E_{lys} was 19.9 mm while E_{EC} measured 20.1 mm with only a 0.2 mm difference which is negligible.

4.4.4 Overall lysimeter/EC accuracy

The lysimeters often measured values of evaporation less than the eddy covariance technique, particularly when energy balance closure was forced. Figure 4.13 shows a scatter plot of E_{lys} versus E_{EC} .

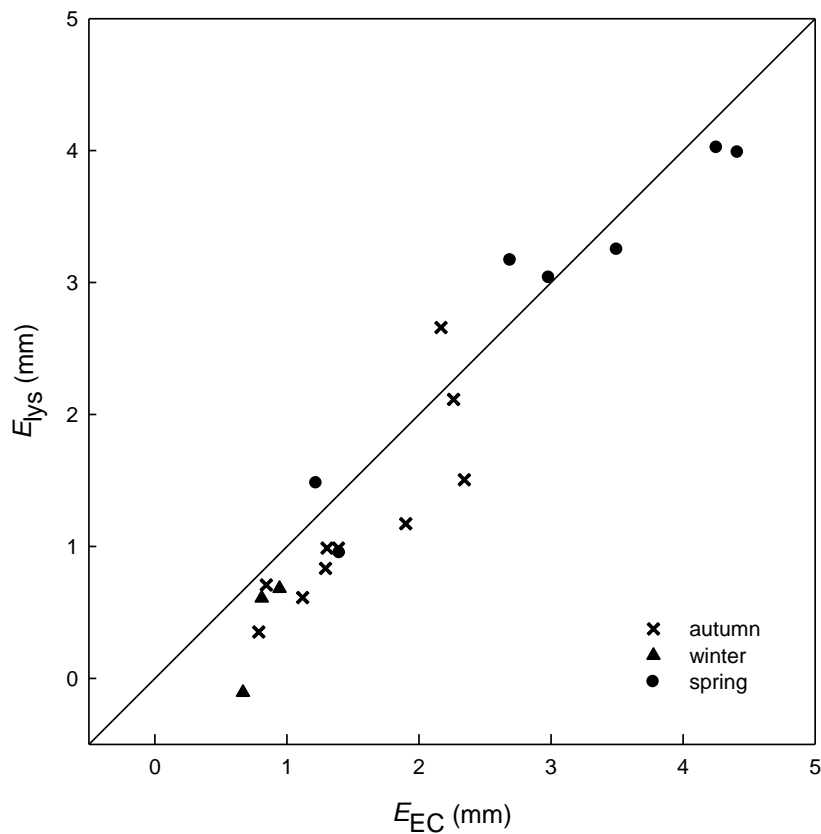


Figure 4.13 Scatter plot of measured eddy covariance and measured lysimeter evaporation for all lysimeter studies.

Most data fell below the one to one line, indicating the lysimeters' tendency to under-measure evaporation. The general under-measurement by lysimeters relative to EC could be the cause of several different factors including:

- 1) The two measurement techniques measured evaporation on different spatial scales. The sample number (10) may not always be adequate to represent evaporation occurring on a hectare scale such as measured by eddy covariance.
- 2) EC measurements were biased by closure forcing and/or night time gap-filling. This may result in an over calculation of evaporation, particularly during winter.
- 3) The depth of the lysimeter pots was not always deep enough to allow vegetation free access to soil water at depths greater than 20 cm. This was particularly the case during autumn when soil moisture contents were very low.
- 4) The lysimeter area may have been measured incorrectly or plant cover may have affected area assumptions.
- 5) Lysimeters may distort soil temperature and soil moisture regimes in comparison to that in the soil outside the lysimeter, affecting measured evaporation rates.

The reason for the autumn lysimeter study resulting in an underestimation is thought to be due to the limitations caused by lysimeter depth. The winter study required a longer sampling time and there may be some doubt as to the effects of night time gap-filling of E_{EC} data during this season, however two of the three days resulted in very similar results. The lysimeter study during spring resulted in good data and provided confidence in the EC method. Forcing energy balance closure led to a greater difference between E_{lys} and E measured by EC, leading to the suggestion that this lysimeter study did not support closure forcing of the energy balance.

4.5 Discussion

Results of energy balance closure and ground-truthing using lysimeters have been analysed and explained and have produced the following deductions:

- Energy balance measurements (30 min data) resulted in a lack of closure by 24% at Scott Farm and was worst during wind directions from 75 – 125°.

- The daily energy balance ratio was 0.81 and was worse, with more scatter, from June – September 2008 most likely due to low available energy during this season.
- Forcing energy balance closure throughout the seasons did result in an increase in EC evaporation, and more so in winter due to poorer closure during this month.
- Lysimeters need to be much deeper to get more accurate measures of E , particularly when measuring E during summer.
- Winter lysimeter results required a longer sampling time and there may be some doubt as to the effects of night time gap-filling on E_{EC} data during this season.
- The lysimeter study done during spring (November) was successful and provided confidence in EC data.

Energy balance closure has been found to be an issue when using the eddy covariance method for measuring evaporation (Twine *et al.* 2000; Wilson *et al.* 2002; Oncley *et al.* 2007). An average daily EBR of about 80% was measured for this study, leaving 20% of the available energy unaccounted for. There are several hypotheses as to the reason for the imbalance in closure. Oncley *et al.* (2007) attempted to account for advection effects and energy used for photosynthesis by vegetation but still could not explain 10% of the imbalance of energy and suggested non-local advection was the cause. Wilson *et al.* (2002) also found an imbalance of 20% and suggested this could be due to an underestimation of the energy storage terms since they are usually assumed to be negligible. Wilson *et al.* (2002) found that the energy imbalance was persistent through all seasons but that the energy balance ratio was closest to 1 during the warmer seasons. This was also true at Scott Farm where, although closure was usually less than 1 through the year (apart from a few days where $EBR > 1$), closure appeared best during the warmer seasons than during winter. Foken (2008) hypothesised that the energy balance closure problem was a scale difficulty in which eddy covariance measures λE and H on a relatively small scale, missing the fluxes of convective energy of larger eddies in the lower boundary layer of the atmosphere which do not make contact with the Earth's surface but interact with the smaller eddies. Because there is not yet a means of measuring these larger turbulent exchanges, Foken (2008)

suggested the Bowen ratio method of Twine *et al.* (2000) as the best means of closing the energy balance currently. To force closure of the energy balance, the Bowen ratio closure method was used at Scott Farm, assuming that the Bowen ratio is measured accurately so the two convective fluxes are increased proportionately (Twine *et al.* 2000). Foken's (2008) hypothesis of the scale issue brings to the point that R_n and G may also not represent the spatial scale of hectares that eddy covariance measures on. This issue should be a key subject for future research.

The most significant physical limitation of lysimeters for this study was the depth of the lysimeter pots which were too shallow during periods of low soil moisture content. During these conditions vegetation becomes stressed and plants are likely to extend their roots deeper into the soil profile than to just the 0.2 m allowed for by the lysimeter pots. Similar results were found by Grimmond *et al.* (1992) who also used small lysimeters during drought conditions with depths of only 0.265 m and 0.198 m. Their study was for a duration of 3 weeks and they found that at the beginning of the period, lysimeters measured greater evaporation rates than eddy covariance, but as the vegetation became more stressed, lysimeters began measuring below eddy covariance rates, similar to what was found in autumn at Scott Farm. Grimmond *et al.* (1992) found that a major limitation of the lysimeter technique for measuring evaporation was that the vegetation must have a rooting depth within the depth of the lysimeter containers, just as was found for this study. This is in comparison to Daamen *et al.* (1993) who compared depths of lysimeters (0.1 m and 0.2 m) but found no significant difference in evaporation rates from either. Although the deeper lysimeter always recorded a higher rate of evaporation, differences were found to be not significant which may mean the difference in depth was not enough to result in a difference. Daamen *et al.* (1993) also only used bare soil cores so no vegetation effects were present.

Using mini-lysimeters to ground-truth eddy covariance measurements at Scott Farm resulted in some interesting findings. The autumn lysimeter study appeared to be most limited by the size of the lysimeters, however evaporation trends were consistent between both methods of measurement. The winter study was also good overall, however this study highlighted the problem of the gap-filling technique at night time over-estimating λE by $\sim 10 \text{ W m}^{-2}$ due to lower available

energy and more gaps in the data set at this time of year. During well-watered and high available energy conditions, such as those experienced during spring, the lysimeter technique compared very favourably with EC. All three lysimeter studies support the need for gap-filling, although an adjustment may need to be considered for night time periods, however the studies did not entirely support closure forcing.

5 Surface energy balance and evaporation

5.1 Introduction

An understanding of the surface partitioning of energy needs to be developed as this is often the main driver of the evaporation process. Energy at the Earth's surface is ultimately derived from solar (or shortwave) radiation, which then becomes terrestrial (or longwave) radiation. These forms of radiation provide the main source of energy to evaporate water. The partitioning of energy into sensible and latent heat varies diurnally and seasonally and is described in this chapter. Advection often plays an important role in providing an extra energy source for evaporation in certain environments and the possibility is described here.

5.2 Surface radiation balances

5.2.1 Longwave and shortwave radiation

Figure 5.1a shows the radiation balance data for three consecutive days in January 2008. The first two days were sunny days with little or no cloud, the third day was partly cloudy. Net radiation (R_n) is controlled largely by incoming shortwave radiation ($K\downarrow$). During cloudy conditions $K\downarrow$ was restricted from reaching the Earth's surface, causing the spiky effect and smaller amount of energy reaching the ground. Reflected shortwave radiation ($K\uparrow$) is also controlled by $K\downarrow$, as Figure 5.1a shows a smooth bell shaped curve during sunny conditions and a more spiky effect during cloudy conditions. No $K\uparrow$ or $K\downarrow$ was present at night as this energy is derived entirely from the sun, giving a diurnal pattern of high values during the day and values of zero at night. Incoming longwave radiation ($L\downarrow$) did not show the same prominent diurnal effect that R_n , $K\downarrow$ and $K\uparrow$ do. This was due to the

effects of clouds and the atmosphere radiating $L\downarrow$ towards the surface both during the day and night, dampening any prominent diurnal patterns, however a peak still occurred during the day with a few hours lag from solar noon. Outgoing longwave radiation ($L\uparrow$) showed a stronger diurnal effect due to its dependence on surface temperatures, peaking just after the maximum $K\downarrow$ due to a slight lag effect for the time taken to heat the soil. $L\uparrow$ exceeded $L\downarrow$ at all times because the surface was warmer than the atmosphere, particularly during the day.

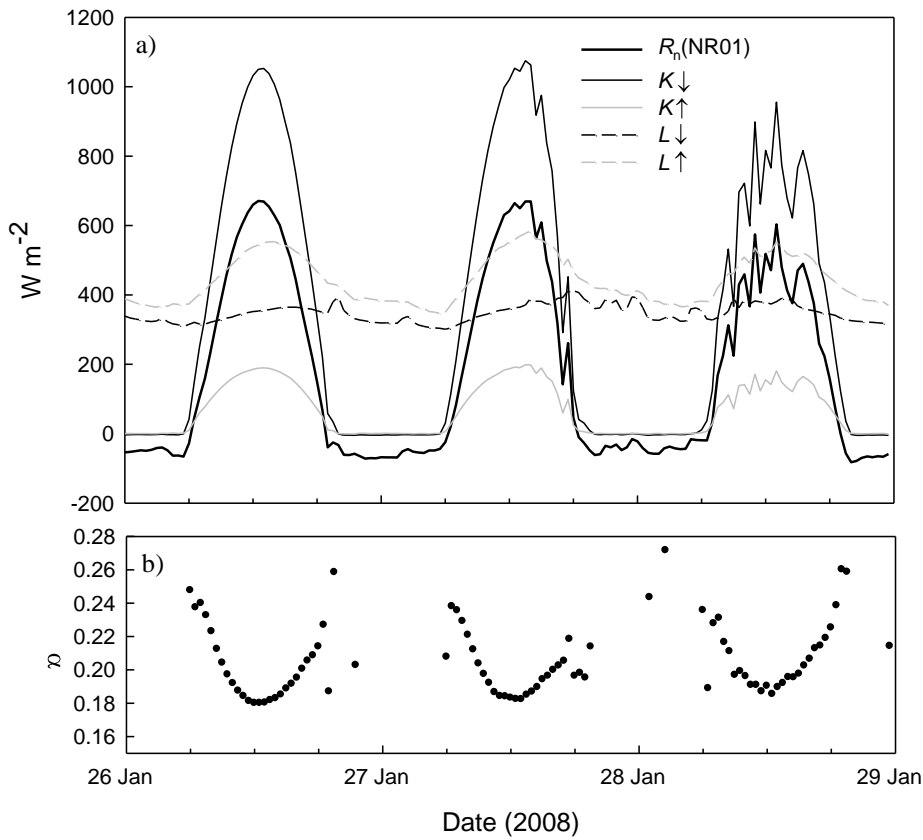


Figure 5.1 a) Radiation balance. R_n , $K\uparrow$, $K\downarrow$, $L\uparrow$ and $L\downarrow$ for 26-28 January 2008 and b) the albedo for the same period. For convenience, $K\uparrow$ and $L\uparrow$ are shown as positive values.

R_n was positive during the day and followed $K\downarrow$ due to the surplus of energy provided by shortwave radiation which exceeded net longwave losses, but R_n became negative at night due to a lack of shortwave input (Spronken-Smith, 2001) with longwave fluxes remaining high. This is because at night $R_n = L^* = L\downarrow + L\uparrow$ so it is the difference between $L\downarrow$ and $L\uparrow$ that determines R_n .

A regression of daily and half hourly R_n on $K\downarrow$ is given in Appendix C to show how $K\downarrow$ can be used to estimate R_n if no R_n measurements are available at a site with similar vegetation.

5.2.2 Albedo

Figure 5.1b shows the diurnal pattern of albedo for the three day period that was described in Section 5.2.1. Because albedo is a ratio, when either $K\downarrow$ or $K\uparrow$ is very small, such as at night, the ratio results in a wild number, causing the scatter of albedo during night time hours or leading to very low ratios. During the day however, for this three day period, albedo averaged about 0.2 with a diurnal cycle of higher values in the morning and evening and lowest values at midday. The reason for this diurnal pattern is the angle of the sun at certain times of day, resulting in more reflection when the sun is at an angle and less when the sun is directly overhead.

Figure 5.2a shows the calculated daily albedo for the period 19 January 2008 to 29 June 2008 when NR01 measurements were available, along with the rainfall (b) and volumetric moisture content (c) for the same period. Albedo was calculated using Equation 2.4 for daily total $K\downarrow$ and $K\uparrow$. The sudden drop in albedo that occurred in the first two weeks of February occurred over 4–5 days and was thought to have been caused by an abrupt change in vegetation conditions for the area the instruments measure above. This coincided with a sudden increase in volumetric soil moisture content, however albedo remained low when soil moisture began to dry again. The albedo averaged 0.2 when measurements first began in mid January 2008, the sudden drop occurred during the second week of February where albedo dropped ~5% to 0.15, after which it began to gradually increase to reach an average of approximately 0.23 from May onwards. The spikes in albedo usually coincided with rainfall events as seen in Figure 5.2a and b, which suggested that water droplets may have impeded the $K\downarrow$ measurement on the up-facing instrument window, during relatively cloudy conditions.

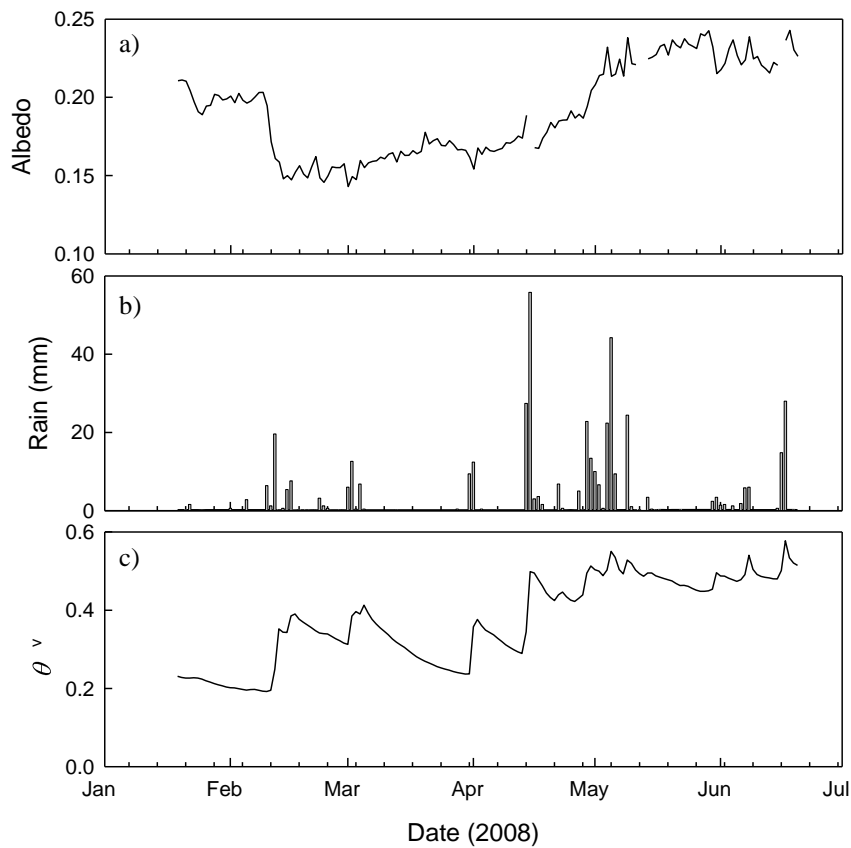


Figure 5.2 a) Daily albedo, b) rain and c) θ_v from 19 Jan to 29 Jun 2008.

5.3 Surface energy balance

5.3.1 Diurnal energy balances

The energy available at the Earth's surface is controlled by the shortwave and longwave radiation fluxes as shown in Figure 5.1. The majority of this energy is then used to heat the air (sensible heat flux H), evaporate water (latent heat flux λE), and transferred into the soil (soil heat flux G). Figure 5.3a shows the net radiation (R_n) and its three partitioned forms of energy for 31 December 2007 to 2 January 2008 showing a combination of sunny and cloudy days. Cloudy days resulted in a more spiky energy balance due to the restriction of solar radiation, while sunny days resulted in a smooth curve. During the night and early morning, fluxes were small and often negative. As net radiation increased following sunrise, other fluxes also began to increase, peaking around solar noon when net

radiation reached its daily maximum. The conditions shown in Figure 5.3a were before drought conditions began having a significant effect on the energy balance. On 1 January 2008 (Figure 5.3a) λE was the dominant energy balance component amounting to 65% of R_n , followed by H (29% of R_n) and G was the smallest at 6% of R_n . At this time of year Bowen ratios were below one (Figure 5.3b) due to the abundance of water for evaporation and ranged from 0.43–0.5 for these days. Occasionally there were some outliers of the Bowen ratio due to the very small values of λE or H . Negative β indicates H and λE have opposite signs, common early morning and late in the day and night. Table 5.1 gives a summary of the energy components for the days shown in Figure 5.3 and 5.4.

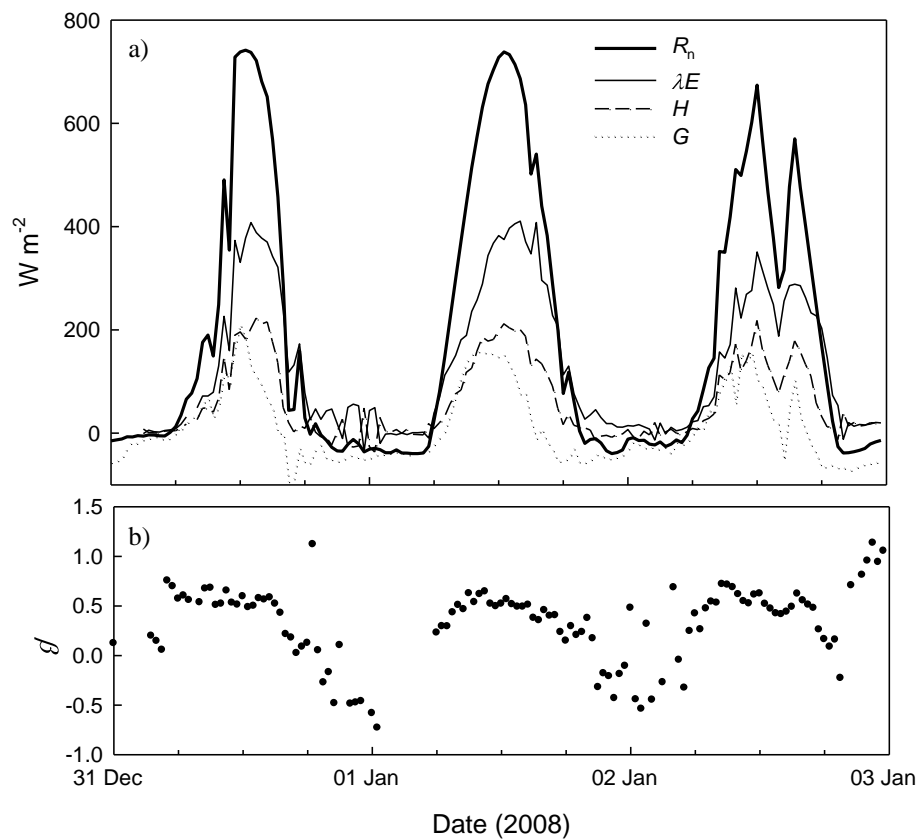


Figure 5.3 a) Diurnal energy balance components and Bowen ratio for the three days 31 December 2007 to 2 January 2008 and b) Bowen ratio for the same period.

Table 5.1 Daily totals of energy fluxes, Bowen ratio, evaporative fraction and θ_v for 31 December 2007 - 2 January 2008 and 4 - 6 February 2008. Refer to Figure 5.3 and 5.4.

	R_n	G	λE	H	β	$\lambda E/R_n$	θ_v
	MJ m ⁻² day ⁻¹					%	%
31 Dec 07	14.8	0.8	9.8	4.2	0.43	66	56
1 Jan 08	19.7	1.2	12.8	5.7	0.44	65	53
2 Jan 08	15.7	0.4	10.2	5.1	0.50	65	50
4 Feb 08	14.5	1.1	4.6	8.8	1.93	32	31
5 Feb 08	16.2	-0.9	7.0	10.0	1.42	44	31
6 Feb 08	16.3	0.4	4.8	11.1	2.32	29	31

Figure 5.4a shows three days of energy partitioning for 4–6 February, but this time it shows the behaviour of the energy components during drought conditions (where Table 5.1 shows the daily totals for each flux). H exceeded λE during the course of each day and even G was greater than λE during the mornings, but decreased quite early and became negative in late afternoon. There were two possible causes (or a combination of the two) for G to peak earlier in the morning than other fluxes. One possible cause was a difference and change in temperature gradients in the soil surface layer. In the mornings the soil was cool, leading to a more rapid change in soil temperature as it was heated from the sun, while near midday the change in soil temperature was no longer as great. The second cause, which most likely acts together with the morning temperature gradient, was turbulent transfer or wind speeds during the course of the day. In the late morning and afternoon, wind speeds increase which helps mixing of the excess surface heat into the atmosphere to enhance λE or H (Oke, 1987).

Under these conditions (5 February 2008), λE was only 44% of R_n , H was 61% and G was -5%. This reversal of partitioning resulted in large Bowen ratios that reached over 2 and were due to the limited availability of water at the land surface. A soil water deficit resulted in less energy being used for evaporation, so the energy that would usually be used to evaporate water was instead used to heat the soil and surrounding air.

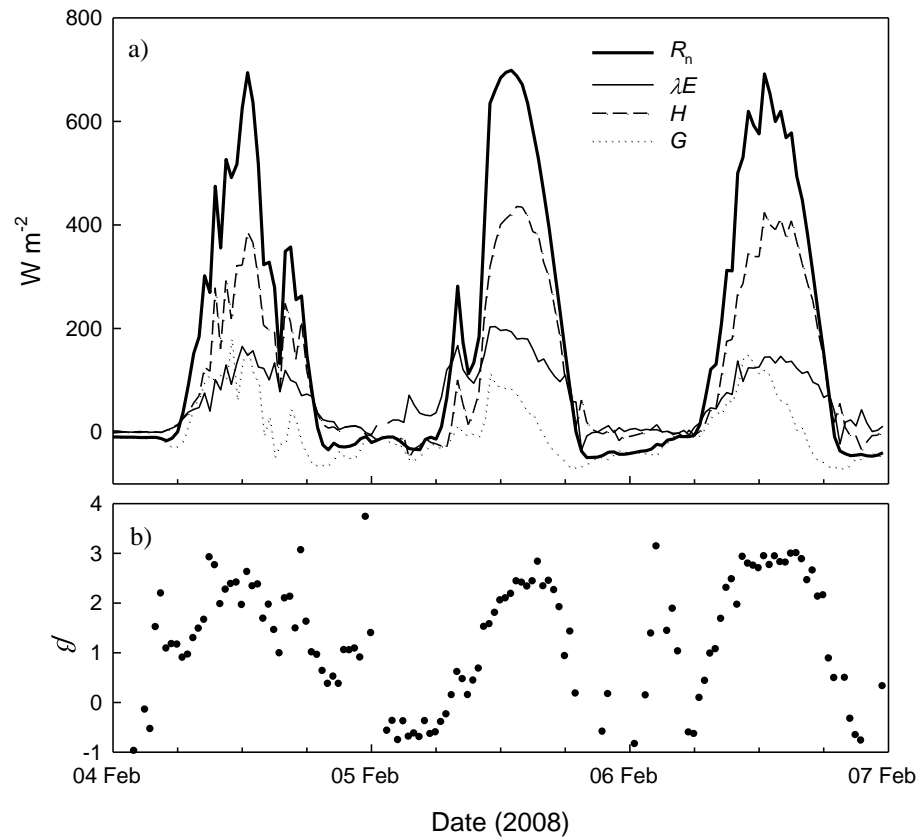


Figure 5.4 a) Diurnal energy components and b) Bowen ratio for the three days 4–6 February 2008.

5.3.2 Seasonal energy balances

Figures 5.5a, b, c and d show an ensemble average energy balance for each season, taken as the average diurnal cycle for the middle month from each season and Table 5.2 shows the daily totals as an average for each month. Figure 5.5a for the month of January (summer) failed to display the most extreme effects of the drought event that occurred predominantly in the months February and March. R_n values reached as high on average as 550 W m^{-2} at solar noon during summer while λE and H both reach an average of about 225 W m^{-2} on average for the month. This resulted in Bowen ratios of around 1 during daylight hours, while G peaked on average at just over 100 W m^{-2} . In autumn (shown as the month of April, Figure 5.5b), average peak R_n values dropped by more than 200 W m^{-2} , down to below 350 W m^{-2} . This resulted in λE and H dropping to about 150 W m^{-2} and 125 W m^{-2} respectively (i.e. λE larger), resulting in Bowen ratios below 1. G

also experienced a drop to approximately 75 W m^{-2} . Winter (July, Figure 5.5c) had the lowest R_n , peaking at below 200 W m^{-2} and λE and H peaking at about 95 W m^{-2} and 50 W m^{-2} respectively with Bowen ratios often below 0.5. G peaked at less than 70 W m^{-2} for the month. As conditions changed from winter to spring (October, Figure 5.5d), flux rates began to increase once again, with R_n reaching over 425 W m^{-2} at midday and λE ($\sim 260 \text{ W m}^{-2}$) becoming largely separated from H ($\sim 100 \text{ W m}^{-2}$) with Bowen ratios around 0.5. G also increased with the onset of spring, reaching a maximum of about 90 W m^{-2} on average for the month. See Appendix D for all twelve months of energy balance ensembles.

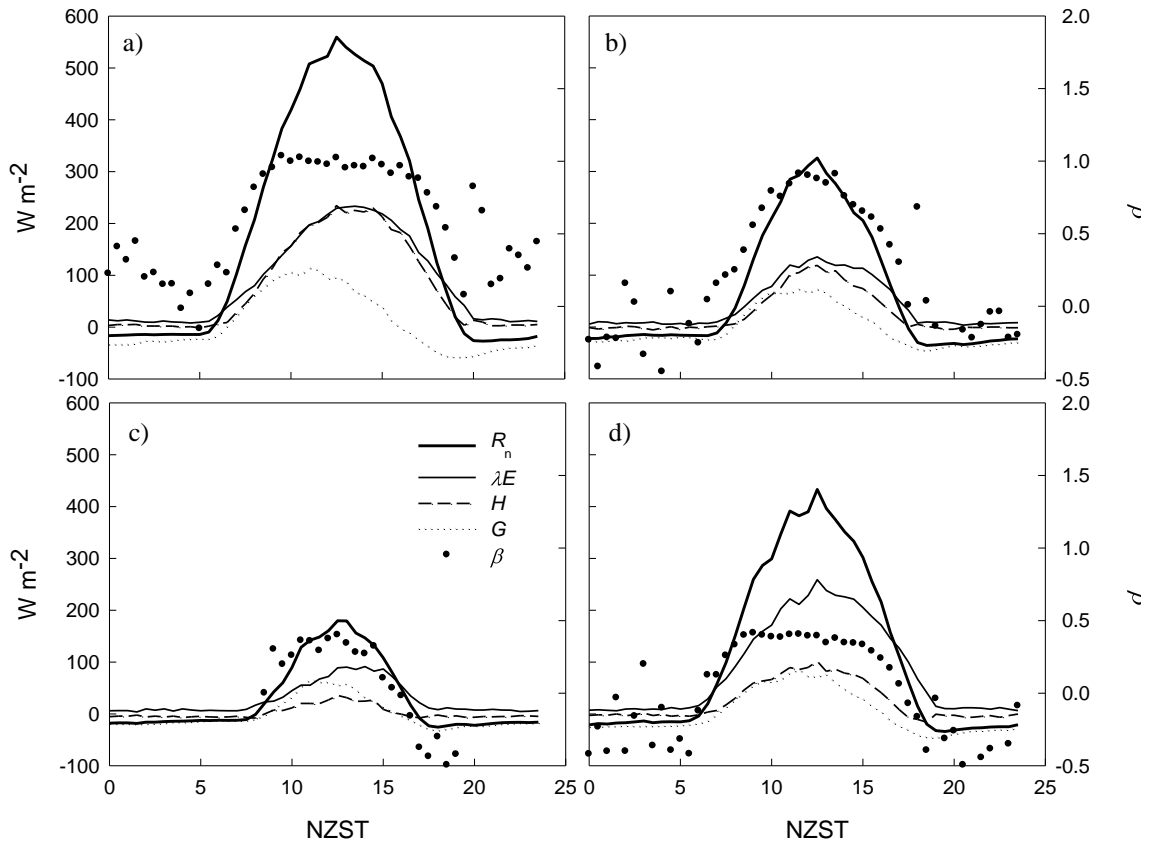


Figure 5.5 Diurnal energy balance ensembles including Bowen ratios for a) January, b) April, c) July, and d) October 2008.

Table 5.2 Daily average total energy fluxes for the months representing each season (Figure 5.5a, b, c and d) including β , evaporative fraction and θ_v .

	R_n	G	λE	H	β	$\lambda E/R_n$	θ_v
2008	MJ m ⁻² day ⁻¹					%	%
January	15.0	0.6	7.6	6.7	0.89	51	40
April	5.6	-0.2	3.7	2.2	0.60	65	60
July	2.5	-0.1	2.4	0.1	0.05	99	82
October	9.8	0.2	7.5	2.1	0.28	77	80

Figure 5.6a displays the annual partitioning (15-day running mean) of the energy balance components so an analysis of the progression through the year could be done. Mean R_n peaked in January and February 2008 at just over 15 MJ m⁻² day⁻¹ and steadily declined down to just over 2 MJ m⁻² day⁻¹ during June and July 2008, then began to steadily rise again with the onset of spring in September. λE declined from the beginning of measurements until near the end of February when it suddenly increased a small amount to then continue its downward trend until reaching a minimum in July at about the same level as R_n (2 MJ m⁻² day⁻¹). When analysing H from Figure 5.6a the reversal of dominance between λE and H during the drought period was obviously due to the initial increase in H where it exceeded λE , then dropped suddenly near the end of February (due to a significant rain event), then H exceeded λE again between March to April during the second most significant drying event of the drought. After this time, H decreased, reaching zero near the end of July, then slowly began increasing again during spring. G stayed very small throughout the year, being positive during summer and turning negative during autumn and winter, and then became positive again in spring when the soil began to gain heat once again.

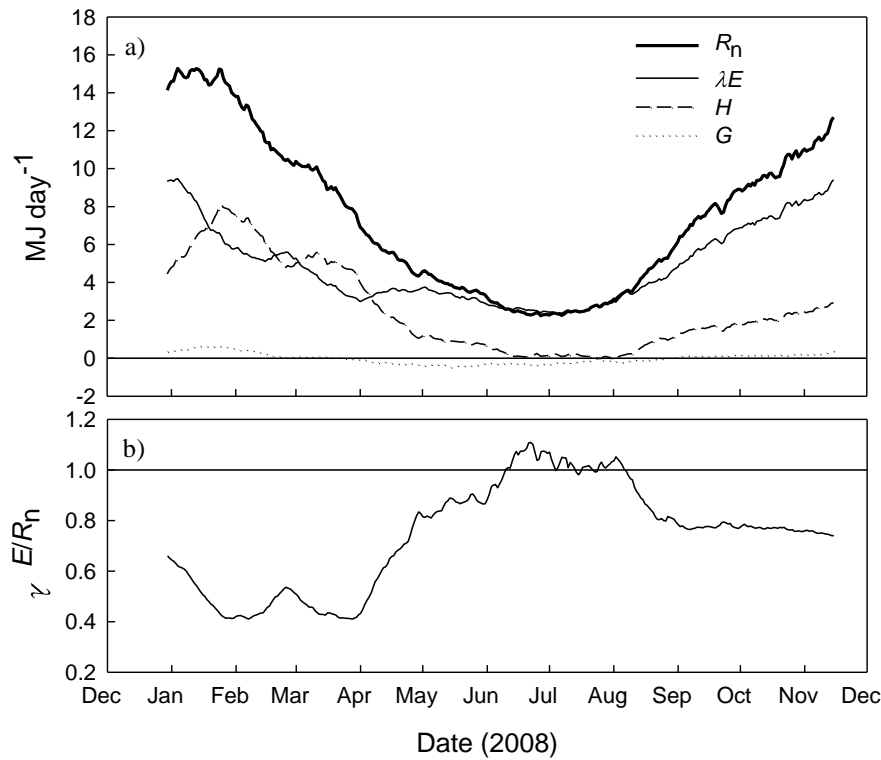


Figure 5.6 a) Annual 15 day running mean energy balance for Scott Farm and b) the ratio $\lambda E/R_n$ for 15 December 2007 to 30 November 2008.

5.3.3 Advection

Figure 5.6b shows a 15-day running mean of the evaporative fraction, $\lambda E/R_n$, through the year. The majority of available energy was portioned into λE through most of the year, but during the very dry conditions over the 2008 summer the partitioning was inverted, with H exceeding λE . The reason for this inversion was the lack of water in the plant canopy and underlying soil, resulting in less energy being used for evaporation and more energy being used to heat the overlying air. In the months of June and July, H and G were ~ 0 or slightly negative and the fraction of λE to R_n was above 1, indicating that another source of energy may exist. It is hypothesised to be energy sourced from the warm ocean surface surrounding New Zealand (Kelliher and Jackson, 2001) causing advection to occur during certain wind conditions during particular seasons of the year and is a suggested topic of future research. Figure 5.7 shows the sea surface temperature of the Tasman Sea at a location west/north-west of Scott Farm compared to the

soil temperature measured at Scott Farm. During summer, sea surface temperatures were cooler than the Scott Farm soil temperature, however during winter, the sea surface was warmer than the Earth, providing a temperature gradient which may explain possible advection. The effect of this was to make $H \sim 0$ or negative on a 24 hour basis. Local advection was unlikely at this site because it is largely surrounded by dairy farms, where roads were a very small portion of the surrounding area to be providing significant amounts of extra energy.

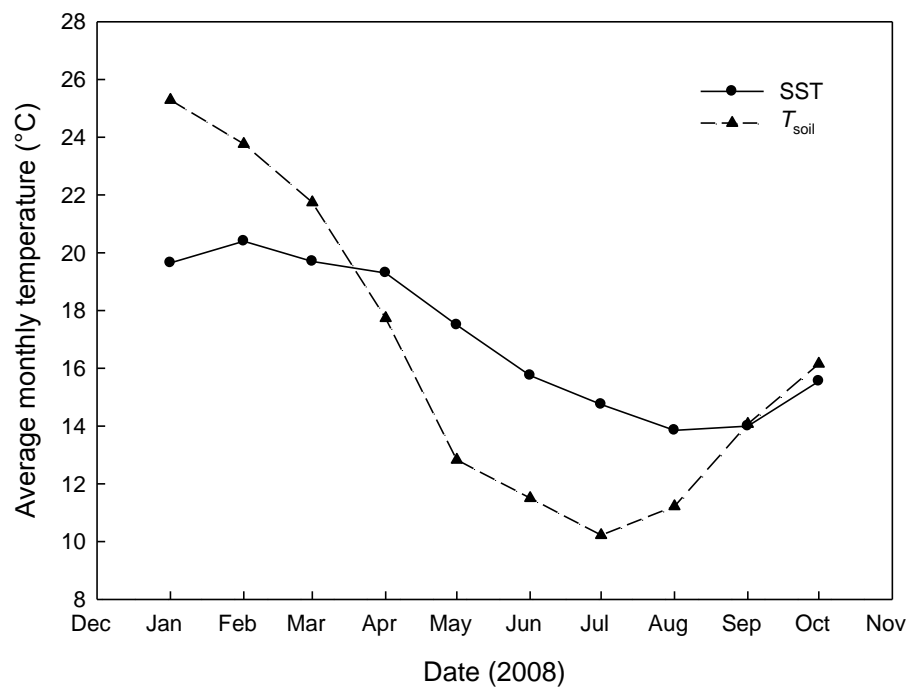


Figure 5.7 Mean monthly sea surface temperature (SST) from the Tasman sea and soil temperature (0.1 m) measured at Scott Farm for January 2008 to October 2008. Coordinates Lat 173.5°(E) Long 38° (S).

5.4 Evaporation

Evaporation can be thought of as either an energy balance term (λE) or a water balance term (E). The previous sections have discussed evaporation in terms of the latent heat flux λE . In a water balance context, evaporation was calculated as a depth of water so it could be compared to measurements of rainfall and discharge. Figure 5.8 shows the mean daily evaporation measured at Scott Farm for each month with maximums and minimums shown as ‘range bars’. Evaporation for December 2007 was high with an average of approximately 4 mm day^{-1} and a large difference between maximum and minimum evaporation for the month. January 2008 has a smaller average evaporation of about 3.1 mm day^{-1} . The difference between daily maximum and minimums was even larger due to the high available energy through the month, and with abundant soil moisture to begin with, which was then depleted quickly, resulting in much lower evaporation near the end of the month. The smallest mean evaporation occurred during the month of July with an average of 1.0 mm day^{-1} with a maximum of 1.9 mm day^{-1} and a minimum of about 0.4 mm day^{-1} . After July, evaporation increased quickly with the onset of spring and summer, ending with fairly high rates of evaporation in November with a large amount of variation for the month.

Table 5.3 shows monthly totals of evaporation and rainfall and the evaporation percentage of rainfall (i.e. the percentage of rainfall that is evaporated). Even before the severe onset of the drought in January, evaporation already exceeded rainfall by 3 times as much in December. January’s evaporation total was almost 20 times greater than rainfall, resulting in the severe drying of the soil and leading to a moisture deficit. February and March were also drying events where evaporation rates exceeded rainfall. The months April through to August were dominated by wetting events and evaporation averaged approximately 25% of rainfall. From September, evaporation began exceeding rainfall again, resulting in the drying of the soil profile once again as summer began to approach.

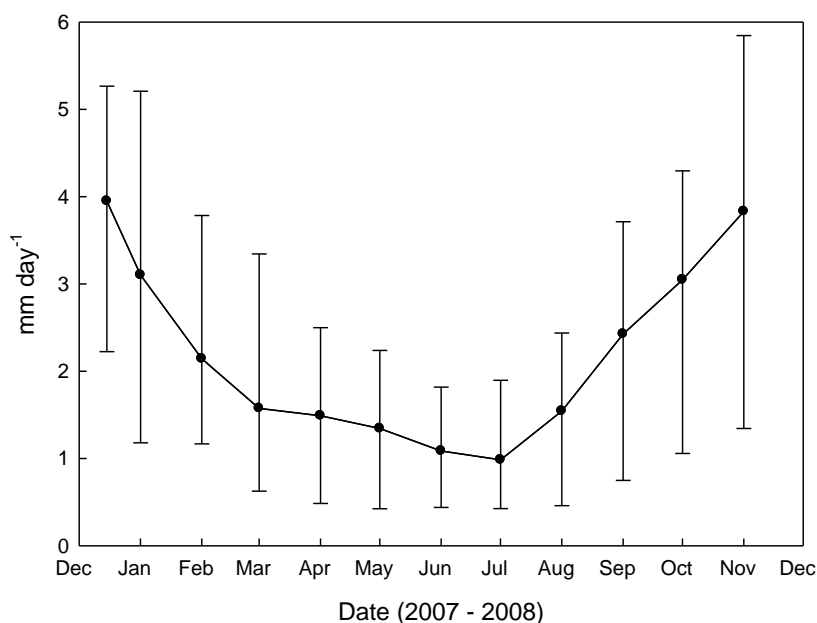


Figure 5.8 Mean, minimum and maximum daily evaporation for each month for Scott Farm from 15 December 2007 to 30 November 2008. Note: December is only a part month from 15 December 2007 to 31 December 2007 so some bias may exist for this month.

Table 5.3 Total monthly evaporation and rainfall (mm) and the evaporation percentage of rainfall showing the months of drying and wetting. Note that December 2007 is only a half month.

Date	<i>E</i> (mm)	Rain (mm)	Percent <i>E</i> of rain	Wetting/Drying
Dec-07 ²	138.7	89	156%	Drying
Jan-08	96.1	4.8	2000%	
Feb-08	62.1	50.4	123%	
Mar-08	48.8	36.2	135%	
Apr-08	44.7	153.2	29%	Wetting
May-08	41.7	129.2	32%	
Jun-08	32.6	151.2	22%	
Jul-08	30.5	193.6	16%	
Aug-08	47.9	184.2	26%	Drying
Sep-08	72.8	70	104%	
Oct-08	94.4	31.6	299%	
Nov-08	114.9	52	221%	
Annual Total	825.2	1145.4	72%	

² Note that December 2007 is only a part month and any monthly December value used here on has been scaled to 31 days in order to allow monthly comparisons.

5.5 Discussion

Diurnal, seasonal and annual cycles in radiation, energy and evaporation were observed and some interesting results were found:

- Radiation and energy partitioning showed strong diurnal and seasonal variation.
- Net radiation was driven primarily by incoming shortwave radiation.
- Albedo varied on a seasonal scale dependent on canopy cover, and vegetation status but once an equilibrium was reached an average of $\alpha = 0.23$ was found during winter, while for summer $\alpha = 0.2$ may be more appropriate.
- During summer, evaporation was controlled by soil moisture availability while during winter and spring evaporation is controlled by available energy.
- Over the study period evaporation rates were highest during spring and summer and lowest during June and July when energy availability is low.
- The evaporative fraction was found to be high in winter (often above 1) which may be an indication of advection.

Both radiation and energy partitioning showed diurnal and seasonal variation in which low values of radiation and energy were present at night and high values during the day. On a seasonal scale, summer values were higher than winter values as expected (Spronken-Smith, 2001; and Sturman and Tapper, 2006).

Diurnal partitioning of energy was driven by R_n and was largely controlled by availability of soil water at Scott Farm. During the drought, when little water was available, H was the dominant sink for energy and λE was small, while during times of abundant water, λE was the dominant sink and H was smaller by comparison. This was a common finding in most energy balance literature as expected (Hunt *et al.* 2002; Alfieri *et al.* 2007; and Aires *et al.* 2008). The result of this reversal in energy partitioning was high Bowen ratios during drought conditions as also observed by Hunt *et al.* (2002) for tussock grassland in NZ during drought conditions.

The seasonal partitioning of energy at Scott Farm began with a fairly severe drought with conditions notably drier than the last 40 years, as also experienced by Humphreys *et al.* (2003) for an energy balance study over forest. The drought for this study lasted from January through to the end of March. Large values of R_n were observed up to a summer midday average of 500 W m^{-2} and winter midday averages of less than 200 W m^{-2} . The annual energy balance (Figure 5.6) shows the changes in energy partitioning from the very dry summer to the wet winter, in which λE was largely controlled by soil moisture conditions as also seen by Aires *et al.* (2008) for a Mediterranean grassland.

Although evaporation was usually driven by the amount of available energy, during the drought the main control on evaporation rates was water availability, resulting in smaller than expected evaporation rates. Aires *et al.* (2008) found, for a Mediterranean C3/C4 grassland, that although they experienced a drought during their study period, their grass type had the ability to extend roots deep into the soil to help augment water uptake which resulted in higher evaporation rates than expected. Alfieri *et al.* (2007) found that, depending on moisture conditions, the moisture content influenced evaporation by 39%. During dry conditions evaporation was mainly controlled by soil moisture content but during wet conditions it was controlled by R_n for the Scott Farm study.

Albedo varied on a seasonal basis at Scott Farm, beginning at an average of about 0.2 in January, suddenly dropping by about 5% during the drought and then slowly increasing to reach an average of about 0.23 from May onwards. Albedo varies with changes in canopy structure, pasture production (Rosset *et al.* 1997), and plant greenness (Ryu *et al.* 2008) and will therefore vary throughout the year depending on vegetation conditions. Ryu *et al.* (2008) found an average albedo value of 0.102 – 0.124 for an annual grassland, however, they saw abrupt decreases down to 0.05 – 0.08 when rainfall and greenness started at the beginning of the growing season. Albedo values for grass are known to range between 0.16 – 0.26, depending on grass height (Sturman and Tapper, 2006) so mean values measured at Scott Farm are what were expected, however a reason for the sudden drop can still not be explained.

The possibility of large scale advection occurring at this site is still not clear however other studies have found that local-scale advection may be a possible cause of lack in energy balance closure, possibly due to an upwind dry to wet transition (Figuerola and Berliner, 2005), or that advection events may occur only at certain times of the day (Oncley *et al.* 2007). At Scott Farm, the evaporative fraction was often above 1.0 during winter, indicating that H was negative, which means the atmosphere was heating the ground, thus indicating large scale advection. After analysing sea surface temperature data from the Tasman Sea, and making comparisons to soil temperature at Scott Farm (at a depth of 0.1 m), it appeared that a strong sea-land temperature gradient existed during winter and could possibly be providing energy via advection to explain the high percentage of λE during this season.

Evaporation during December 2007 was high with rates of about 4 mm day^{-1} , and began dropping over the next seven months, decreasing quickly at first and reaching a minimum of $\sim 1 \text{ mm day}^{-1}$ in July 2008. After this date, rates began increasing very quickly again, back to a mean of about 4 mm day^{-1} in November 2008. The year can be split into periods of drying and wetting, depending on the percentage of rainfall that is evaporated. December 2007 – March 2008 were months of drying, where evaporation exceeded rainfall. April – August 2008 were months of wetting where rainfall exceeded evaporation. From September 2008 onwards, drying occurred again in which rainfall was less than evaporation rates. On an annual basis, evaporation was only 72% of rainfall, however due to significant seasonal variability, one standard number is not applicable over an entire year.

6 Evaporation estimation

6.1 Introduction

Two evaporation estimation models were tested to determine their accuracy when compared to the eddy covariance technique for measuring evaporation. These were the Priestley-Taylor (PT) model and the Food and Agricultural Organisation, Irrigation and Drainage Paper No. 56, Penman-Montieth (FAO₅₆) model. Evidence for a critical soil moisture content value was examined for FAO₅₆, below which the model did not accurately predict evaporation when compared with measured values during soil drying events. From this analysis, a crop coefficient can also be derived during moist conditions. A water stress correction factor, which was applied to both models during drought conditions, was assessed to find how much results can be improved when field conditions were not ideal for the use of potential evaporation models such as the standard PT or FAO₅₆ models. A discussion then compares findings with published literature in order to give an indication of how the given models react under New Zealand conditions, particularly during a drought.

A description of the models used is given in Section 2.3.3, and their application is described in Section 3.5. For data analysis, closure forced data has been used for this chapter as recommended by literature.

6.2 Priestley-Taylor and FAO₅₆ models

Figure 6.1 shows cumulative evaporation over the year-long study period, showing measured evaporation (E_{EC}) compared to both FAO₅₆ (E_o) and Priestley-Taylor (E_{PT}) estimated evaporation. During January 2008, the models began over-predicting evaporation relative to E_{EC} leading to the large separation between

measured and modelled E , however near the end of the period the gap became smaller again. This would suggest that models over predicted evaporation during the summer/early autumn months, but during winter and spring, models under predicted evaporation. The relationship between daily measured and estimated evaporation for E_o and E_{PT} are shown in Figures 6.2 and 6.3 respectively. At low daily measured evaporation the majority of E_o were usually estimated correctly for which data fell close to the 1:1 line with a small trend of systematic underestimation (i.e. slope <1). This was an indication of the need for a crop coefficient to be applied to E_o after Allen *et al.* (1998), which will be discussed in more detail in the following sections. However at high rates of evaporation, a large scatter existed between E_{EC} and E_o , indicating a need for an adjustment during drought conditions.

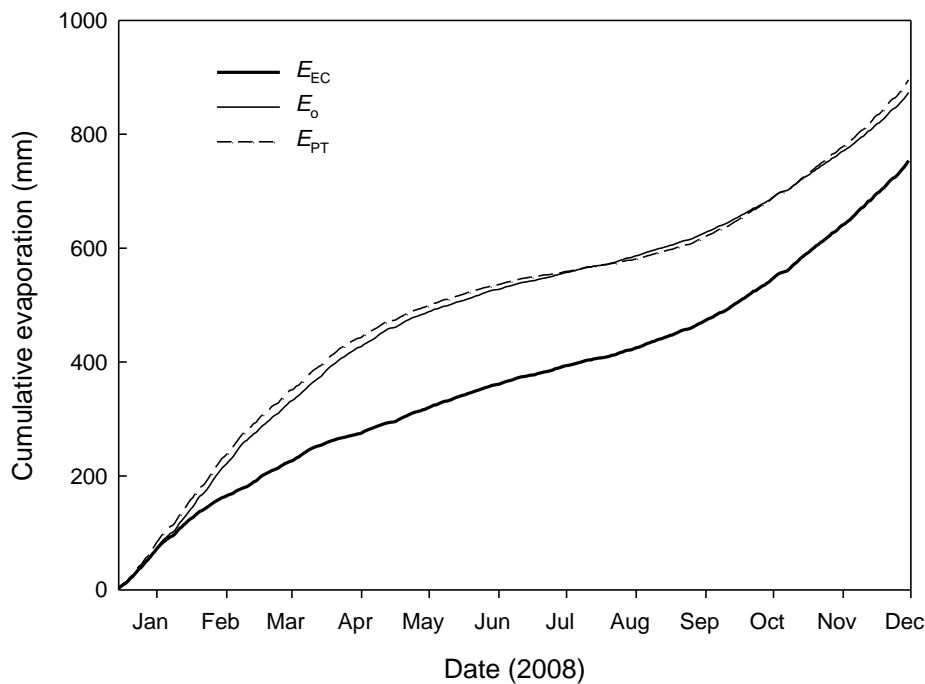


Figure 6.1 Cumulative evaporation for measured (E_{EC}), modelled FAO_{56} (E_o) and Priestley-Taylor (E_{PT}) for 15 December 2007 to 30 November 2008.

When comparing E_{PT} to E_{EC} (Figure 6.3), it appeared that at low evaporation rates, the model under estimated E , possibly indicating α was not large enough. There was also considerably more scatter at low E , with E_{PT} estimating near-zero at times, in contrast to minimum E_{EC} of approximately 0.5 mm day^{-1} . At higher

measured rates of evaporation a large scatter existed in which estimates were higher than measured evaporation, showing the limitations of the model during drought conditions.

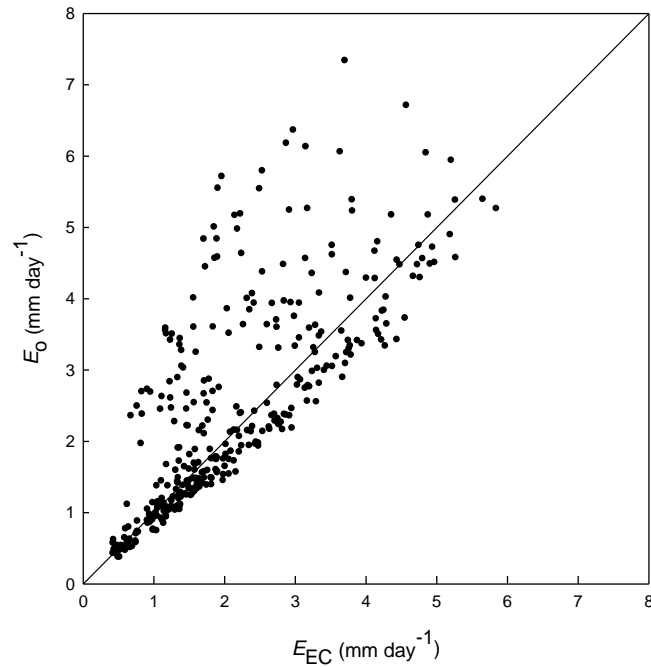


Figure 6.2 Scatter plot of estimated E_o evaporation versus measured E_{EC} . All values are 24 hour totals.

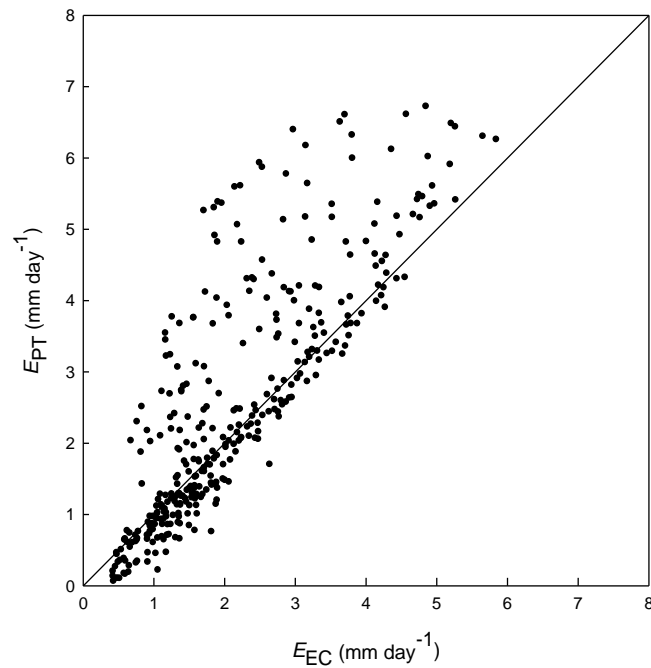


Figure 6.3 Scatter plot of estimated E_{PT} evaporation versus measured E_{EC} where α is set to the standard 1.26. All values are 24 hour totals.

6.2.1 The Priestley-Taylor alpha (α)

E_{PT} was calculated using the equilibrium equation (Equation 2.10, Section 2.3.3) multiplied by a constant variable α , which is often set to 1.26. This α term attempts to account for other variables that may be affecting evaporation other than available energy such as crop conditions or advected energy (which vary throughout the year). The ‘real’ α value can be calculated by dividing the measured daily evaporation by the equilibrium evaporation and this was plotted against time in Figure 6.4. From this it was clear that during very dry conditions during summer α was much smaller than the standard 1.26 value (down to below 0.5), while during very wet conditions during winter, such as those experienced in the 2008 winter, α values were often much higher than the standard 1.26 value (sometimes above 4). During the months of September, October, and November values were closer to $\alpha = 1.26$.

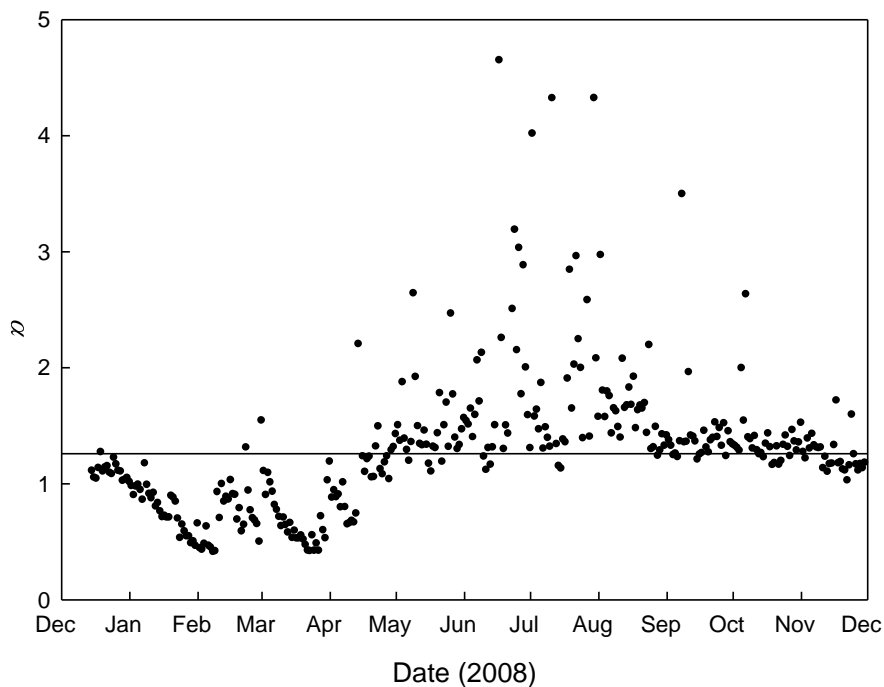


Figure 6.4 Time series of daily Priestley-Taylor alpha values calculated as $\alpha = E_{EC}/E_{EQ}$. Horizontal line is $\alpha = 1.26$.

Figure 6.5 shows the regression of E_{EQ} to E_{EC} for data not including drought effects (after 1 May 2008) where the slope, when forced through the origin, was

equivalent to $1/\alpha$. This resulted in an average α of 1.31 for Scott Farm during normal conditions when there were no drought effects, however the regression was poor and still resulted in seasonal over and under estimation. It would be most ideal to use a seasonally adjusted α where possible. Figure 6.6 shows the regression of E_{EQ} to E_{EC} from 15 December 2007 to 30 April 2008 which encompassed the drought. A large scatter existed leading to an r^2 of only 0.61. The calculated α for these conditions was 0.86, well below the 1.26 standard. Spring conditions appeared very close to the standard $\alpha = 1.26$ (Figure 6.4) so a regression analysis was also carried out for the months September – November (Figure 6.7), resulting in $\alpha = 1.26$ exactly matching that of the standard value. However it was evident that a regression forced through zero was inappropriate because of significant underestimation at low E and over estimation at high E . These results demonstrated the importance of using a seasonally adjusted α at Scott Farm since the suggested standard was not valid throughout the whole year.

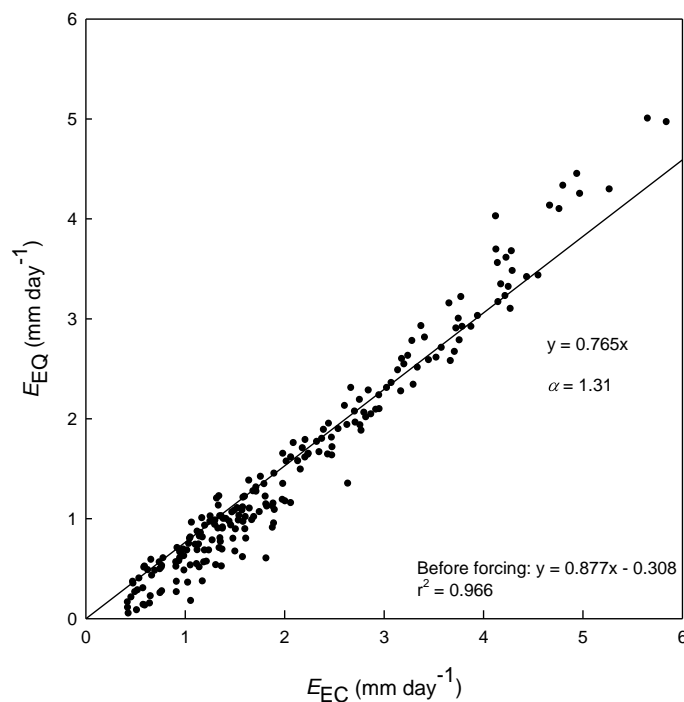


Figure 6.5 Regression of E_{EQ} to E_{EC} for data after 1 May 2008 (no drought effects) forced through the origin where the slope is equal to $1/\alpha$. The initial regression equation is also shown to display the magnitude of change when forced through zero.

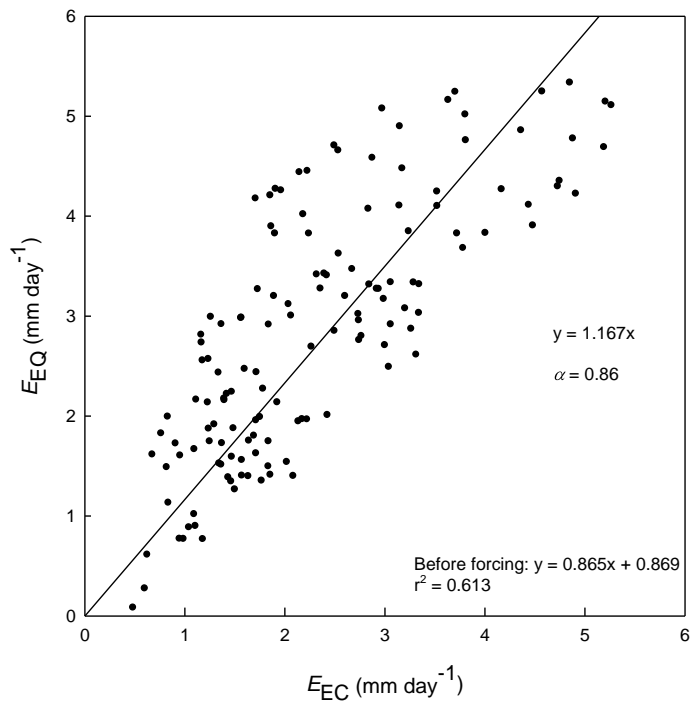


Figure 6.6 Regression of E_{EQ} to E_{EC} for data from 15 December 2007 to 30 April 2008 (during drought conditions) forced through the origin where the slope is equal to $1/\alpha$.

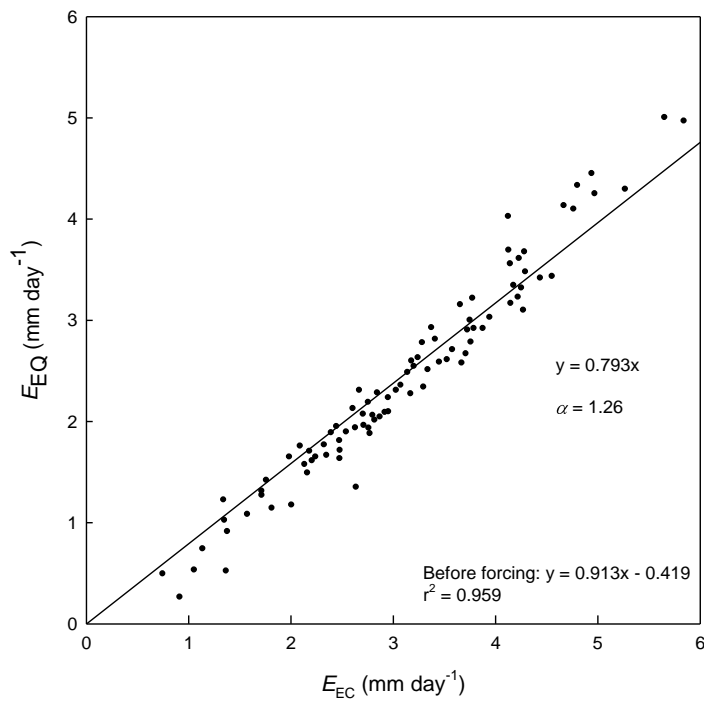


Figure 6.7 Regression of E_{EQ} to E_{EC} for data from 1 September 2008 to 30 November 2008 forced through the origin where the slope is equal to $1/\alpha$.

6.2.2 Critical soil moisture values during drought

A critical soil moisture content can be derived by assessing the relationship between E_o and E_{EC} when compared to soil moisture content. Only the FAO₅₆ model was analysed for a critical moisture content value because the PT model relied on the α constant that was not adequate for the conditions experienced at Scott Farm (see Section 6.2.1). Figure 6.8 shows the ratio between daily E_o and E_{EC} against θ_v . During high soil moisture conditions ratios were less than 1, not providing a very accurate estimation in comparison to E_{EC} and indicating a crop coefficient may need to be applied. The average ratio at this high moisture content range was the inverse of what can be considered the crop coefficient (K_c), which will be discussed in more depth below. A critical volumetric soil moisture content can be estimated from Figure 6.8 at 0.42–0.46, below which the ratio E_o/E_{EC} increased to values substantially greater than 1.0 and with considerable scatter. For days where soil moisture contents were below approximately 0.44 the ratio trended upwards, indicating an over estimation in estimated evaporation values in comparison to measured E values. The estimated critical soil moisture content of 0.44 matches well with published soil data for this area. Singleton (1991) gave the lower limit of readily available water for a Horotiu silt loam and Te Kowhai silt loam (which were both similar to the soil type present at this site) to be ~42% and ~45% respectively. Below this value, plants can no longer easily extract water from the soil for transpiration.

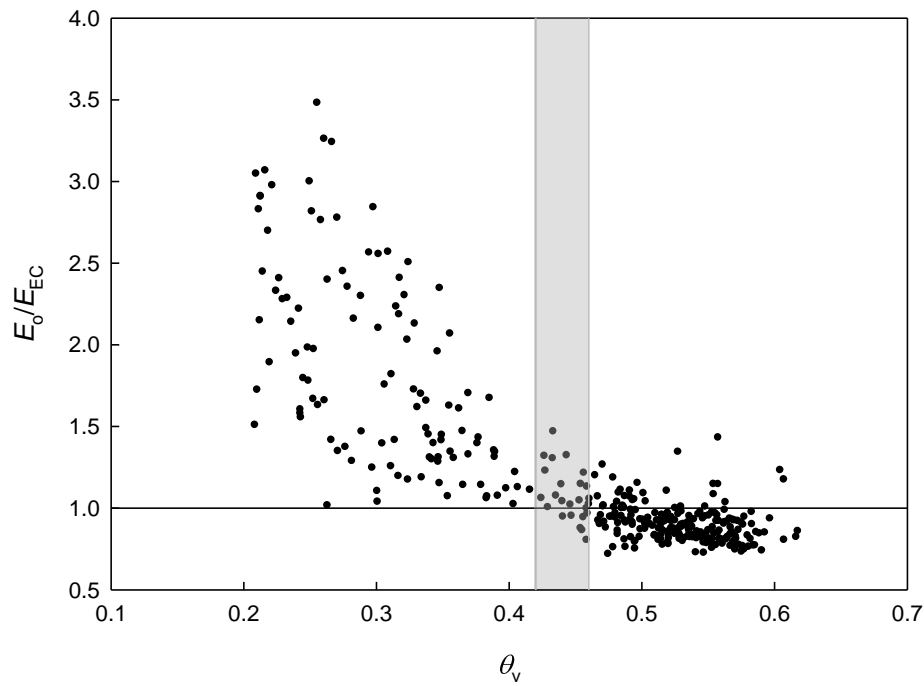


Figure 6.8 Ratio of E_o to E_{EC} evaporation against θ_v . Shaded area represents the estimated critical moisture content limit. θ_v probes are 5 and 10 cm deep.

Figure 6.9 shows rainfall and volumetric moisture content data with the summer drying events annotated for the period 15 December 2007 to 30 June 2008. Figure 6.10 shows the ratio E_o/E_{EC} for the two major drying events. This shows that the first drying event from 22 December 2007 to 10 February 2008 affected the estimated E values differently to the second drying event which occurred from 5 March 2008 to 31 March 2008 (Figure 6.10). During event 1, $E_o/E_{EC} < 1.5$ until soil moisture content reached below 0.26. At the same moisture content during the second drying event, E_o/E_{EC} was much higher, up to about 2.5. The most likely reason for the difference in behaviour of the ratio in comparison to moisture content was the status of the vegetation at the time of the drying event. During the first drying event, pasture was still alive and transpiring, however with some control over water loss. Once the second drying event occurred, vegetation had either died off completely or was struggling to extract enough soil moisture so evaporation estimates were affected.

Figure 6.11 shows the regression between E_o and E_{EC} during high soil moisture conditions (after 1 May 2008) where the slope of the regression, when forced

through the origin, was the inverse of the crop coefficient, which was calculated to be 1.13. This regression appeared to fit the data well, particularly in contrast to the PT model in Figure 6.5. Figure 6.11 does not have a seasonal over or under estimation trend and the effect on the regression equation of forcing the regression through zero was very small.

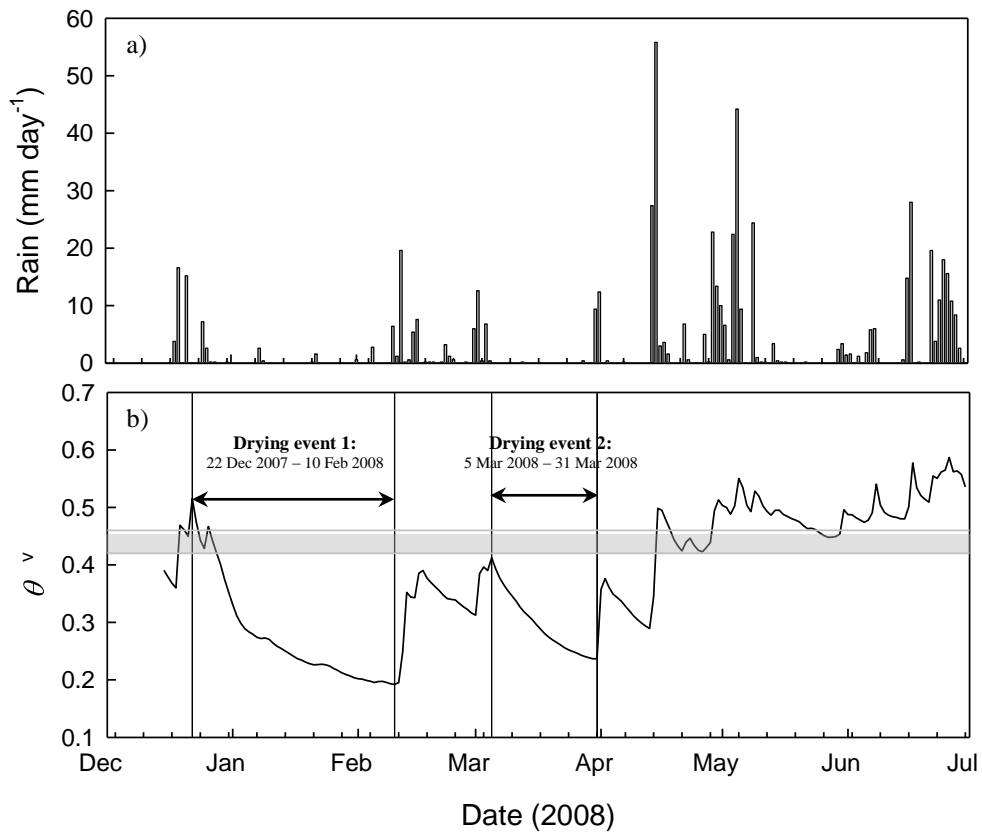


Figure 6.9 a) Daily rainfall and b) θ_v for 15 December 07 to 30 June 08 with two drying events indicated during the 2008 summer drought. Shaded area is estimated critical moisture content.

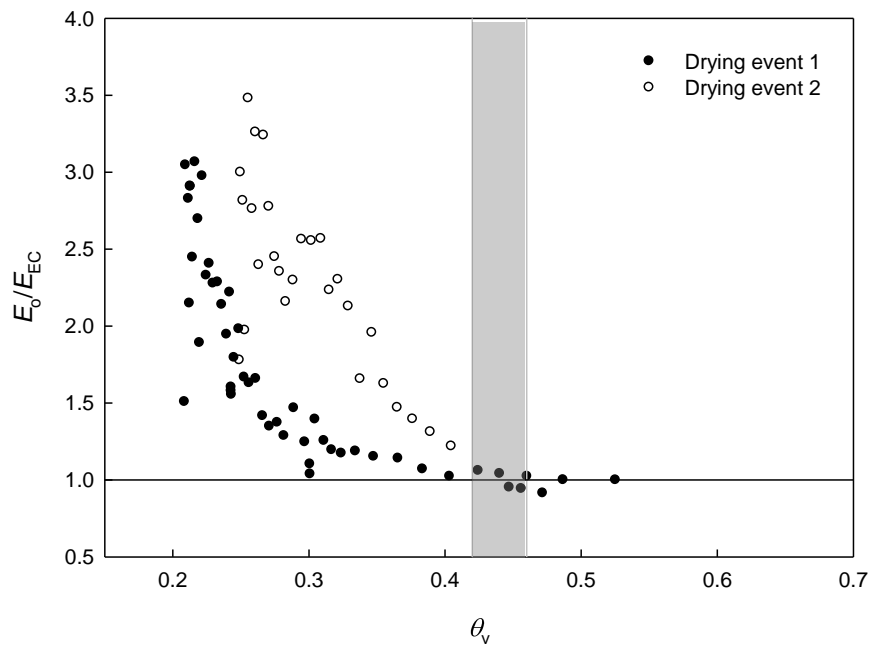


Figure 6.10 E_o/E_{EC} against θ_v for the two major drying events during the 2008 drought. Shaded area shows estimated critical moisture content.

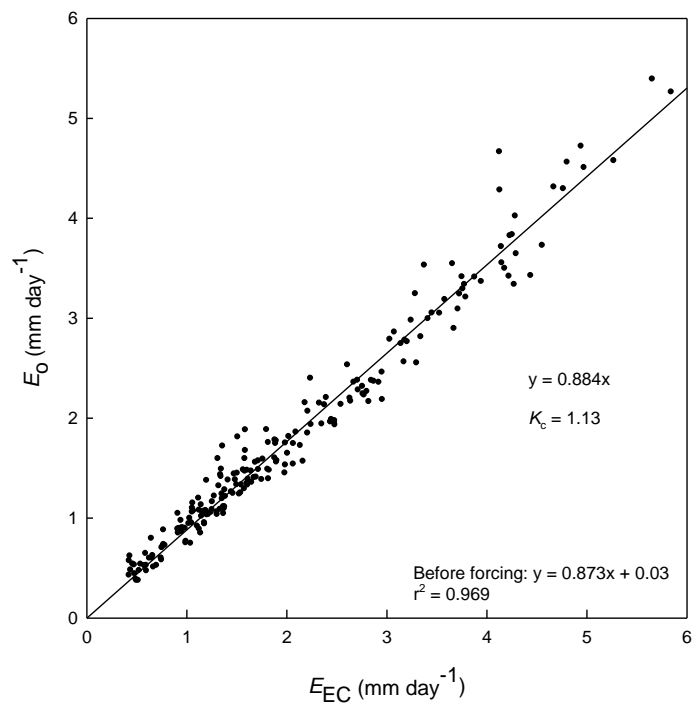


Figure 6.11 Regression of E_o to E_{EC} for data after 1 May 2008 (no drought effects) forced through the origin where the slope is equal to the inverse of the crop coefficient, K_c .

6.2.3 Model corrections

Although Section 6.2.2 gave a critical soil moisture value below which E_o significantly began to overestimate actual E , soil moisture content was not the direct factor recommended by Allen *et al.* (1998) to adjust E_o under drying conditions. Allen *et al.* (1998) acknowledged that under water stress conditions the FAO₅₆ model had limited use, and described the steps needed to adjust evaporation estimates. This adjustment was specifically developed for the use with the FAO₅₆ equation but the water stress coefficient has also been applied to the Priestley-Taylor equation to see how it improves the model performance during water stress conditions. The water stress correction is explained in Section 2.3.4 in which a crop coefficient (K_c) and a water stress coefficient (K_s) are applied to the estimated reference crop evaporation (or for the case of E_{PT} , just K_s is applied). The coefficients used in the model are given in Table 6.1. Figure 6.12 gives an example of the extent that values are adjusted when using this water stress adjustment factor by comparing the estimated E_o data with that measured by E_{EC} . Adjusted values generally lay closer to the one to one line, indicating that estimated values were adjusted to be much closer to measured evaporation than the non-adjusted evaporation estimates, however at high E the model was still not very good.

Table 6.1 Values used for the estimated evaporation adjustment after Allen *et al.* (1998).

Coefficient	Value	Notes
K_c – crop coefficient	1.13	Calculated in Section 6.2.2 using a regression approach for non-limiting θ_v
Z_r – effective rooting depth	1 m	Value most sensitive in summer (see Section 6.2.2.1)
FC – field capacity	0.5	50% volumetric moisture content field capacity (derived from θ_v data and Singleton (1991))
WP – wilting point	0.2	20% volumetric moisture content wilting point (derived from Singleton (1991))
p – depletion fraction	0.6	Allen <i>et al.</i> (1998) Table 22. Value for grazed pasture

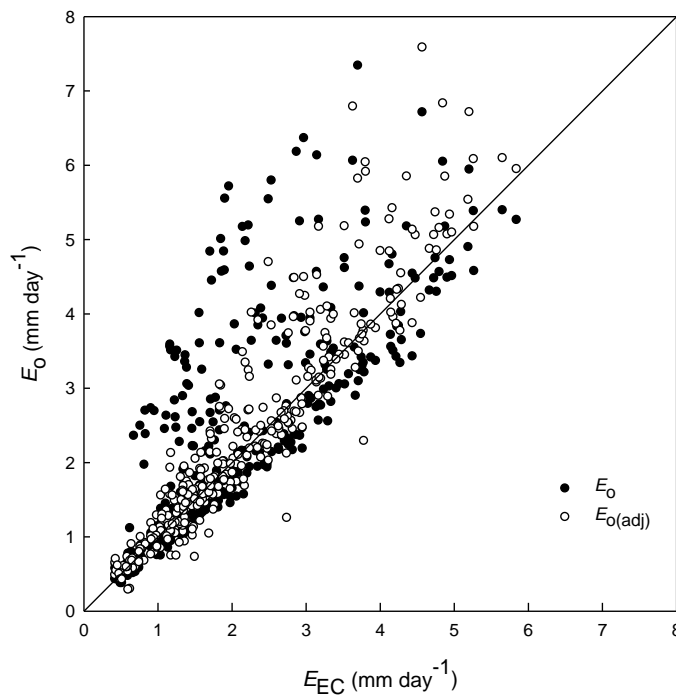


Figure 6.12 Effect the water stress adjustment model (using $K_c = 1.13$) has on estimated evaporation data by showing regression of E_o and E_{EC} .

Figure 6.13 shows the evaporation estimates compared to those measured by E_{EC} as monthly totals for the year for non-adjusted evaporation. Note that because December is only a part month (beginning 15 December 2007) this value has been scaled to a 31-day month. Both E_o and E_{PT} resulted in a large over-estimation during the months January, February, March and April and E_{PT} then under-estimated evaporation during the months May – October. After the water stress adjustment was applied using the constants listed in Table 6.1, both estimated values were reduced as expected and reasonable results were found for February, March and April (Figure 6.14). However January was not adjusted far enough due to the model requiring time to reach the required adjustment magnitude. The E_o adjustment also resulted in the best estimation during the wet months April – August where evaporation values matched very well with E_{EC} . The E_{PT} adjusted values consistently under-estimated throughout the wet months and began over estimating E after September.

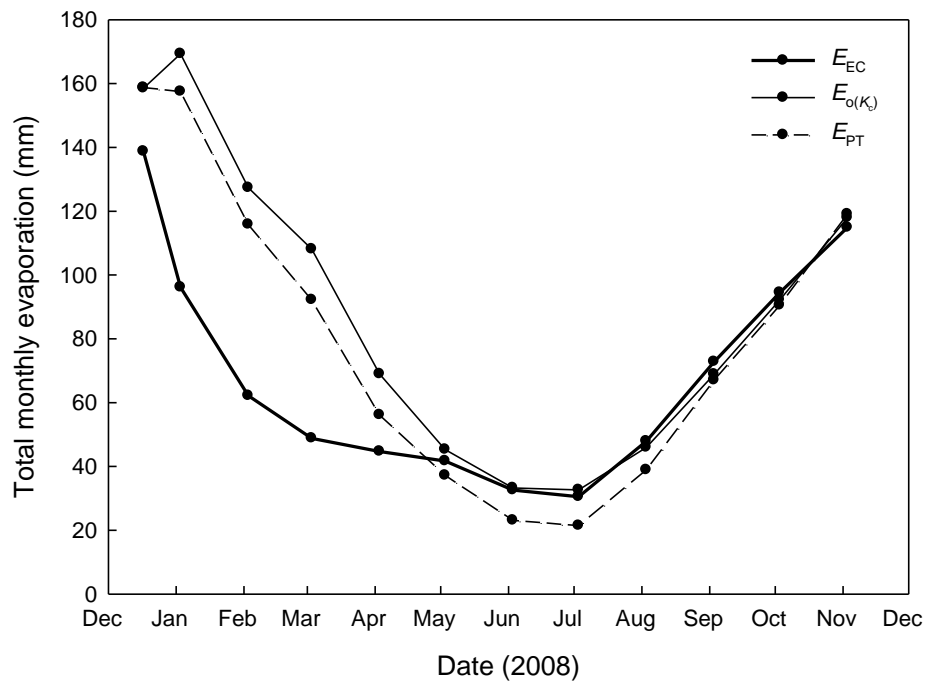


Figure 6.13 Measured E_{EC} evaporation and estimated E_o (using $K_c = 1.13$) and E_{PT} ($\alpha = 1.26$) evaporation throughout the year (December 2007 only part month so adjusted to equivalent of a 31-day month).

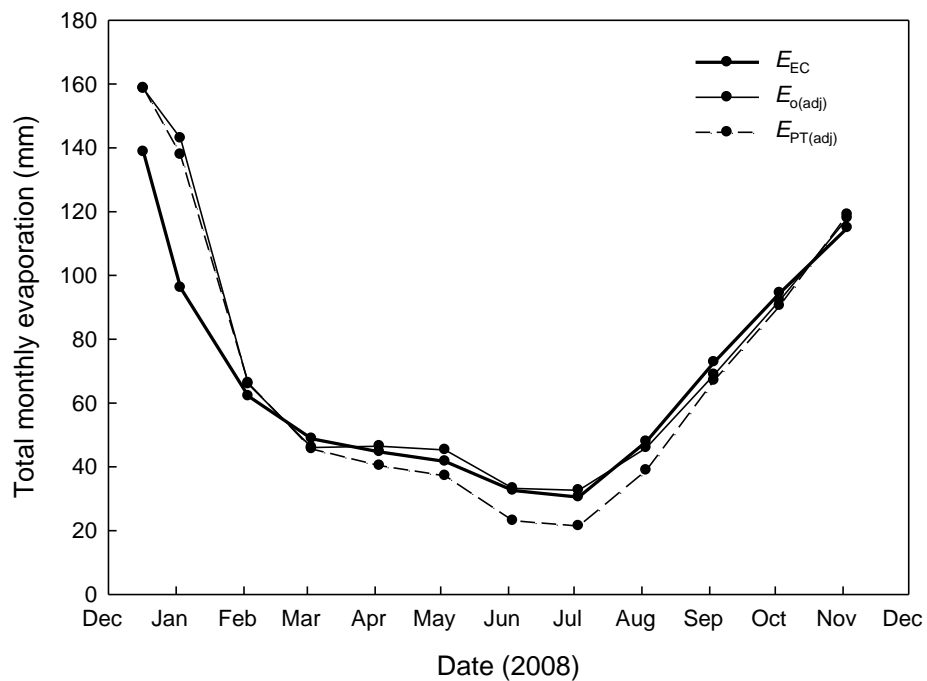


Figure 6.14 Measured E_{EC} evaporation and estimated E_o (using $K_c = 1.13$) and E_{PT} ($\alpha = 1.26$) evaporation adjusted for water stress conditions throughout the year (December 2007 only part month so adjusted to equivalent of a 31-day month).

Figure 6.15 shows the cumulative evaporation for all five variables (E_{EC} , E_o , $E_{o(adj)}$, E_{PT} and $E_{PT(adj)}$). It helps display the accuracy of the models throughout the changing seasons and shows how large the overestimation during the summer/autumn period is. The reason for the significant over-estimation in January was due to the time it takes for the adjustment model to take effect for the limited moisture conditions, however thereafter the slope of $E_{o(adj)}$ and E_{EC} are similar for the rest of the year. The under-estimation by the $E_{PT(adj)}$ model during winter was also very clear in this figure which would suggest that the $E_{o(adj)}$ model appeared to estimate evaporation best under the conditions experienced in the Waikato during 2008.

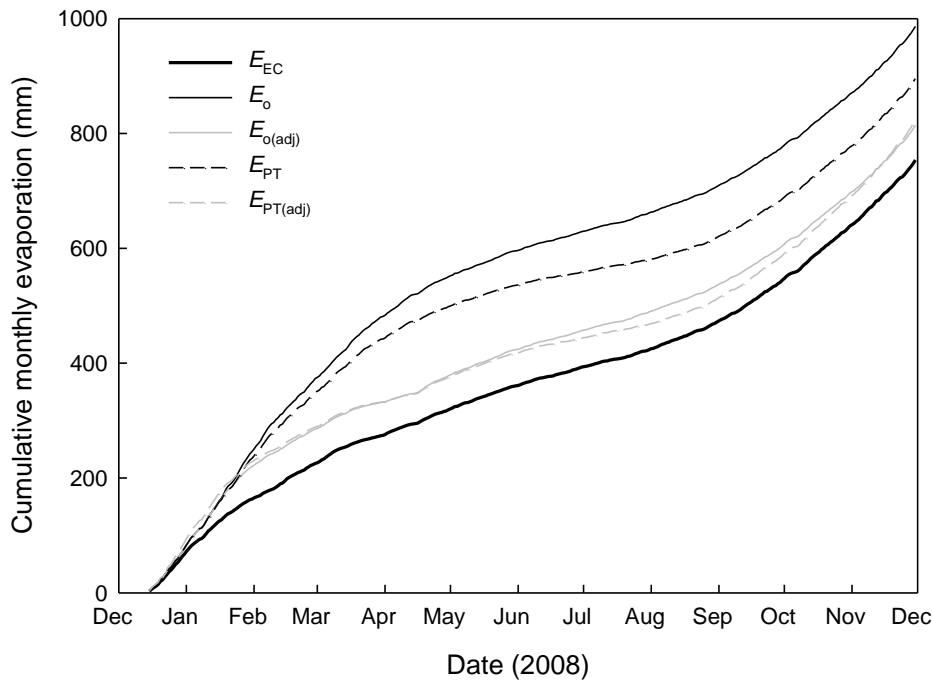


Figure 6.15 Cumulative evaporation for measured E_{EC} and estimated E_o , E_{PT} and $E_{o(adj)}$ and $E_{PT(adj)}$ for water stress conditions using $K_c = 1.13$.

To gain an idea of the magnitude the models miscalculate as a percentage of measured evaporation, Table 6.2 shows both the monthly total measured and estimated evaporation rates for each model (including adjustments) in millimetres and finishes with the total percentage of measured evaporation that the models predict. The unadjusted values for E_o and E_{PT} were over predicted over the measurement period basis by 116% and 119% of measured E_{EC} respectively. The

adjusted equations perform much better with over predictions (over the entire study period) of only 108% and 109% of measured E_{EC} respectively. The reason that $E_{PT(adj)}$ appeared to perform fairly well with these results was because study period totals were displayed. Large over estimations during summer were compensated by large underestimations during winter (Figure 6.14). If the monthly total E measures were compared, it was evident that the E_o model was much better at estimating evaporation on a shorter time scale, the exception being for January 2008, the first month of the drought.

Table 6.2 Monthly total measured, estimated and adjusted evaporation rates and total percentage of estimated from measured E (* December only half month from 15 December 2007).

	Total Monthly Evaporation (mm)				
	E_{EC}	E_o	$E_{o(adj)}$	E_{PT}	$E_{PT(adj)}$
Dec 07*	67.12	67.89	76.72	76.80	86.78
Jan 08	96.13	149.82	142.97	157.46	141.30
Feb	62.14	112.71	65.91	115.83	61.14
Mar	48.78	95.64	46.08	92.19	43.00
Apr	44.69	61.04	46.46	56.12	43.28
May	41.68	40.10	45.31	37.15	41.98
Jun	32.58	29.43	33.25	23.10	26.10
Jul	30.50	28.87	32.62	21.40	24.18
Aug	47.86	40.67	45.96	38.89	43.94
Sep	72.80	60.94	68.86	67.06	75.78
Oct	94.45	81.57	92.18	90.43	102.19
Nov	114.87	104.38	117.95	119.04	134.52
TOTAL	753.60	873.07	814.27	895.47	824.19
% of total measured E_{EC}	100%	116%	108%	119%	109%

6.2.4 Sensitivity analysis

6.2.4.1 Rooting depth

When $K_s = 1$, the water stress correction does not apply, but with the onset of dry conditions K_s becomes less than one so the soil moisture correction applies. The model was sensitive to the effective rooting depth of the vegetation, which can become quite deep during periods of soil moisture stress. Figure 6.16a shows how K_s changes over time with the onset of dry conditions using three different estimated rooting depths (where Figure 6.16b shows volumetric soil moisture content). In Figure 6.16c the E_o modelled evaporation using different rooting depths was compared to E_{EC} , both as cumulative totals. With a shallow estimated rooting depth of 0.6 m, K_s declined very quickly from 1.0, resulting in an over adjustment in estimated evaporation (Figure 6.16c). Using a rooting depth of 1.4 m, K_s had a more gradual decline (Figure 6.16a), but resulted in a lack of adjustment in evaporation (Figure 6.16c), while a rooting depth of 1.0 m appeared most acceptable for the conditions at Scott Farm because the slope of the cumulative $E_{o(adj)}$ line was parallel to the E_{EC} cumulative line (Figure 6.16c). Figure 6.16a shows the decrease in K_s from 1.0 (no water stress effects) to $K_s < 1$ where a constant change in rooting depth did not result in a constant linear change in K_s . The overall result in assessing the effect of Z_r was that it did not control the timing of when the water stress model reacts to the drying conditions, but thereafter affects water availability.

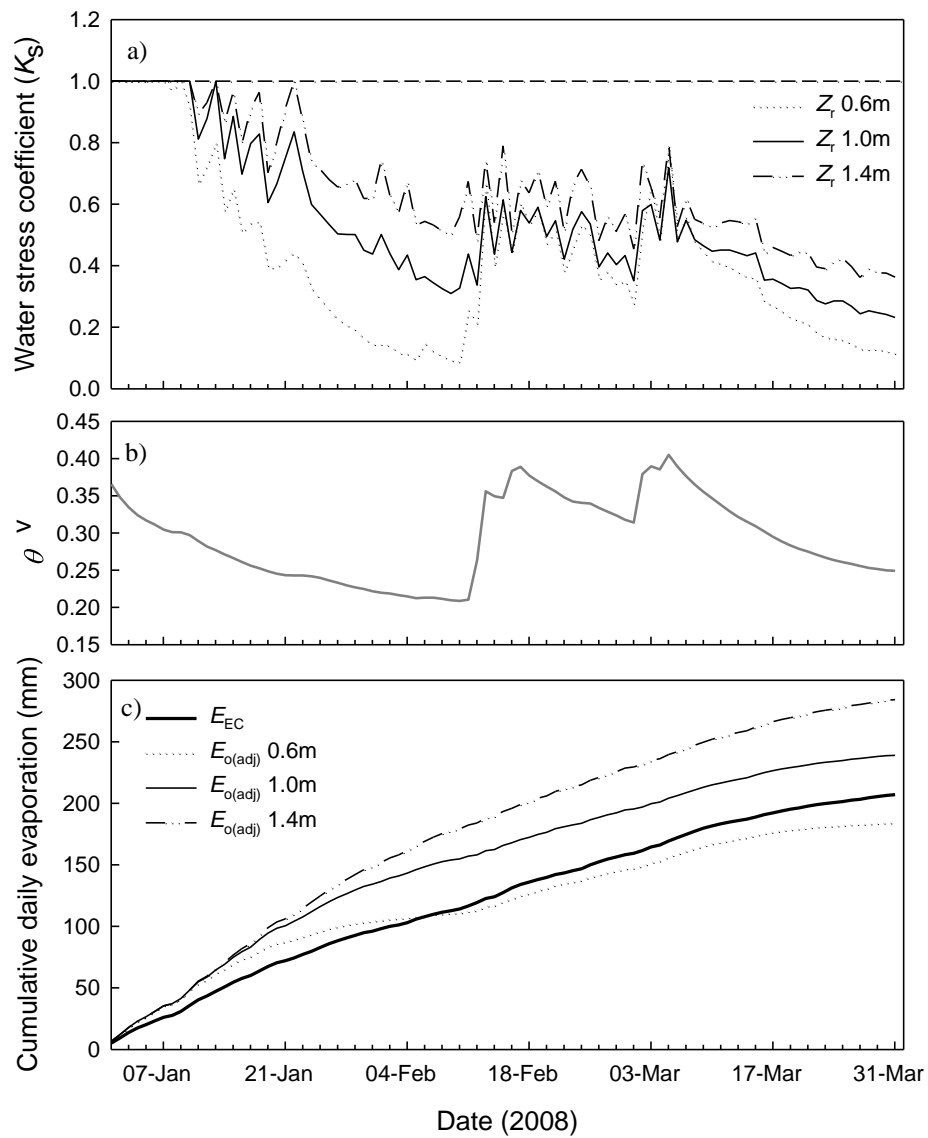


Figure 6.16 For the time period 1 January 2008 to 31 March 2008 a) change in water stress coefficient with different rooting depths, b) volumetric moisture content and c) cumulative E_o using different rooting depths and $K_c = 1.13$ and E_{EC} evaporation.

The important thing to note for Figure 6.16c is the slope of the cumulative modelled evaporation compared to the slope of the measured E_{EC} . At the onset of dry conditions, models for all three rooting depths took time to adjust to the drying conditions (slopes were steeper for the modelled evaporation to begin with). Around 2 February 2008, the shallow rooting depth model over-adjusted (slope becomes less than E_{EC}), while the 1.0 m rooting depth model developed a very similar slope to the E_{EC} , and the 1.4 m rooting depth model maintained a

slope steeper than E_{EC} . This would suggest that $Z_r=1.0$ m most realistically adjusted the E_o estimation equation during drought conditions when the water stress coefficient drops below zero. This resulted in the implication that during very dry soil conditions like those experienced at Scott Farm in the summer of 2008, grazed pasture had the ability to extend their roots to depths of 1.0 m in the soil profile to extract water. Figure 6.17 shows the final regression of $E_{o(adj)}$ against E_{EC} where $Z_r=1.0$ m to show scatter of data. This was most likely caused by drought conditions in early January 2008 because the adjustment model did take some time to adjust estimated evaporation to acceptable values.

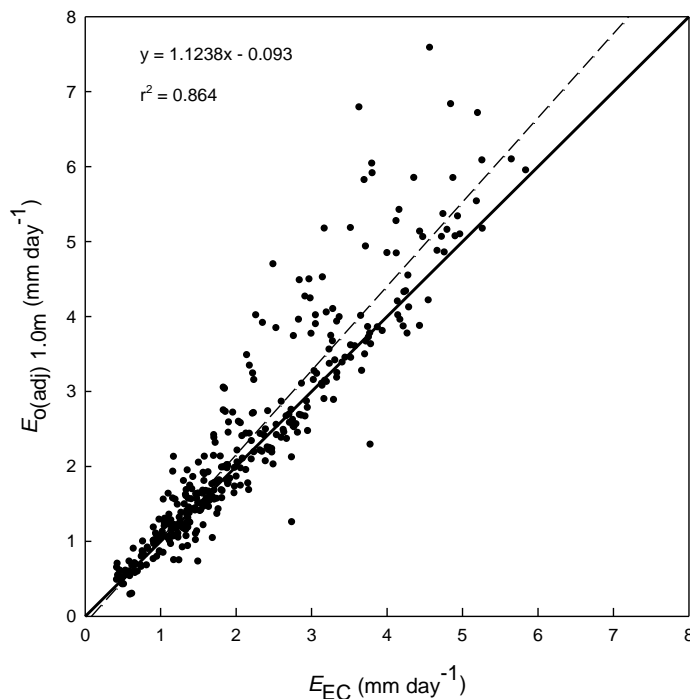


Figure 6.17 Scatter plot with regression of $E_{o(adj)}$ with a rooting depth of 1.0 m against daily E_{EC} for data from 15 December 2007 to 30 November 2008.

6.2.4.2 Other model sensitivities

Sensitivity analyses were also carried out on the field capacity (FC) and wilting point (WP) variables that were used in the adjustment model. The values used in the model were estimated using published data for the soil type and an estimate after assessing θ_v data. The sensitivity analyses used $\pm 5\%$ of the final moisture

values used for both FC (0.5) and WP (0.2). Results showed that differences in FC (Figure 6.18) resulted in negligible changes in the water stress coefficient (K_s) and that all three values resulted in similar values when cumulative evaporation was plotted.

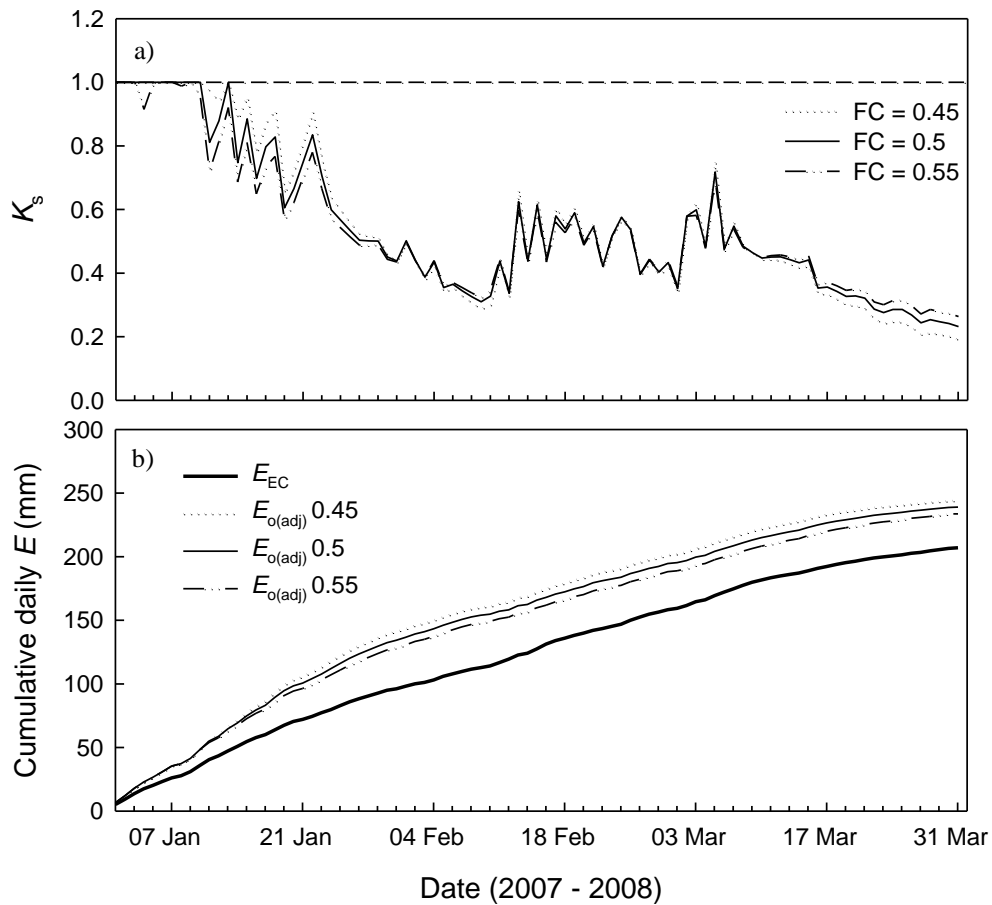


Figure 6.18 For the time period 1 January 2008 to 31 March 2008 a) change in water stress coefficient with different field capacity (FC) values, and b) cumulative E_o using different field capacity values where $K_c = 1.13$ and cumulative E_{EC} evaporation.

Wilting point had more of an effect on the adjustment model because WP was used to calculate K_s in dry conditions. WP made the model sensitive to the timing of K_s and also the magnitude when the model first applied (Figure 6.19). The final chosen WP=0.2 developed the same slope as the E_{EC} cumulative daily evaporation so appeared to be the most adequate value for use at this site. All sensitivity

analyses (Z_r , FC and WP) failed to adjust adequately to the initial onset of soil drying at the beginning of the drought.

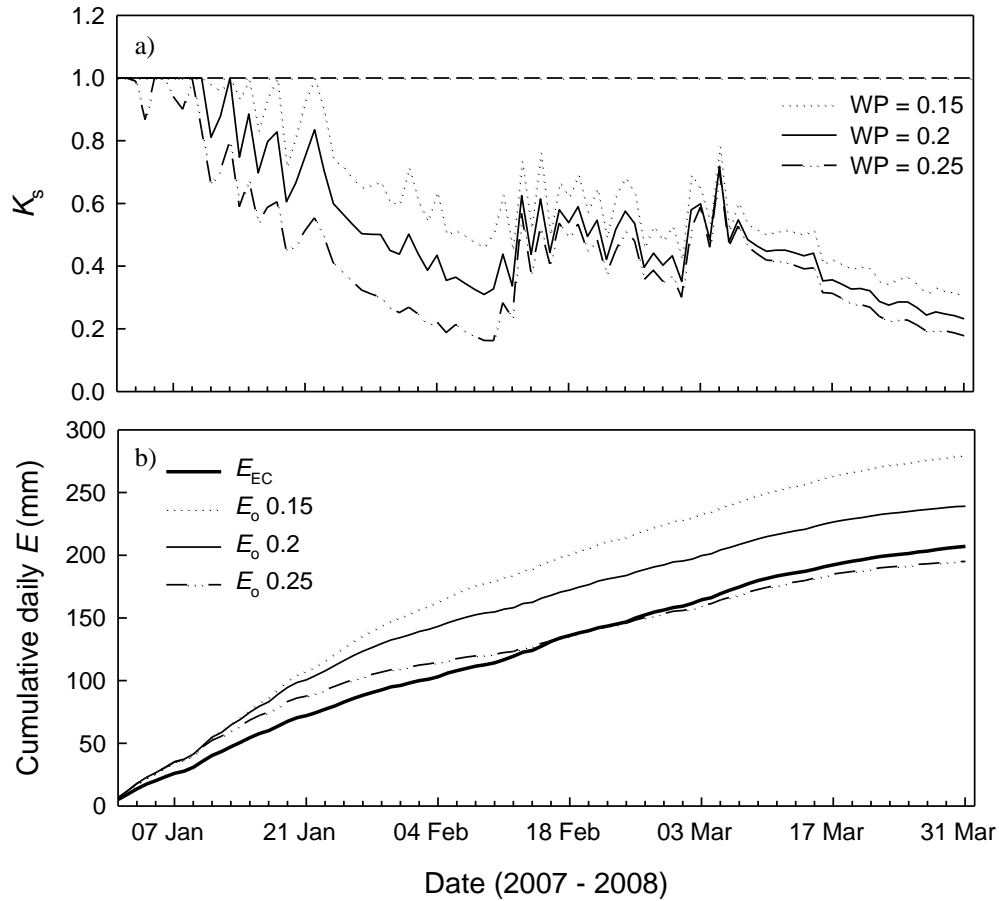


Figure 6.19 For the time period 1 January 2008 to 31 March 2008 a) change in water stress coefficient with different wilting point (WP) values, and b) cumulative E_o using different wilting point values where $K_c = 1.13$ and cumulative E_{EC} evaporation.

6.3 Discussion

The key findings for the analysis of estimation methods are as follows:

- E_o and E_{PT} models both overestimated evaporation when conditions became dry.
- E_{PT} underestimated evaporation during winter.

- The E_{PT} α coefficient was not constant throughout the year. It was much lower during summer and autumn and higher and more variable during winter. In spring average α was very close to 1.26. During ‘non-limiting’ soil moisture conditions $\alpha = 1.31$ at this site so the model simply doesn’t fit well.
- The E_o model began over estimating evaporation when soil moisture contents drop below 44%.
- The crop coefficient for this site was estimated to be 1.13 under well watered conditions.
- The FAO₅₆ water stress adjustment improved estimated evaporation to a satisfactory standard, but early onset of drying was not able to be adjusted for.
- The water stress adjustment was most realistic when a rooting depth of 1.0 m was used.
- The water stress adjustment was not sensitive to field capacity but more to wilting point because it related to water stress conditions. A field capacity of 0.5 and a wilting point of 0.2 were adequate for use at Scott Farm.

E_o appeared to predict better than E_{PT} . The reason for the more accurate measure using E_o was likely to be due to the extra forcing variables that were used within the equation, such as temperature, vapour pressure deficit and wind speed as well as the parameterisation of vegetation and aerodynamic resistances (Allen *et al.* 1998). E_{PT} attempted to account for these variables by using a constant variable alpha (α) often set to 1.26, which was then multiplied by the equilibrium evaporation (E_{EQ}) (see Section 2.3.3) to calculate E_{PT} . For Scott Farm α was calculated to be 1.31 during non drought conditions, however it would be most appropriate to estimate a seasonal α to develop a more realistic value for the Waikato region due to the extreme dry and wet conditions during 2008. Until this has been done, the PT model is not considered accurate enough to estimate E if data are available for the application of the FAO₅₆ model.

Methods to estimate evaporation have been used by the scientific and agricultural communities for many years and improvements are continuously being made as methods of measurement and hence understanding also improve. Published

studies have found various results as to which estimation method is most accurate. Here we found that the FAO_{56} method was more accurate than the E_{PT} model which reinforces studies such as Irmak *et al.* (2003), Scotter and Heng (2003) (where Scotter and Heng (2003) assessed the suitability of the FAO_{56} model under New Zealand conditions), Allen *et al.* (2005), Berengena and Gavilan (2005), Lopez-Urrea *et al.* (2006a, 2006b), and Gavilan and Berengena (2007). However many other studies found that the standard Penman-Montieth model and E_{PT} models adequately reproduced evaporation effectively while the FAO_{56} method was not as accurate (Ventura *et al.* 1999; Sumner and Jacobs, 2005). Here it was found that both models over-predicted E during summer and PT also under-predicted E during winter months. The better result with E_o was thought to be because E_o included temperature, vapour pressure deficit and wind speed data to help account for other energy sources (such as horizontal advection) as well as vegetation parameters, while E_{PT} tried to use a constant value to account for local advection only. It became evident that the E_{PT} α coefficient had a strong seasonal variation, where during summer α was well below the standard 1.26 value (sometimes below 0.5) and during winter it was highly variable and often much greater than 1.26. The only months it behaved as expected (coming close to 1.26 on average) was during September and October. Similar results were also found by Pauwels and Samson (2006), who discovered that at high moisture contents α was very high, however when vapour pressure deficits were high, α was low. Pauwels and Samson (2006) suggested the use of monthly averages of α would improve the E_{PT} model considerably, while Clothier *et al.* (1982) state the improvement of the E_{PT} model via local calibration of the α constant would also help.

During dry conditions evaporation rates were most often limited by soil moisture content (Aires *et al.* 2008). It was possible to find an approximate critical soil moisture content to determine when evaporation estimation models began to overestimate E during such conditions. A critical θ_v was found to be 42–46% at Scott Farm. This range corresponded with the readily available water limit for this soil type (~42–45%) in a study done by Singleton (1991) at a field site very close to Scott Farm.

The use of the FAO_{56} water stress adjustment was not often mentioned in literature. The reason for this is probably because those crops where evaporation is measured or estimated are usually irrigated during drought periods so critical soil water deficits are rare. It was found that the adjustment defined by Allen *et al.* (1998) for drought conditions resulted in a much more accurate estimation of evaporation when applied to both the E_o and the E_{PT} models. However caution should be taken due to its sensitivities to rooting depth during summer and to the crop coefficient when water is abundant at a site during winter (for New Zealand conditions). It became evident that there was a possibility that rooting depths may increase significantly during summer when moisture became limited in the surface soil so plant roots grew much deeper than they usually would in search for more water. For this model, rooting depth was best set at 1 m with a crop coefficient of 1.13 which accounted for any underestimations during winter. Both these coefficients will change depending on soil type and vegetation at a site so caution is recommended for the sensitivities of this adjustment model. The water stress adjustment model appeared to work well, however the initial timing of the onset of drying conditions was not accurately estimated and cannot be entirely explained from this research.

7 Conclusions

A year-long measurement campaign was undertaken using eddy covariance to measure energy fluxes and evaporation rates from pasture at a Waikato dairy farm. The study period was from 15 December 2007 to 30 November 2008 during which a drought was experienced during the summer months followed by a very wet winter.

The overall findings are summarised below and are structured following the objectives listed in Section 1.3

7.1 Accuracy of eddy covariance measurements of evaporation

Energy balance closure at Scott Farm was deficient by 24% on average which falls within reported literature values of up to 30%. Closure was worst during wind directions from 75–125° and during winter. Energy balance closure was forced by adjusting λE and H while maintaining the measured Bowen ratio, as recommended by Twine *et al.* (2000) and Foken (2008).

Overall the lysimeter studies were successful, particularly the spring study, however one main limitation was identified. Lysimeters should be deeper than the 0.2 m used for this study to ensure plant roots are able to extend to natural depths, particularly during summer/autumn. During spring when soil moisture was non-limiting, the lysimeter measurements of evaporation agreed closely with non-closure forced eddy covariance measurements, although closure-forced measurements were within the 95% confidence intervals of lysimeter measurements on some days. Some uncertainty still exists as to the accuracy of

both lysimeter and EC methods of evaporation measurement because both methods still have potential biases, however for the purpose of this study, it would appear data are sufficiently accurate to have confidence in results.

7.3 Radiation and energy balances, and evaporation

The radiation and energy partitioning at the pasture surface showed a strong diurnal cycle, with small or negative fluxes at night and peaking near midday. Some fluxes were often lagged due to the time it takes for energy to be transferred (i.e. soil temperature) or some fluxes peaked earlier (i.e. soil heat flux) due to the stronger temperature gradient and wind conditions at certain times of day.

Incoming shortwave radiation is the primary source of radiation and therefore drives net radiation at the Earth's surface. If no net radiation measurements are available for future studies, shortwave radiation data can be used to estimate a net radiation value (see Appendix B), for example to estimate evaporation.

Albedo is largely dependent on vegetation colour so therefore it varies on a seasonal scale, depending on vegetation conditions. At Scott Farm, common albedo is around 0.20–0.23, consistent with other research for pasture.

At Scott Farm, available energy fluxes were high during summer, however evaporation was constrained by soil moisture availability. During winter soil moisture was non-limiting but evaporation was limited by available energy which was relatively low.

During winter at Scott Farm, it is possible that an extra energy source was available because λE commonly exceeded R_n on a 24-hour basis. Because of New Zealand's maritime environment, it is possible that warmer maritime air masses could provide an extra source of energy during this time of year, known as advection. This hypothesis is supported by land and Tasman Sea surface temperature data, which showed strong seasonal gradient reversals.

Total evaporation at Scott Farm was 755 mm during the study period, 72% of rainfall.

7.4 Estimating evaporation

The Priestley-Taylor model has been used to estimate evaporation (E_{PT}) in New Zealand for many years (e.g. Clothier *et al.* 1982; and McAneney and Judd, 1983), while the FAO₅₆ Penman-Monteith model (E_o) has more recently been recommended for New Zealand conditions (Scotter and Heng, 2003).

When E_o and E_{PT} models were compared to measured E_{EC} , it became clear that the models over-estimated evaporation during dry conditions and E_{PT} also underestimated evaporation during winter.

The E_o model began over estimating E during summer when soil moisture contents dropped below about 44%. The model also required a crop coefficient adjustment of 1.13 for this site during well-watered conditions. Overall the FAO₅₆ model resulted in a very good comparison with EC measurements when soil moisture was not limiting. No seasonal trends in model performance stood out and estimated values showed only a small amount of scatter around the forced regression line.

The α coefficient that is applied to the E_{PT} model (usually set to 1.26) is not constant throughout the year. It was calculated to be much lower during summer and autumn (< 0.8) and higher and more variable during winter. Spring α was very close to 1.26. During non-limiting soil moisture conditions $\alpha = 1.31$ at Scott Farm, however a seasonally adjusted value would be most appropriate if this model is to be used. When the regression was analysed to find the accuracy of E_{PT} in comparison to E_{EC} , seasonal trends were apparent for which, during low evaporative conditions, E_{PT} significantly underestimated E , and over-estimated E during high evaporative conditions. This model is not recommended if input data are available for E_o .

A water stress adjustment was applied to both E_o and E_{PT} models which resulted in an improvement in estimated summer/autumn evaporation. Early onset of

drying was not able to be adjusted for within the model which causes problems when estimating evaporation at the beginning of seasonal drought. Possible reasons for this difficulty may be the changing vegetation conditions and composition during the dry-down phase of a drought. The water stress adjustment was most realistic using an estimated a rooting depth of 1.0 m, field capacity of 0.5 and wilting point of 0.2 (v/v). The model was not very sensitive to field capacity however it was to wilting point due to the relation to water stress conditions.

7.5 Further research recommendations

This study has resulted in some recommendations for future research as well as some extended areas that could be possible research topics:

Further research using lysimeter studies to develop more confidence in eddy covariance measurements would be beneficial for this field of research. When conducting a lysimeter study, it is important to ensure the depth of the lysimeter is deep enough to allow for maximum rooting depth of the contained vegetation, especially during dry conditions when roots may extend deeper than usual in order to extract deeper water for survival. The surface area of lysimeters may also be a critical factor for lysimeter results so an assessment of the effect of large and small lysimeters would be valuable.

An area of interest that presented itself as a result of this study is the effects and sources of large-scale advection. Due to New Zealand's maritime climate and environment, advection of warm maritime air masses may provide a significant source of energy for evaporation especially in winter. This may also assist in understanding lack of energy balance closure at this eddy covariance site during some times of year. Foken (2008) proposed a hypothesis about larger atmospheric turbulent transfers which may help gain a good understanding of processes relevant to this type of research and could be used as a hypothesis for future research.

The soil moisture correction applied to the FAO₅₆ model suffered one major downfall when applied to estimated E data; the initialisation of the correction was too slow at the onset of drying. Research into the reasons for this shortfall would be very beneficial for which a more accurate model could be developed to correct for drying conditions. Possible reasons may be site vegetation conditions and composition or differences due to soil type variations.

Recent studies into decadal climate change effects on pan evaporation have found that pan evaporation rates have been decreasing (Peterson *et al.* 1995; Roderick and Farquhar, 2002; Linacre, 2004; Roderick and Farquhar, 2005; and Jovanovic *et al.* 2008). With the confidence gained in the FAO₅₆ estimation method for estimating E , this model may be used to assess climate change impacts on evaporation rates over the past few decades or longer if sufficient data are available. Most variables required to calculate E_o have been measured for long time periods and could be used to gain a more accurate understanding of how a changing climate may affect evaporation in New Zealand.

References

- Aires, L.M., Pio, C.A., and Pereira, J.S., (2008). The effect of drought on energy and water vapour exchange above a Mediterranean C3/C4 grassland on Southern Portugal. *Agricultural and Forest Meteorology*, 148, 565-579.
- Alfieri, J.G., Blanken, P.D., Yates, D.N., and Steffen, K., (2007). Variability in the environmental factors driving evapotranspiration from a grazed rangeland during severe drought conditions. *Journal of Hydrometeorology*, 8, 207-220.
- Allen, R.G., Clemmens, A.J., Burt, C.M., Solomon, K., and O'Halloran, T., (2005). Prediction accuracy for projectwide evapotranspiration using crop coefficients and reference evapotranspiration. *Journal of Irrigation and Drainage Engineering*, 131, 1, 24-36.
- Allen, R.G., Pereira, L.S., Raes, D., and Smith, M., (1998). *Crop evapotranspiration – Guidelines for computing crop water requirements – FAO Irrigation and drainage paper 56*. FAO – Food and Agriculture Organization of the United Nations, Rome.
- Allen, R.G., Pruitt, W.O., and Jensen, M.E., (1991). Environmental requirements of lysimeters. *Proceedings of the International Symposium on Lysimetry*. American Society of Civil Engineers, New York, 170-181.
- Baldocchi, D., (2008). 'Breathing' of the terrestrial biosphere: lessons learned from a global network of carbon dioxide flux measurement systems. *Australian Journal of Botany*, 56, 1-26.
- Baldocchi, D.D., Xu, L., and Kiang, N., (2004). How plant functional-type, weather, seasonal drought, and soil physical properties alter water and energy fluxes of an oak-grass savanna and an annual grassland. *Agricultural and Forest Meteorology*, 123, 13-39.
- Baumgartner, A., and Reichel, E., (1975). *The world water balance*. Elsevier Scientific Publishing Company, Amsterbam, The Netherlands.

- Berengena, J., and Gavilan, P., (2005). Reference evapotranspiration estimation in a highly advective semiarid environment. *Journal of Irrigation and Drainage Engineering*, 131, 2, 147-163.
- Beyrich, F., Leps, J., Mauder, M., Bange, J., Foken, T., Huneke, S., Lohse, H., Lüdi, A., Meijninger, W.M.L., Mironov, D., Weisensee, U., and Zittel, P., (2006). Area-averaged surface fluxes over the Litfass region based on eddy-covariance measurements. *Boundary-Layer Meteorology*, 121, 33-65.
- Burman, R. and Pochop, L.O. (1994). Evaporation, Evapotranspiration and Climatic Data. Developments in Atmospheric Science, 22. University of Wyoming, USA.
- Calder, I.R., (1990). *Evaporation in the uplands*. John Wiley & Sons Ltd, Chichester, England.
- Campbell Scientific, Inc, (2007). *Instruction Manual: CSAT3 Three dimensional sonic anemometer, revision: 2/07*. Campbell Scientific, Inc. Logan, Utah.
- Campbell, D. I. (1989). Energy balance and transpiration from tussock grassland in New Zealand. *Boundary-Layer Meteorology*, 46, 133-152.
- Campbell, D., and Nieveen, J., (2005). Seasonal controls on evaporation from pasture. *New Zealand Hydrological Society Conference Presentation 2005*, Auckland, New Zealand.
- Campbell, D.I., and Murray, D.L., (1990). Water balance of snow tussock grassland in New Zealand. *Journal of Hydrology*, 118, 229-245.
- Campbell, D.I., and Nieveen, J.P., (in prep). Forcing energy balance closure provides realistic estimates of evaporation from eddy covariance measurements over pasture.
- Campbell, D.I., and Williamson, J.L., (1997). Evaporation from a raised peat bog. *Journal of Hydrology*, 193, 142-160.
- Clothier, B. E., Kerr, J. P., Talbot, J.S., and Scotter, D.R. (1982). Measured and estimated evapotranspiration from well-watered crops. *New Zealand Journal of Agricultural Research* 25: 301-307.

- Daamen, C.C., and McNaughton, K.G., (2000). Modelling energy fluxes from sparse canopies and understories. *Agronomy Journal*, 92, 837-847.
- Daamen, C.C., Simmonds, L.P., Wallace, J.S., Laryea, K.B., and Sivakumar, M.V.K., (1993). Use of microlysimeters to measure evaporation from sandy soils. *Agricultural and Forest Meteorology*, 65, 159-173.
- DehghaniSanij, H., Yamamoto, T., and Rasiah, V., (2004). Assessment of evapotranspiration estimation models for use in semi-arid environments. *Agricultural Water Management*, 64, 91-106.
- Dugas, W.A., and Bland, W.L., (1989). The accuracy of evaporation measurements from small lysimeters. *Agricultural and Forest Meteorology*, 46, 119-129.
- Dugas, W.A., Fritschen, L.J., Gay, L.W., Held, A.A., Matthias, A.D., Reicosky, D.C., Steduto, P., and Steiner, J.L., (1991). Bowen ratio, eddy correlation, and portable chamber measurements of sensible and latent heat flux over irrigated spring wheat. *Agricultural and Forest Meteorology*, 56, 1-20.
- Dyer, A.J., and Maher, F.J., (1965). Automatic eddy-flux measurements with the Evapotron. *Journal of Applied Meteorology*, 4, 622-625.
- Fahey, B. D., and Watson, A.J., (1991). Hydrological impacts of converting tussock grassland to pine plantation, Otago, New Zealand. *New Zealand Journal of Hydrology*, 30, 1, 1-15.
- Fahey, B., and Jackson, R., (1997). Hydrological impacts of converting native forests and grasslands to pine plantations, South Island, New Zealand. *Agricultural and Forest Meteorology*, 84, 69-82.
- Falge, E. *et al.* (2001). Gap filling strategies for defensible annual sums of net ecosystem exchange. *Agricultural and Forest Meteorology*, 107, 1, 92-102.
- Figuerola, P.I., and Berliner, P.R., (2005). Evapotranspiration under advective conditions. *International Journal of Biometeorology*, 49, 403-416.
- Foken, T., (2008). The energy balance closure problem: An overview. *Ecological Applications*, 18, 6, 1351-1367.

- Fong, A., (2001). Evaporation from hillslope pasture at Mahurangi, Northland. MSc Thesis, University of Waikato.
- Gavilan, P., and Berengena, J., (2007). Accuracy of the bowen ratio-energy balance method for measuring latent flux in a semiarid advective environment. *Irrigation Science*, 25, 127-140.
- Grimmond, C.S.B., Isard, S.A., and Belding, M.J., (1992). Development and evaluation of continuously weighing mini-lysimeters. *Agricultural and Forest Meteorology*, 62, 205 – 218.
- Hewitt, A.E., (1993). New Zealand soil classification, Manaaki Whenua – Landcare Research New Zealand Ltd, Lincoln.
- Hillel, D., (2004). *Introduction to environmental soil physics*. Elsevier Academic Press, San Diego, USA.
- Humphreys, E.R., Black, T.A., Ethier, G.J., Drewitt, G.B., Spittlehouse, D.L., Jork, E.M., Nesic, Z., and Livingston, N.J., (2003). Annual and seasonal variability of sensible and latent heat fluxes above a coastal Douglas-fir forest, British Columbia, Canada. *Agricultural and Forest Meteorology*, 115, 109-125.
- Hunt, J.E., Kelliher, F.M., McSeveny, T.M., and Byers, J.N., (2002). Evaporation and carbon dioxide exchange between the atmosphere and a tussock grassland during a summer drought. *Agriculture and Forest Meteorology*, 111, 65-82.
- Irmak, S., Irmak, A., Allen, R.G., and Jones, J.W., (2003). Solar and net radiation-based equations to estimate reference evapotranspiration in humid climates. *Journal of irrigation and drainage engineering*, 336-347.
- Jovanovic, B., Jones, D.A., and Collins, D., (2008). A high-quality monthly pan evaporation dataset for Australia. *Climatic Change*, 87, 517-535.
- Kelliher, F.M., and Jackson, R., (2001). Evaporation and the water balance, in A. Struman and R. Spronken-Smith (eds), *The Physical Environment, A New Zealand Perspective*. Oxford University Press, Melbourne, 206-217.

- Kelliher, F.M., Lloyd, J., Rebman, C., Wirth, C., Schulze, E.E., and Baldocchi, D.D., (2001). *1.11 Evaporation in the boreal zone during summer – physics and vegetation*. In: Schulze, E.D., Heimann, M., Harrison, S., Holland, E., Lloyd, J., Prentice, I.C., and Schimel, D. *Global Biogeochemical Cycles in the Climate System*. Academic Press.
- Klocke, N.L., Martin, D.L., Todd, R.W., Dehaan, D.L., and Polymenopoulos, A.D., (1990). Evaporation measurements and predictions from soils under crop canopies. *Transactions of the ASAE*, 33, 5, 1590-1596.
- Law, B.E., Falge, E., Gu, L., Baldocchi, D.D., Bakwin, P., Berbigier, P., Davis, K., Dolman, A.J., Falk, M., Fuentes, J.D., Goldstein, A., Granier, A., Grelle, A., Hollinger, D., Janssens, I.A., Jarvis, P., Jensen, N.O., Katul, G., Mahli, Y., Matteucci, G., Meyers, T., Monson, R., Munger, W., Oechel, W., Olson, R., Pilegaard, K., Paw U, K.T., Thorgeirsson, H., Valentini, R., Verma, S., Vesala, T., Wilson, K., and Wofsy, S., (2002). Environmental controls over carbon dioxide and water vapor exchange of terrestrial vegetation. *Agricultural and Forest Meteorology*, 113, 97-120.
- LI-COR, (2001). *CO₂/H₂O Gas Analyzers: The LI-7000 and LI-7500*. LI-COR Biosciences, Lincoln, Nebraska.
- Linacre, E.T., (2004). Evaporation trends. *Theoretical and Applied Climatology*, 79, 11-21.
- Lopez-Urrea, R., Martin de Santa Olalla, F., Febeiro, C., and Moratalla, A., (2006a). Testing evapotranspiration equations using lysimeter observations in a semiarid climate. *Agricultural Water Measurements*, 85, 15-26.
- Lopez-Urrea, R., Martin de Santa Olalla, F., Febeiro, C., and Moratalla, A., (2006b). An evaluation of two hourly reference evapotranspiration equations for semiarid conditions. *Agricultural Water Management*, 86, 277-282.
- Marc, V., and Robinson, M. (2007). The long-term water balance (1972-2004) of upland forestry and grassland at Plynlimon, mid-Wales. *Hydrology and Earth System Sciences*, 11, 1, 44-60.

- McAneney, K.J., and Judd, M.J., (1983). Pasture production and water use measurements in the central Waikato. *New Zealand Journal of Agricultural Research*, 26, 7-13.
- McConchie, J. (2001). Water transport processes. In; Sturman, A. & Spronken-Smith, R. (eds). *The physical environment, a New Zealand perspective*. Oxford University Press, Melbourne, 175-205.
- McMillen, R.T., (1988). An eddy correlation technique with extended application to non-similar terrain. *Boundary-Layer Meteorology*, 43, 231-245.
- McNaughton, K. G., Clothier, B.E., and Kerr, J.P., Ed. (1979). Evaporation from land surfaces. *Physical Hydrology. New Zealand Experience*. Wellington, The Caxton Press.
- McNaughton, K.G., (1976). Evaporation and advection I: evaporation from extensive homogeneous surfaces. *Quarterly Journal of the Royal Meteorological Society*, 102, 181-191.
- McNaughton, K.G., and Jarvis, P.G., (1983). Effects of vegetation on Transpiration and Evaporation, in T.T. Kozlowski (ed). *Water deficits and plant growth, Vol. VII*. Academic Press, New York.
- McNaughton, K.G., and Jarvis, P.G., (1991). Effects of spatial scale on stomatal control of transpiration. *Agricultural and Forest Meteorology*, 54, 279-301.
- McNaughton, K.G., Clothier, B.E., and Kerr, J.P., (1979). Evaporation from land surfaces. In: *Physical Hydrology. New Zealand Experience*. Eds D.L. Murraray and P. Ackroyd. The Caxton Press, Wellington, New Zealand.
- Ministry for the Environment (2001/2002). Landcover Database B2, Wellington, New Zealand.
- Monteith, J.L., and Unsworth, M.H., (1990). *Principles of Environmental Physics, Second Edition*. Edward Arnold, London.
- Moore, C.J., (1986). Frequency response corrections for eddy correlation systems. *Boundary-Layer Meteorology*, 37, 17-35.

- Nieveen, J.P., Campbell, D.I., Schipper, L.A. and Blair, I.J., (2005). Carbon exchange of grazed pasture on a drained peat soil. *Global Change Biology*, 11, 607–618.
- NIWA (National Institute of Water and Atmospheric Research), CliFlo national climate database: <http://cliflo.niwa.co.nz/>. Accessed on 4 and 29 September 2008.
- Oke, T.R., (1987). *Boundary Layer Climates*. Routledge, London and New York.
- Oncley, S.P., Foken, T., Vogt, R., Kohsiek, W., DeBruin, H.A.R., Bernhofer, C., Christen, A., Gorsel, E., Grantz, D., Feigenwinter, C., Lehner, I., Liebenthal, C., Liu, H., Mauder, M., Pitacco, A., Ribeiro, L., and Weidinger, T., (2007). The energy balance experiment EBEX-2000. Part I: overview and energy balance. *Boundary-Layer Meteorology*, 123, 1-28.
- Paco, T.A., Ferreira, M.I., and Conceicao, N., (2006). Peach orchard evapotranspiration in a sandy soil: Comparison between eddy covariance measurements and estimates by the FAO 56 approach. *Agricultural Water Management*, 85, 305-313.
- Pauwels, V. R. N., and Samson, R. (2006). Comparison of different methods to measure and model actual evapotranspiration rates for a wet sloping grassland. *Agricultural Water Management*, 82, 1-24.
- Pearce, A.J., and Rowe, L.K., (1979). Forest management effects on interception, evaporation, and water yield. *Journal of Hydrology NZ*, 18, 73-87.
- Pearce, A.J., Rowe, L.K., and Stewart, J.B., (1980). Nighttime, wet canopy evaporation rates and the water balance of an evergreen mixed forest. *Water Resources Research*, 16, 5, 955-959.
- Peterson, T.C., Golubev, V.S., and Groisman, P.Ya., (1995). Evaporation losing its strength, *Nature*, 377, 687-688.
- Priestley, C.H.B., and Taylor, R.J., (1972). On the assessment of surface heat flux and evaporation using large-scale parameters. *Monthly weather review*, 100, 81-92.

- REBS, (1995). REBS Q*6.7.1 Net Radiometer Manual. Radiation and Energy Balance Systems, Inc., Seattle, WA, USA.
- Roderick, M.L., and Farquhar, G.D., (2002). The cause of decreased pan evaporation over the past 50 years. *Science*, 298, 1410-1411.
- Roderick, M.L., and Farquhar, G.D., (2005). Changes in New Zealand pan evaporation since the 1970s. *International Journal of Climatology*, 25, 2031-2039.
- Rodriguez-Iturbe, I., (2000). Ecohydrology: A hydrologic perspective of climate-soil-vegetation dynamics. *Water Resources Research*, 36, 1, 3-9.
- Rosset, M., Riedo, M., Grub, A., Geissmann, M., and Fuhrer, J., (1997). Seasonal variation in radiation and energy balances of permanent pastures at different altitudes. *Agricultural and Forest Meteorology*, 86, 245-258.
- Ryu, Y., Baldocchi, D.D., Ma, S., and Hehn, T., (2008). Interannual variability of evapotranspiration and energy exchange over an annual grassland in California. *Journal of Geophysical Research*, 113, D09104.
- Schotanus, P., Nieuwstadt, F.T.M., and de Bruin, H.A.R., (1983). Temperature measurement with a sonic anemometer and its application to heat and moisture fluxes. *Boundary-Layer Meteorology*, 26, 81-93.
- Schuepp, P.H., Leclerc, M.Y., MacPherson, J.I., and Desjardins, R.L., (1990). Footprint prediction of scalar fluxes from analytical solutions of the diffusion equation. *Boundary-Layer Meteorology*, 50, 355-373.
- Scotter, D., and Heng, L. (2003). Estimating reference crop evapotranspiration in New Zealand. *Journal of Hydrology (NZ)*, 42, 1, 1-10.
- Scotter, D., and Kelliher, F., (2004). Evaporation and transpiration, in J.S. Harding, M.P. Mosley, C.P. Pearson, and B.K. Sorrell (eds), *Freshwaters of New Zealand*. New Zealand Hydrological Society Inc. and New Zealand Limnological Society Inc., Christchurch, New Zealand, chp 3.
- Shuttleworth, W.J., (2007). Putting the ‘vap’ into evaporation. *Hydrology and Earth System Sciences*, 11, 1, 210-244.

- Singleton, P.L., (1991). Soils of Ruakura – a window on the Waikato, New Zealand, *Department of Scientific and Industrial Research Land Resources. Scientific Report Number 5*.
- Smith, J., (2003). Fluxes of carbon dioxide and water vapour at a Waikato peat bog. PhD Thesis, University of Waikato, Hamilton.
- Spronken-Smith, R., (2001). Microclimates and Earths-surface energy exchanges. In; Sturman, A. & Spronken-Smith, R. (eds). *The physical environment, a New Zealand perspective*. Oxford University Press, Melbourne, 113-129.
- Stewart, J.B., (1977). Evaporation from the wet canopy of a pine forest. *Water Resources Research*, 13, 6, 915-921.
- Stiles, S., (1998). A soil survey of an AgResearch farm. BSc Technology Industry Report. University of Waikato, Hamilton.
- Sturman, A., and Tapper, N., (2006). *The weather and climate of Australia and New Zealand, second edition*. Oxford University Press, Melbourne, Australia.
- Sumner, D. M., and Jacobs, J.M. (2005). Utility of Penman-Monteith, Priestley-Taylor, reference evapotranspiration, and pan evaporation methods to estimate pasture evaporation. *Journal of Hydrology*, 308, 81-104.
- Swinbank, W.C., (1951). The measurement of vertical transfer of heat and water vapor by eddies in the lower atmosphere. *Journal of Meteorology*, 8, 3, 135-145.
- Teuling, A.J., Seneviratne, S.I., Williams, C., and Troch, P.A., (2006). Observed timescales of evapotranspiration response to soil moisture. *Geophysical Research Letters*, 33, L23403.
- Thompson, M.A., Campbell, D.I., and Spronken-Smith, R.A., (1999). Evaporation from natural and modified raised peat bogs in New Zealand. *Agricultural and Forest Meteorology*, 95, 85-98.
- Thornburrow, B. R., (2005). Fluxes of CO₂ and water vapour at Opuatia wetland. MSc Thesis, University of Waikato.

- Twine, T.E., Kustas W.P., Norman, J.M., Cook, D.R., Houser, P.R., Meyers, T.P., Prueger, J.H., Starks, P.J., and Wesely, M.L., (2000). Correcting eddy-covariance flux underestimates over a grassland. *Agricultural and Forest Meteorology*, 103, 279-300.
- Ventura, F., Spano, D., Duce, P., and Snyder, R.L., (1999). An evaluation of common evapotranspiration equations. *Irrigation Science*, 18, 163-170.
- Villa Nova, N. A., Pereira, A.B., and Shock, C.C. (2007). Estimation of reference evapotranspiration by an energy balance approach. *Biosystems Engineering*, 96, 4, 604-615.
- Villalobos, F.J., (1997). Correction of eddy covariance water vapor flux using additional measurements of temperature. *Agricultural and Forest Meteorology*, 88, 77-83.
- Ward, R.C., and Robinson, M., (1999). *Principles of Hydrology (4th ed)*. McGraw-Hill Publishing, UK.
- Webb, E.K., Pearman, G.I., and Leuning, R., (1980). Correction of flux measurements for density effects due to heat and water vapour transfer. *Quarterly Journal of the Royal Meteorology Society*, 106, 447, 85-100.
- Welten, B.G., (2005). The role groundwater and surface runoff processes play in facilitating nutrient movement at a Waikato dairy farm. MSc Thesis. University of Waikato, Hamilton.
- Wilson, K., Goldstein, A., Falge, E., Aubinet, M., Baldocchi, D., Berbigier, P., Bernhofer, C., Ceulemans, R., Dolman, H., Field, C., Grelle, A., Ibrom, A., Law, B.E., Kowalski, A., Meyers, T., Moncrieff, J., Monson, R., Oechel, W., Tenhunen, J., Valentini, R., and Verma, S., (2002). Energy balance closure at FLUXNET sites. *Agricultural and Forest Meteorology*, 113, 223-243.
- Wilson, K.B., Hanson, P.J., Mulholland, P.J., Baldocchi, D.D., and Wullschlegel, S.D., (2001). A comparison of methods for determining forest evapotranspiration and its components: sap-flow, soil water budgets, eddy covariance and catchment water balance. *Agricultural and Forest Meteorology*, 106, 153-168.

- Zhang, Y., Kadota, T., Ohata, T., and Oyunbaatar, D., (2007). Environmental controls on evapotranspiration from sparse grassland in Mongolia. *Hydrological Processes*, 21, 2016-2027.
- Zhou, M.C., Ishidaira, H., and Takeuchi, K., (2008). Comparative study of potential evapotranspiration and interception evaporation by land cover over Mekong basin. *Hydrological Processes*, 22, 1290-1309.

Appendices

A Appendix A

Soil water stress adjustment

$$E_{o(\text{adj})} = K_s K_c E_o$$

where K_s is the water stress coefficient, K_c is the crop coefficient (refer to Allen *et al.* (1998) for typical values), and E_o is the reference crop evaporation. When $K_s < 1$ soil water is limited while when $K_s = 1$ there is no soil water stress. K_s defines the water stress on plant transpiration rates and can be calculated using the following equation:

$$K_s = \frac{\text{TAW} - D_r}{\text{TAW} - \text{RAW}} = \frac{\text{TAW} - D_r}{(1 - p)\text{TAW}}$$

where TAW is total available water:

$$\text{TAW} = 1000 (\theta_{\text{FC}} - \theta_{\text{WP}}) Z_r$$

D_r is the root zone depletion:

$$D_{r(i=1)} = 1000 * (\theta_{\text{FC}} - \theta_{v,1}) * Z_r$$

$$D_{r(i)} = D_{r(i-1)} - P_i + E_{o(i)}$$

where θ_{FC} is field capacity, θ_{WP} is wilting point, Z_r is rooting depth, $\theta_{v,1}$ is volumetric soil moisture content on day 1, P is rainfall (mm), and i is the current day. See Allen *et al.* (1998) for equation including parameters where runoff and drainage need including.

RAW is readily available water:

$$\text{RAW} = p * \text{TAW}$$

where p is the depletion factor:

$$p = \frac{\text{RAW}}{\text{TAW}}$$

K_c can be estimated by regressing E_o on E_{EC} during well watered conditions.

B Appendix B

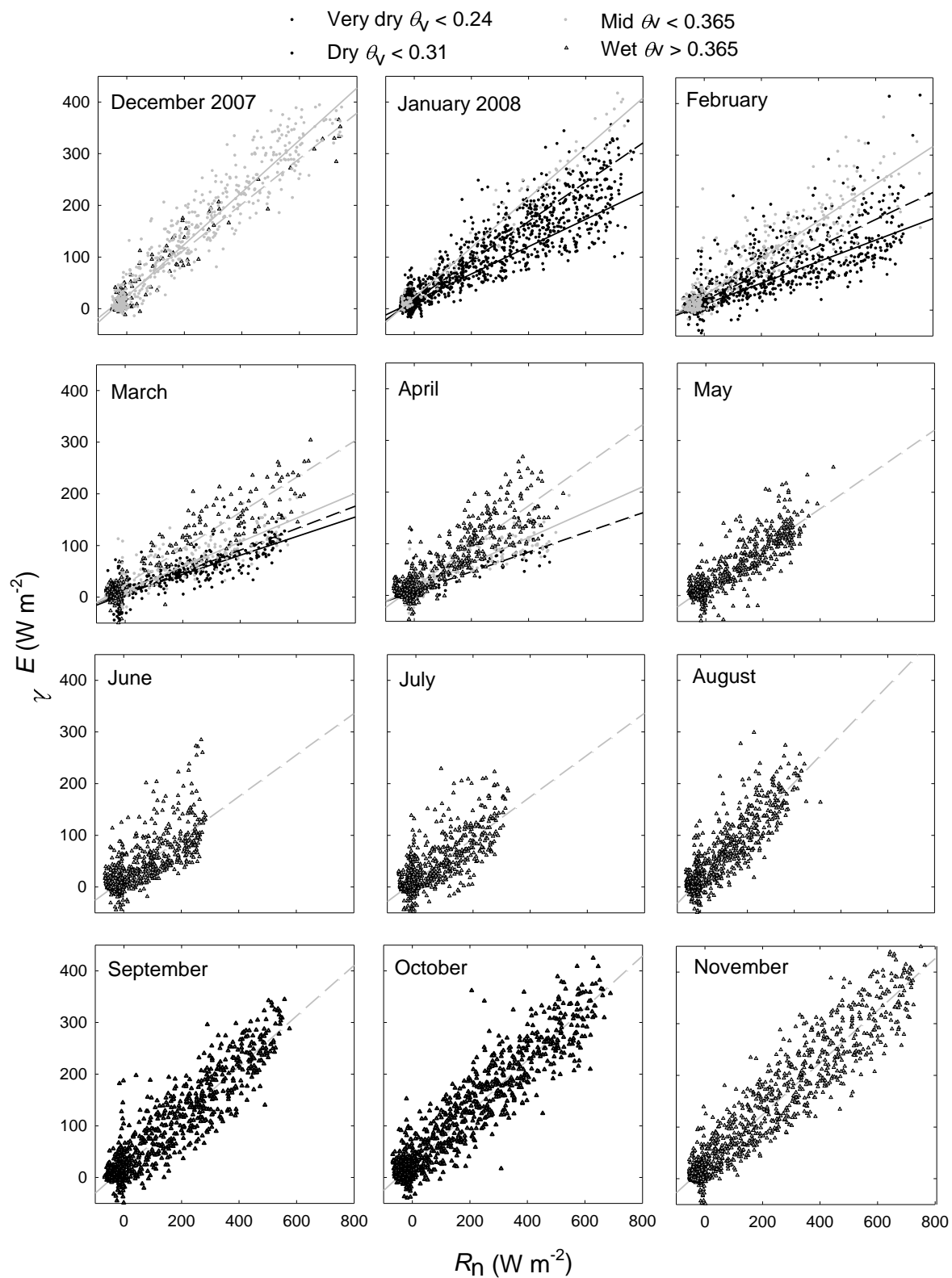


Figure B.1 Monthly plots of LE vs. R_n for December 2007 to November 2008 showing regression curves used for LE gap-filling model.

Table B.1 Monthly quadratic regression coefficients for λE vs. R_n during very dry soil moisture conditions where $\lambda E = m_1 R_n^2 + m_2 2R_n + c$. Refer to Figure A.1.

Month 2008	m_1	m_2	c	r^2
January	-0.0001	0.31	13.64	0.85
February	-0.00001	0.22	10.59	0.61
March	0.00001	0.18	7.23	0.75

Table B.2 Monthly quadratic regression coefficients for λE vs. R_n during dry soil moisture conditions where $\lambda E = m_1 R_n^2 + m_2 2R_n + c$. Refer to Figure A.1.

Month 2008	m_1	m_2	c	r^2
January	-0.0001	0.46	15.59	0.90
February	-0.00001	0.22	10.59	0.78
March	0.00001	0.18	7.23	0.91
April	-0.0002	0.25	7.87	0.75

Table B.3 Monthly quadratic regression coefficients for λE vs. R_n during mid soil moisture conditions where $\lambda E = m_1 R_n^2 + m_2 2R_n + c$. Refer to Figure A.1.

Month 2008	m_1	m_2	c	r^2
December '07	-0.0002	0.60	20.88	0.92
January	0.00004	0.46	22.23	0.97
February	-0.0001	0.31	18.10	0.82
March	-0.0001	0.27	12.68	0.80
April	-0.0002	0.31	13.78	0.84

Table B.4 Monthly quadratic regression coefficients for λE vs. R_n during wet soil moisture conditions where $\lambda E = m_1 R_n^2 + m_2 2R_n + c$. Refer to Figure A.1.

Month 2008	m_1	m_2	c	r^2
March	-0.0002	0.46	23.57	0.86
April	-0.0001	0.41	15.97	0.79
May	0.0002	0.32	14.95	0.77
June	0.0004	0.33	13.18	0.58
July	0.0004	0.33	11.32	0.59
August	-0.00003	0.48	14.90	0.77
September	0.0001	0.47	18.84	0.86
October	-0.0001	0.54	25.02	0.89
November	-0.0001	0.53	22.29	0.90

C Appendix C

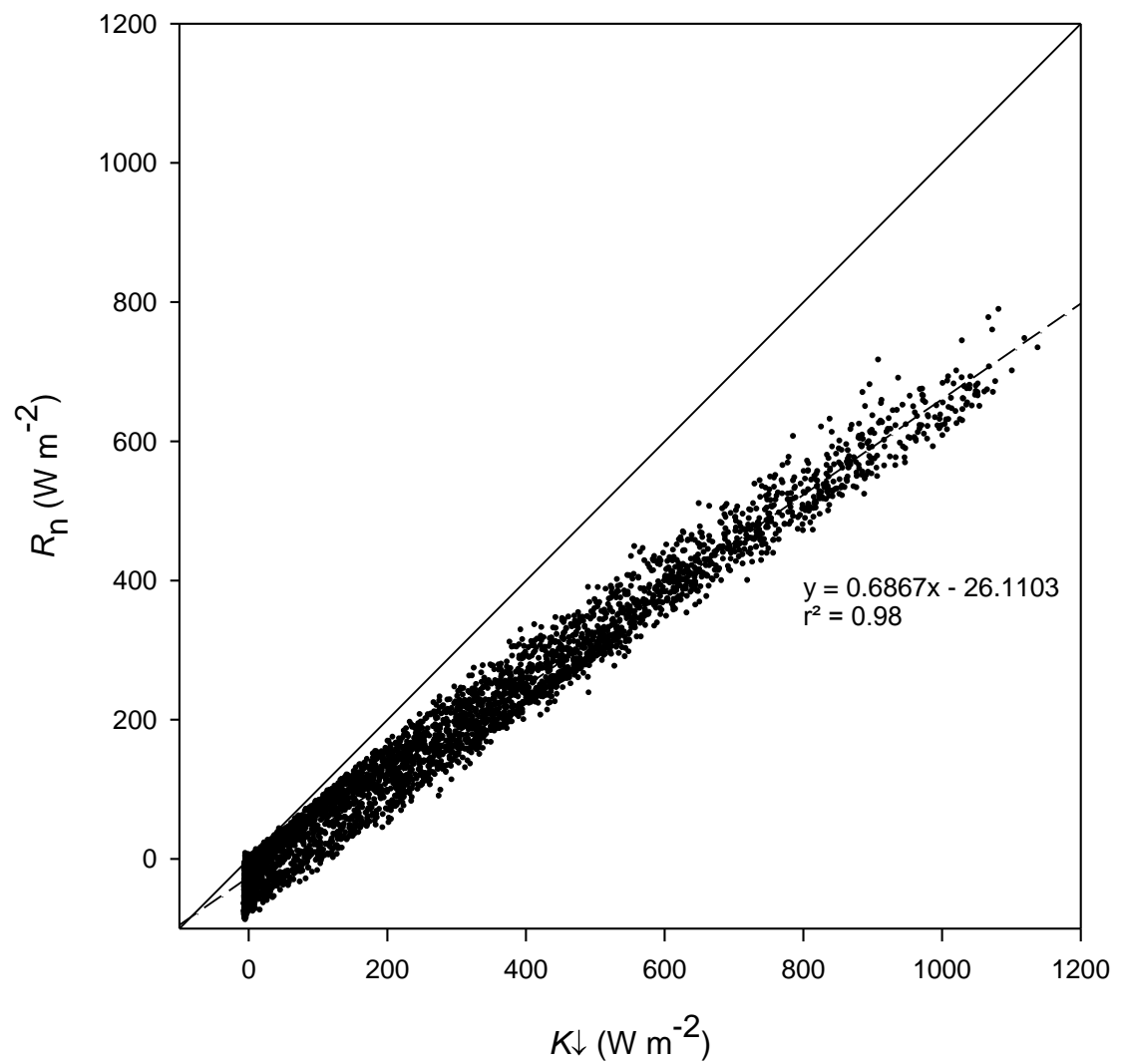


Figure C.1 Regression of half hourly data from 19 January 2008 to 20 June 2008 comparing R_n to K_{\downarrow} .

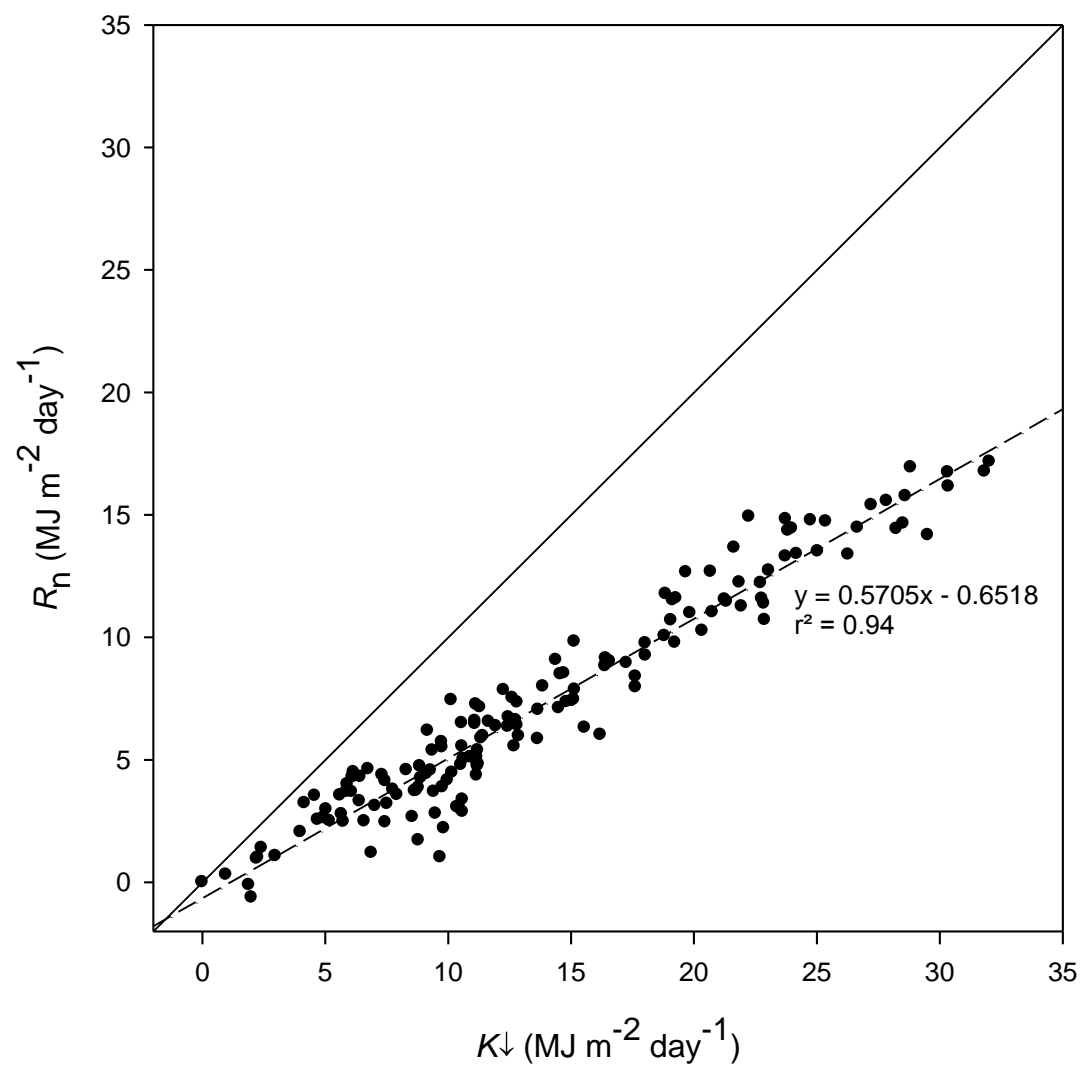


Figure C.2 Regression of daily data from 19 January 2008 to 20 June 2008 comparing R_n to K_{\downarrow} .

D Appendix D

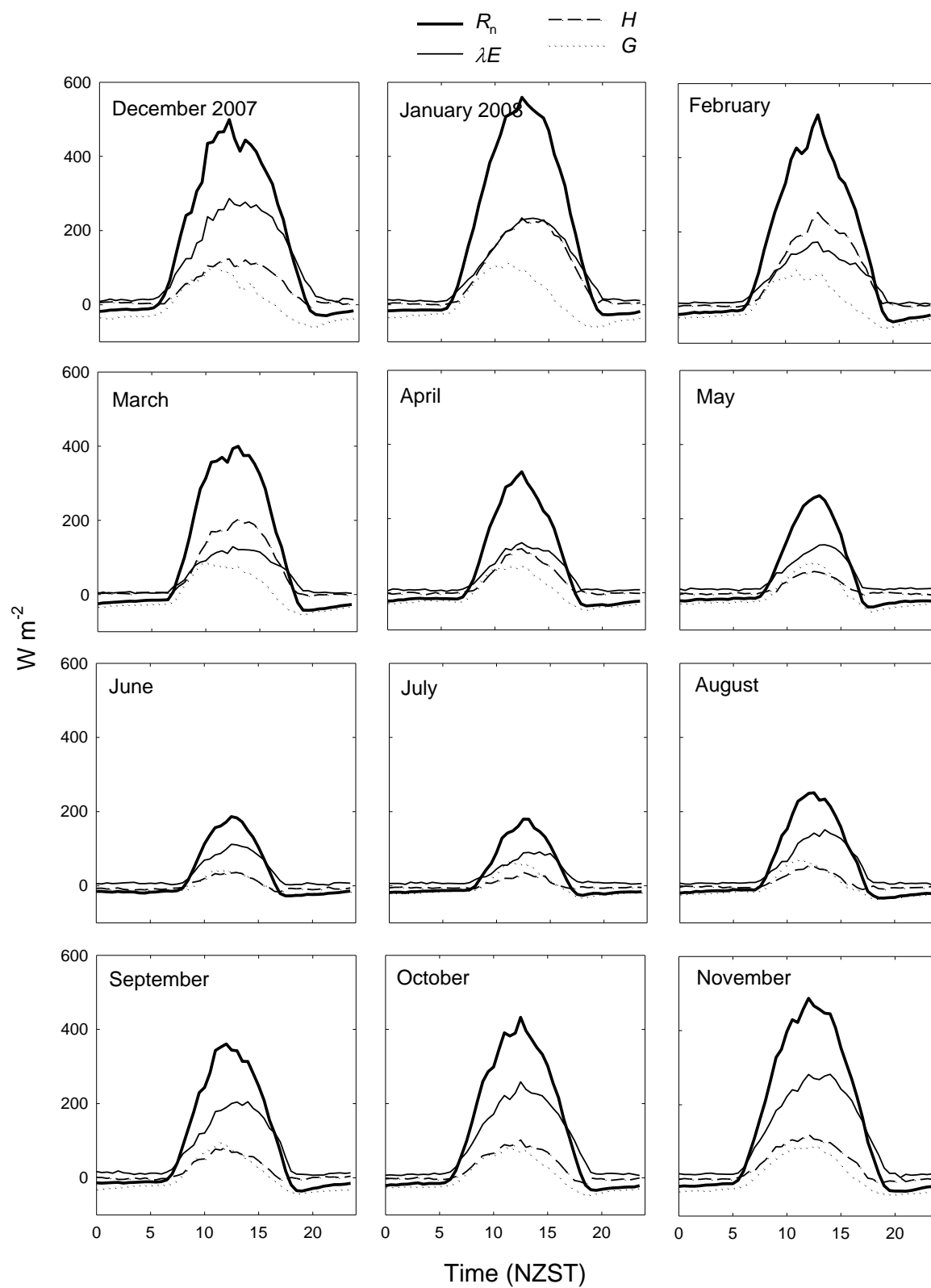


Figure D.1 Monthly energy balance ensembles for the months December 2007 to November 2008 where December 2007 is only a part month.

E Appendix E

The attached CD-ROM contains relevant information for this thesis:

- PDF and Word document of thesis.
- All MatLab functions and scripts that were used in order to produce and analyse data and develop relevant graphs and tables.
- Digital files of all figures made using Sigmaplot.

